Measurement of the Higgs self-coupling λ_{3H} using the Matrix Element Method at Next-to Leading-Order (NLO) in the $gg \rightarrow HH \rightarrow b\bar{b}\gamma\gamma$ channel for the ATLAS experiment at the LHC.

by Matthias TARTARIN

Measurement of the Higgs self-coupling λ_{3H} using the Matrix Element Method at Next-to Leading-Order (NLO)
in the $gg \rightarrow HH \rightarrow b\bar{b}\gamma\gamma$ channel
for the ATLAS experiment at the LHC.

.1 : The Higgs Sector: Spontaneous Symmetry Breaking (SSB)

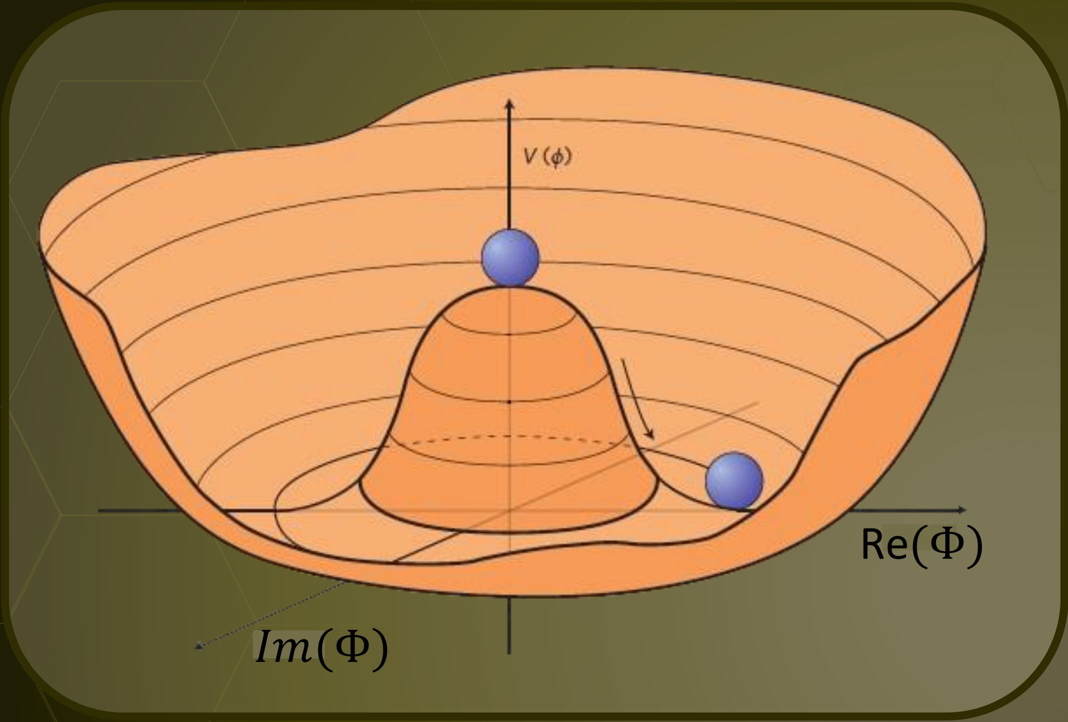

Assumption on the form of the potential of the Higgs field ϕ :

$$V(\phi^2) = \mu^2\phi^2 + \lambda\phi^4$$

(with $\mu^2 < 0$ and $\lambda > 0$)

Rewrite the potential in term of the Higgs boson H:

$$V(H) = 2\lambda v^2\frac{H^2}{2} + 6\lambda v\frac{H^3}{3!} + 6\lambda\frac{H^4}{4!} - \frac{v^4\lambda}{4}$$

$$V(H) = m_H{}^2\frac{H^2}{2} + \lambda_{3H}\frac{H^3}{3!} + \lambda_{4H}\frac{H^4}{4!} - \frac{v^4\lambda}{4}$$

- mass of the Higgs $m_H{}^2$ (squared)
- Coupling constant for 3 Higgs interacting
- Coupling constant for 4 Higgs interacting

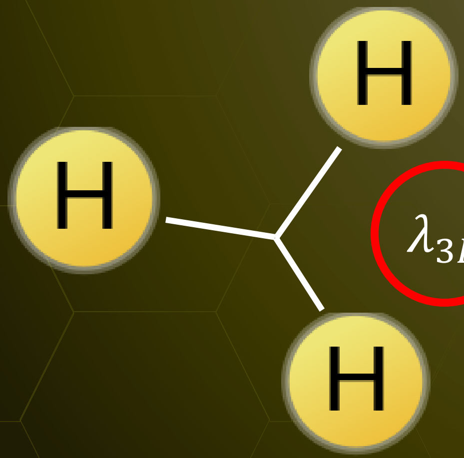

$$\lambda_{3H} = 6\sqrt{-\lambda\mu^2}$$

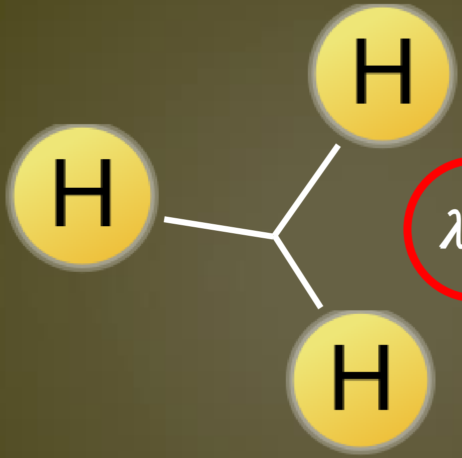

$$\lambda_{3H} = 6\sqrt{-\lambda\mu^2}$$

Objective:

Measure $\boldsymbol{\lambda_{3H}}$

For now, we only have theoretical prediction on the value of λ_{3H}^{SM} (≈ 190 GeV).

We would like to measure it **experimentally**, to test the theory.

1

Motivation

.2 : The LHC: Plan

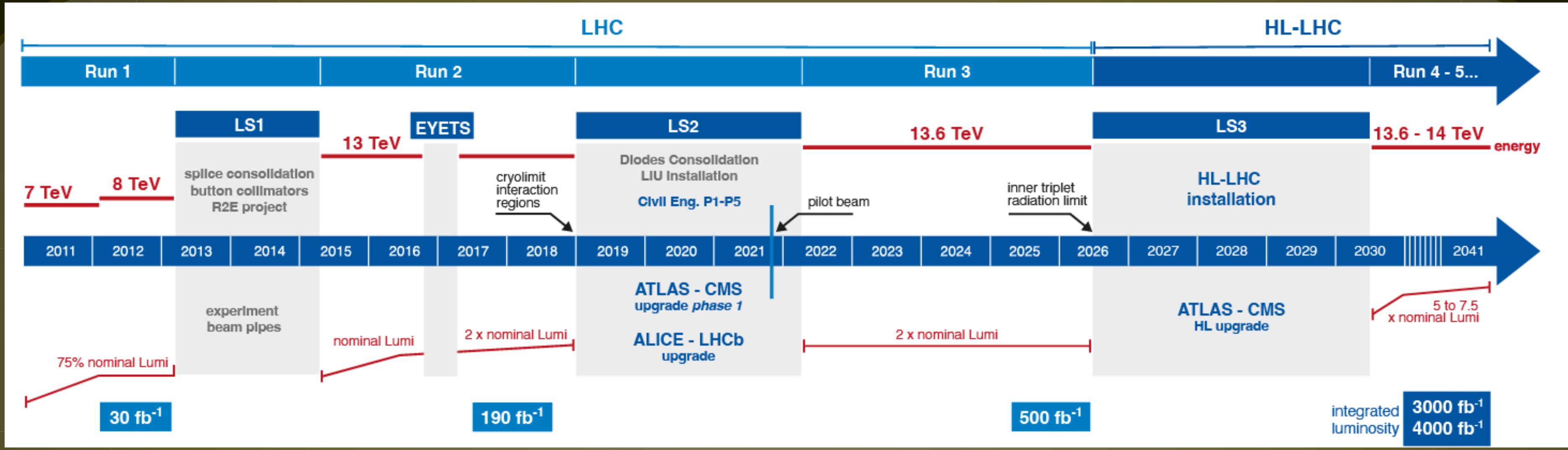

Objective:
Measure λ_{3H}

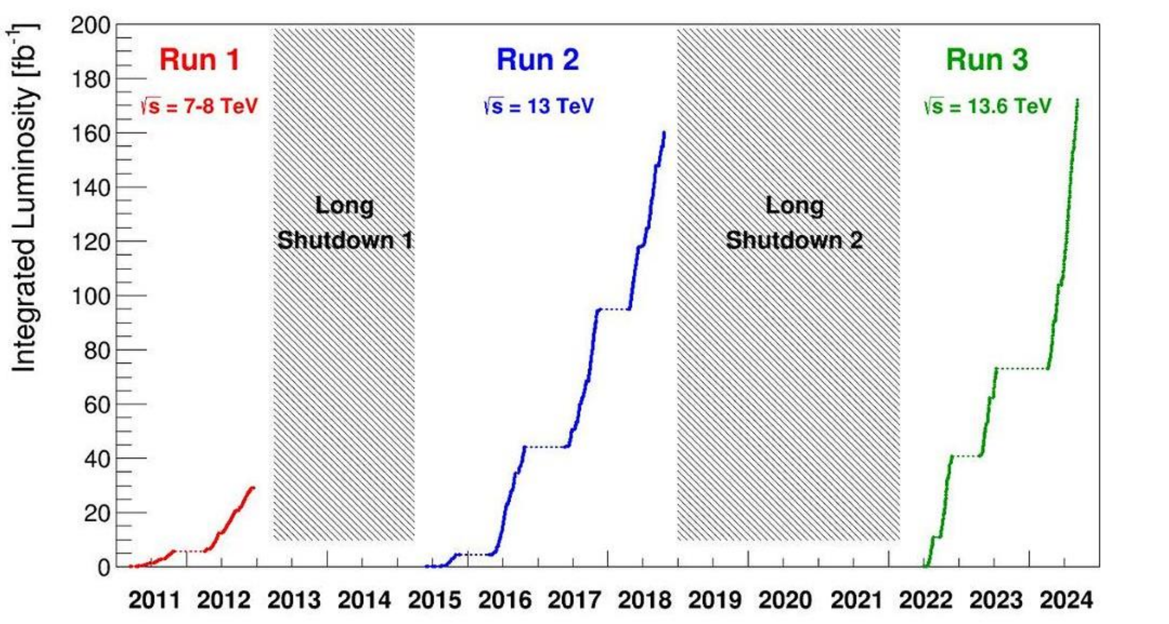

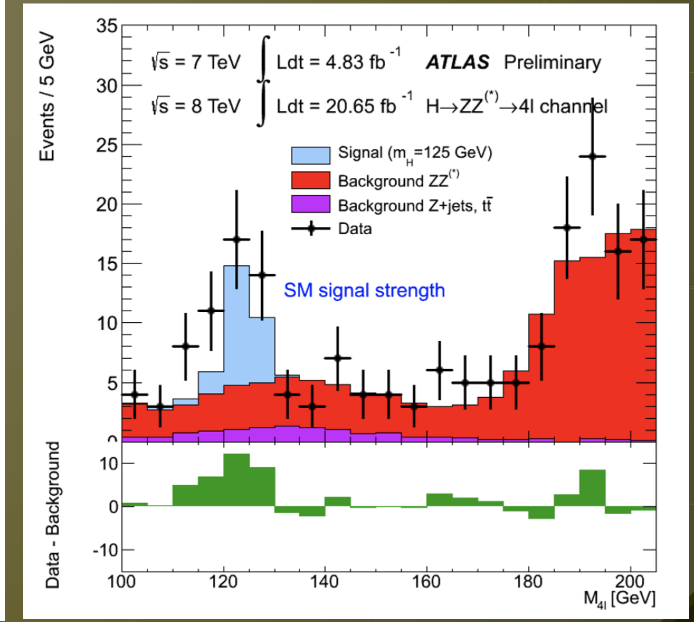

Discovery of the Higgs boson in 2012 by both CMS and ATLAS.
$m_H \cong 125\ GeV$

.2 : The LHC: The High-Luminosity LHC

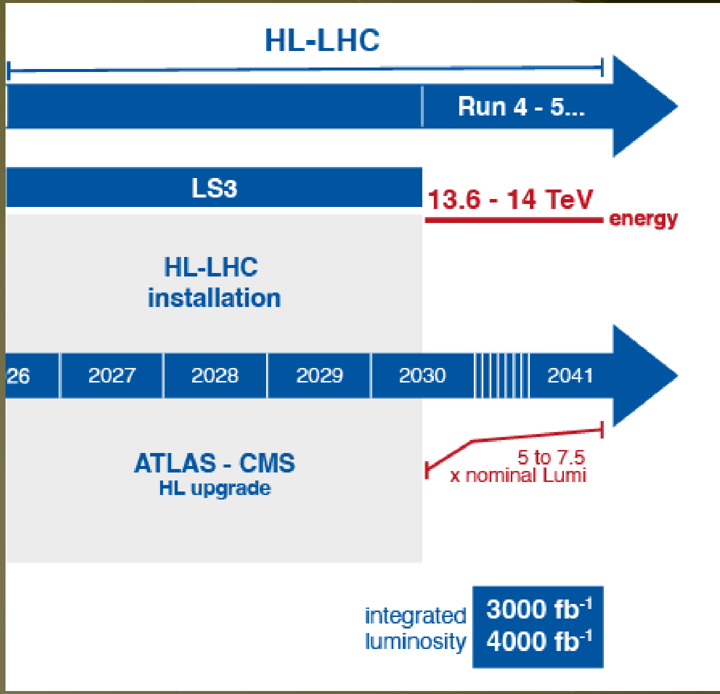

Objective:
Measure λ_{3H}

MadMax framework (Pr.Plehn et al.)

MadMax predicts that the HL-LHC with an integrated luminosity of 3 ab^{-1} could constrain the Higgs self-coupling λ_{3H} (ratio over the SM value) in the range:

$$\frac{\lambda_{3H}}{\lambda_{3H}^{\mathrm{SM}}} = 0.4\text{–}1.7 \qquad \text{at } 68\%\ \mathrm{CL}\ (3\ \mathrm{ab}^{-1})$$

1

Qualification Project

.4 : The HL-LHC: My Qualification project (QP)

Duration: 1 year, from November 2022 → November 2023

On the integration of the **ACTS** (A Common Tracking Software) Kalman Filter (KF) into the ATLAS software **Athena**, to enable precision tracking at the HL-LHC.

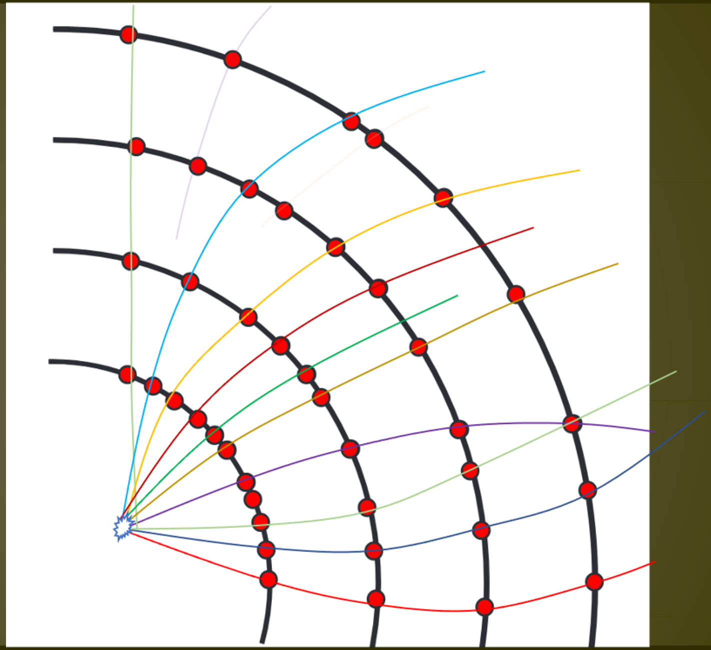

ACTS is an experiment-independent C++ software toolkit designed to support high-performance for track reconstruction.
The integration of **ACTS** into **Athena** is part of broader effort to transition ATLAS tracking software ahead of HL-LHC.

.3 : The HL-LHC: My Qualification project (QP)

My main input inside **Athena**: The interface with ACTS KF

1. Start from PRD (PrepRawData) stored tracks.
2. Fit the track from the PRD.
3. Got into calibration as PRD in the form of a sourceLink.
4. Tranform into ROT (RIO On Track) during calibration with fit-updated parameters.

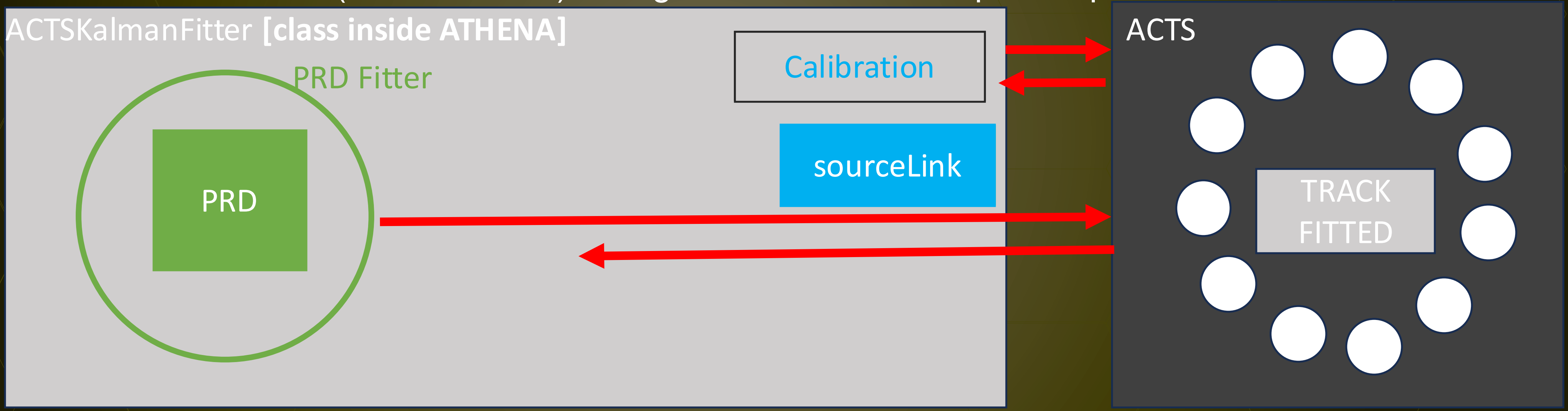

- PrepRawData (PRD): Raw hit information, 'raw data' (needs to be calibrated).
- RIO On Track (ROT): Calibrated hits (i.e translated into well-defined spatial position with its corresponding uncertainty, accounting for alignement and detector response)

.3 : The HL-LHC: My Qualification project (QP)

Qualification Project

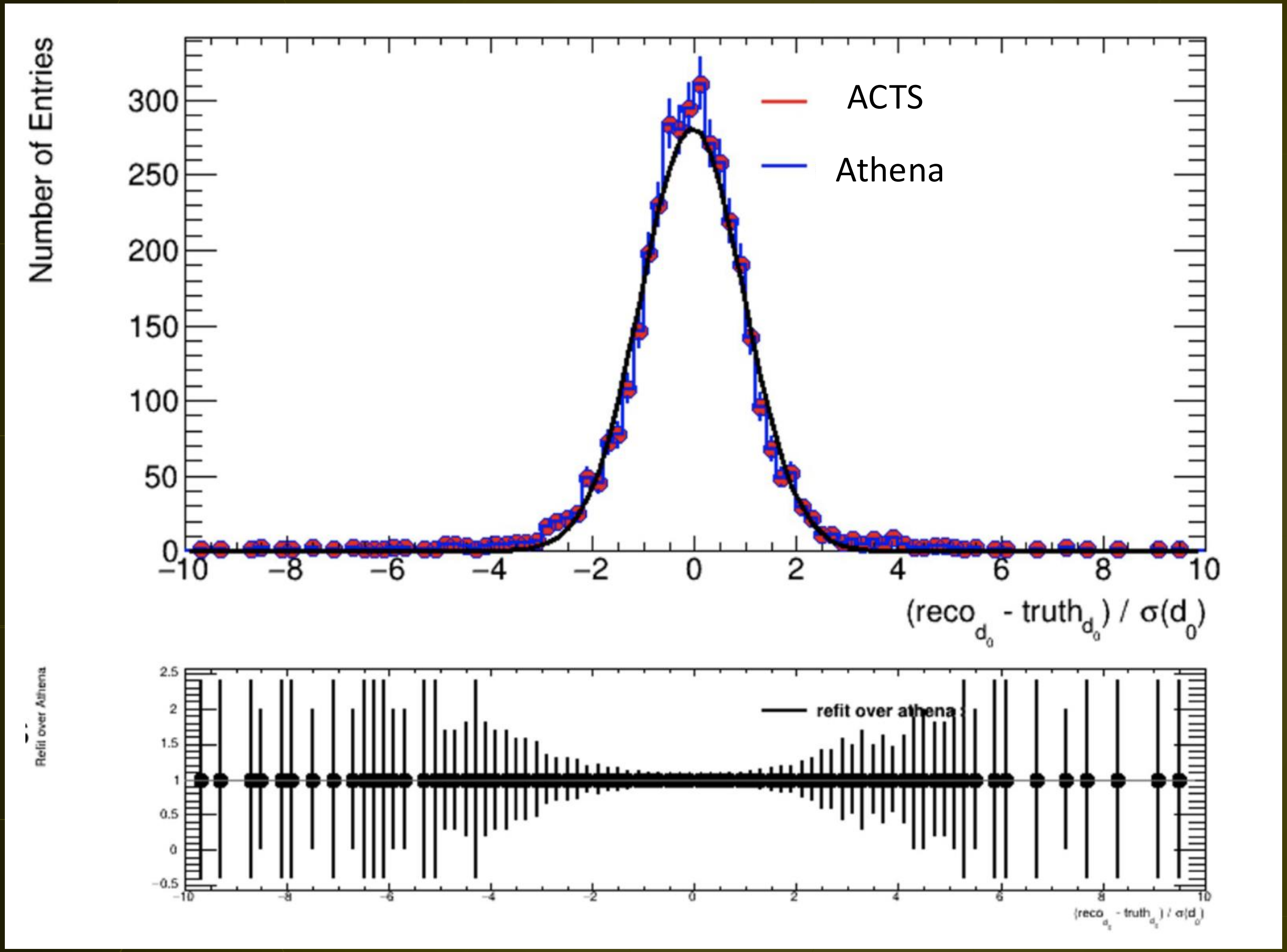

Histogram constructed from the file MuonPt100pull_d0

d_0 is a tracking parameter (~distance of the track to the primary vertex point)

This plot validates the working interface with ACTS.

.3 : The HL-LHC: My Qualification project (QP)

1

Qualification Project

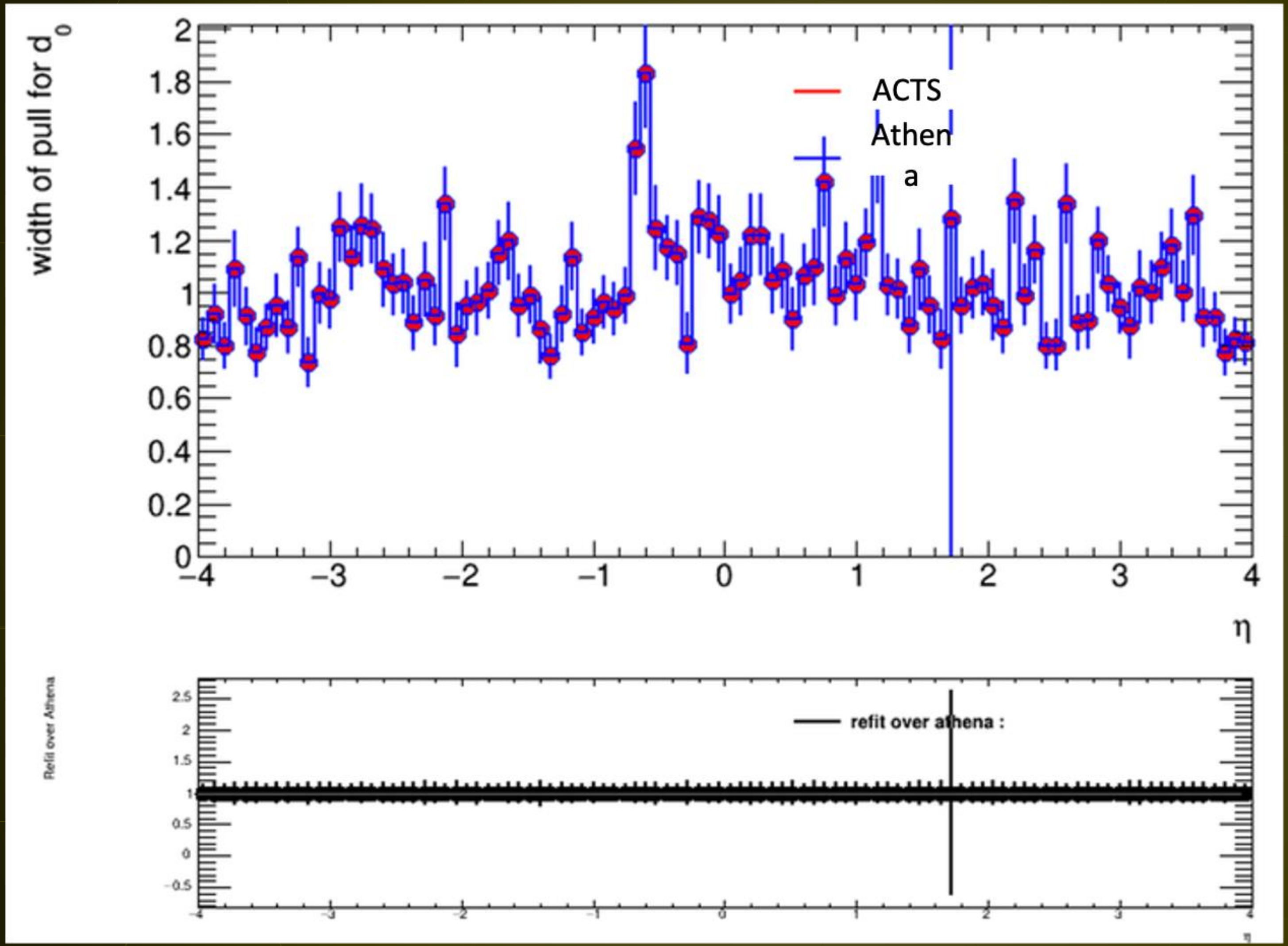

This plot validates the working interface with ACTS.

Histogram constructed from the file MuonPt100pullwidth_eta_vs_d0

.4 : Inside the ATLAS detector: General informations

ATLAS EXPERIMENT

ATLAS detector cross section

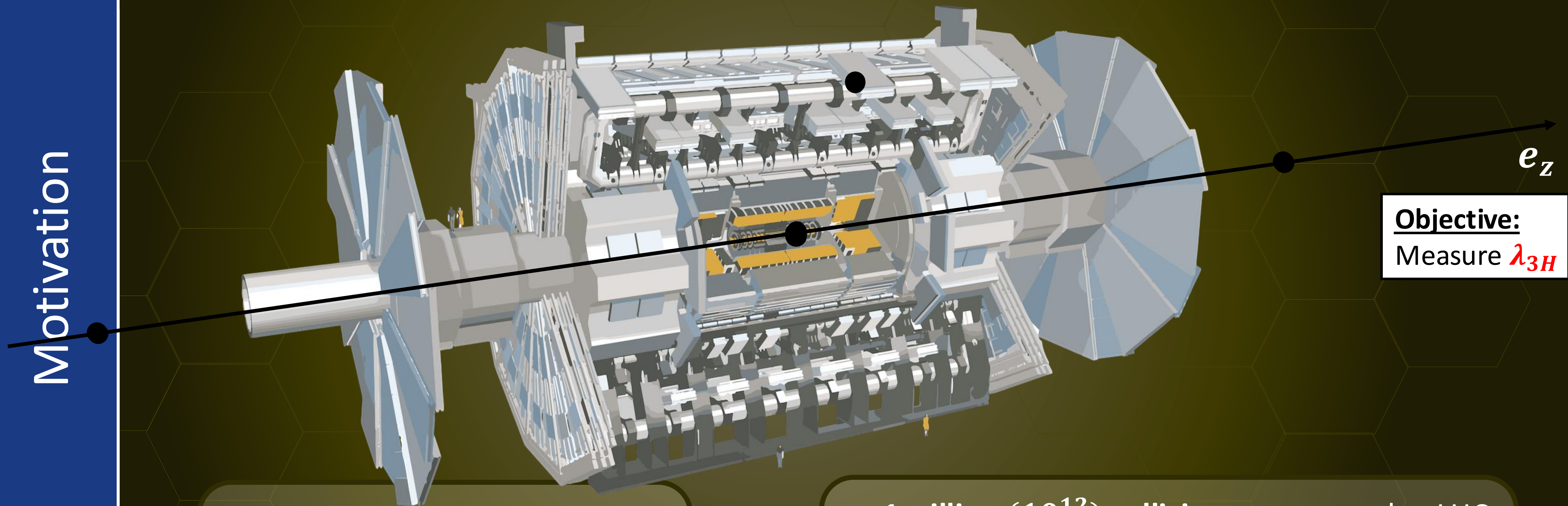

Objective:
Measure λ_{3H}

What we can measure:
- Angles: azimutal η , polar ϕ
- Energies: E,
- Transverse momentum: p_T

~ **1 trillion** (10^{12}) **collisions** per second at LHC (Run2).
Difficulty to isolate/measure/reconstruct trajectories and quantities precisely

.4 : Inside the ATLAS detector: The $b\bar{b}\gamma\gamma$ final state

Objective:
Measure λ_{3H}

Choice for the final state particles: a story about compromise

	bb	WW	ττ	ZZ	γγ
bb	34%				
WW	25%	4.6%			
ττ	7.3%	2.7%	0.39%		
ZZ	3.1%	1.1%	0.33%	0.069%	
γγ	0.26%	0.10%	0.028%	0.012%	0.0005%

Table of possible Di-Higgs decays combinations, and the associated relative percentage.

Excellent trigger & reconstruction efficiency.
High diphoton invariant mass resolution (1-2 GeV).

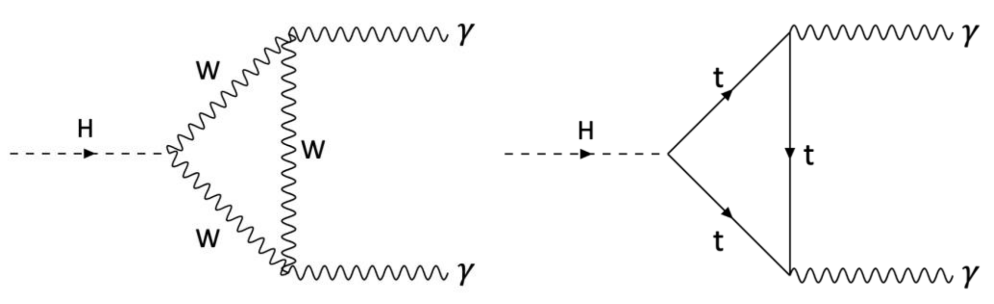

But very low branching ratio for Higgs decay (0.23%).

1

Motivation

.4 : Inside the ATLAS detector: The $b\bar{b}\gamma\gamma$ final state

Objective: Measure λ_{3H}

Choice for the final state particles: a story about compromise

	bb	WW	ττ	ZZ	γγ
bb	34%				
WW	25%	4.6%			
ττ	7.3%	2.7%	0.39%		
ZZ	3.1%	1.1%	0.33%	0.069%	
γγ	0.26%	0.10%	0.028%	0.012%	0.0005%

Table of possible Di-Higgs decays combinations, and the associated relative percentage.

Highest branching ratio (58%).

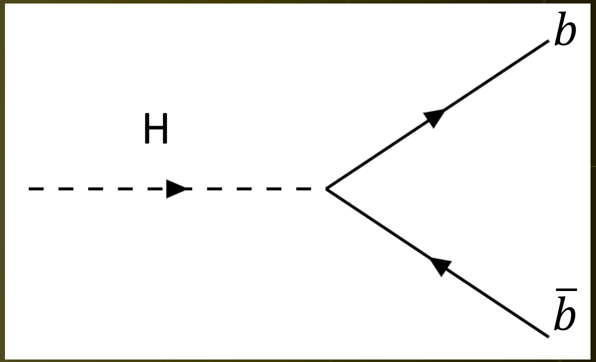

But huge QCD background (risk of confusion with surrounding generic jets);
+ b-tagging limitations (risk of mistag);
+ poorer energy resolution for jets.

.4 : Inside the ATLAS detector: The $b\bar{b}\gamma\gamma$ final state

ATLAS EXPERIMENT

Objective:
Measure λ_{3H}

Choice for the final state particles: a story about compromise

	bb	WW	ττ	ZZ	γγ
bb	34%				
WW	25%	4.6%			
ττ	7.3%	2.7%	0.39%		
ZZ	3.1%	1.1%	0.33%	0.069%	
γγ	0.26%	0.10%	0.028%	0.012%	0.0005%

Table of possible Di-Higgs decays combinations, and the associated relative percentage.

$b\bar{b}$ + $\gamma\gamma$

.4 : Inside the ATLAS detector: Collision

ATLAS EXPERIMENT

ATLAS detector cross section

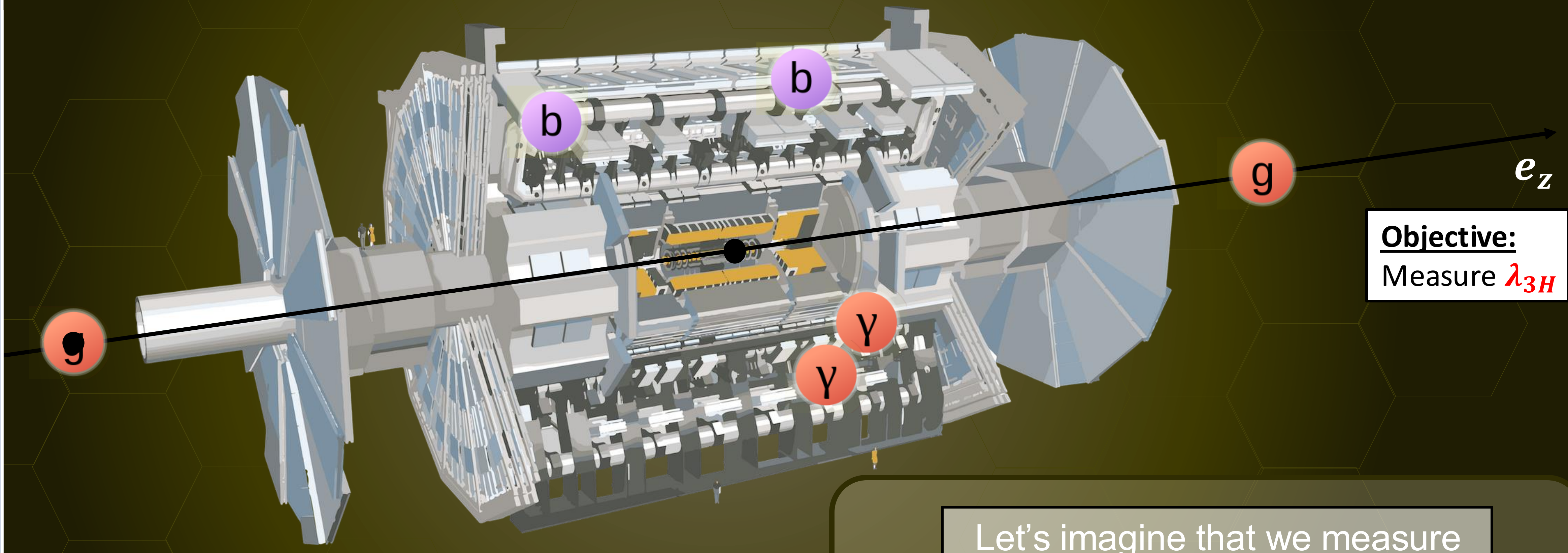

Objective:
Measure λ_{3H}

Let's imagine that we measure
$gg \to \cdots \to b\bar{b}\gamma\gamma$.
What to do next?

.4 : Inside the ATLAS detector: Understanding collisions

Signal **gluon fusion ggF**
Feynman diagram

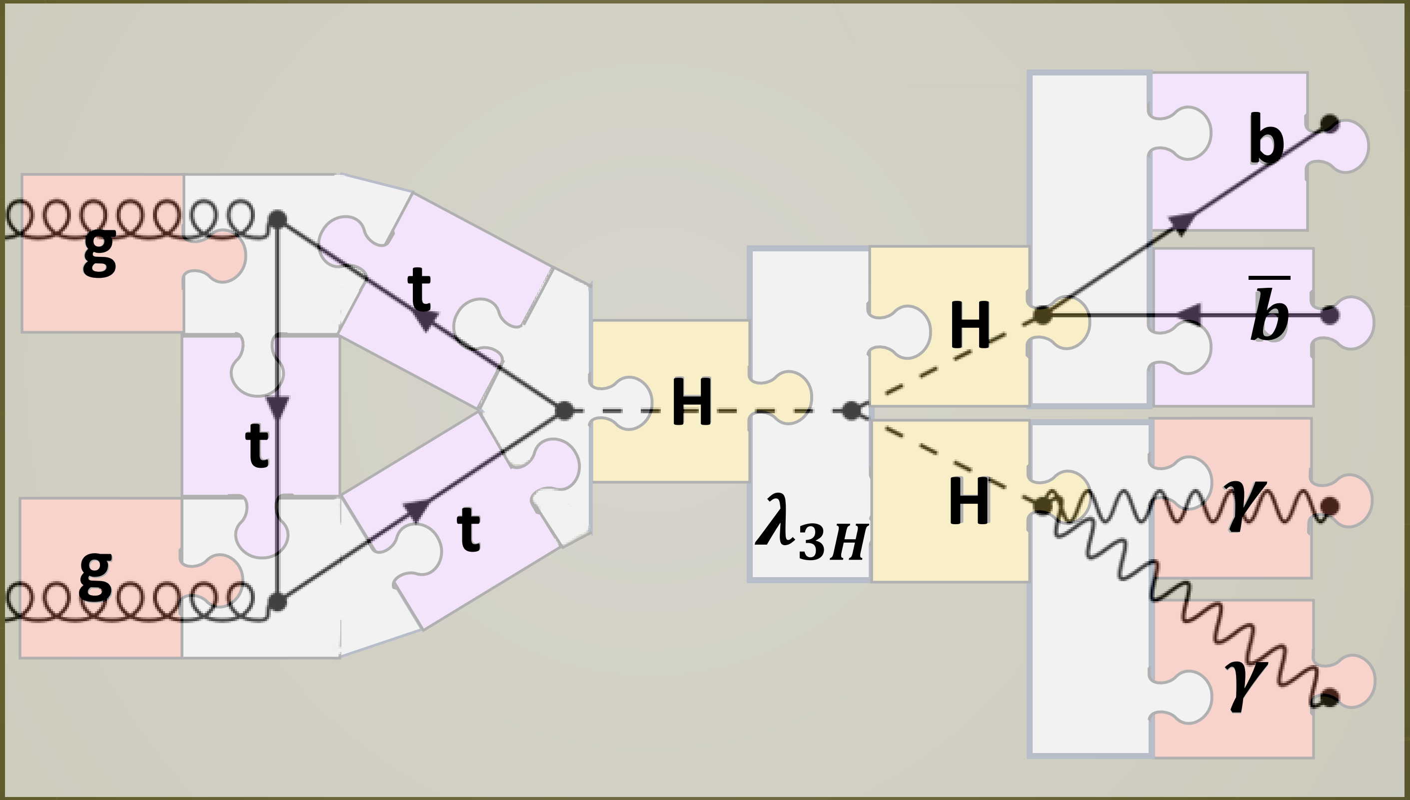

Objective:
Measure λ_{3H}

Motivation

1

.4 : Inside the ATLAS detector: Signal cross-section σ

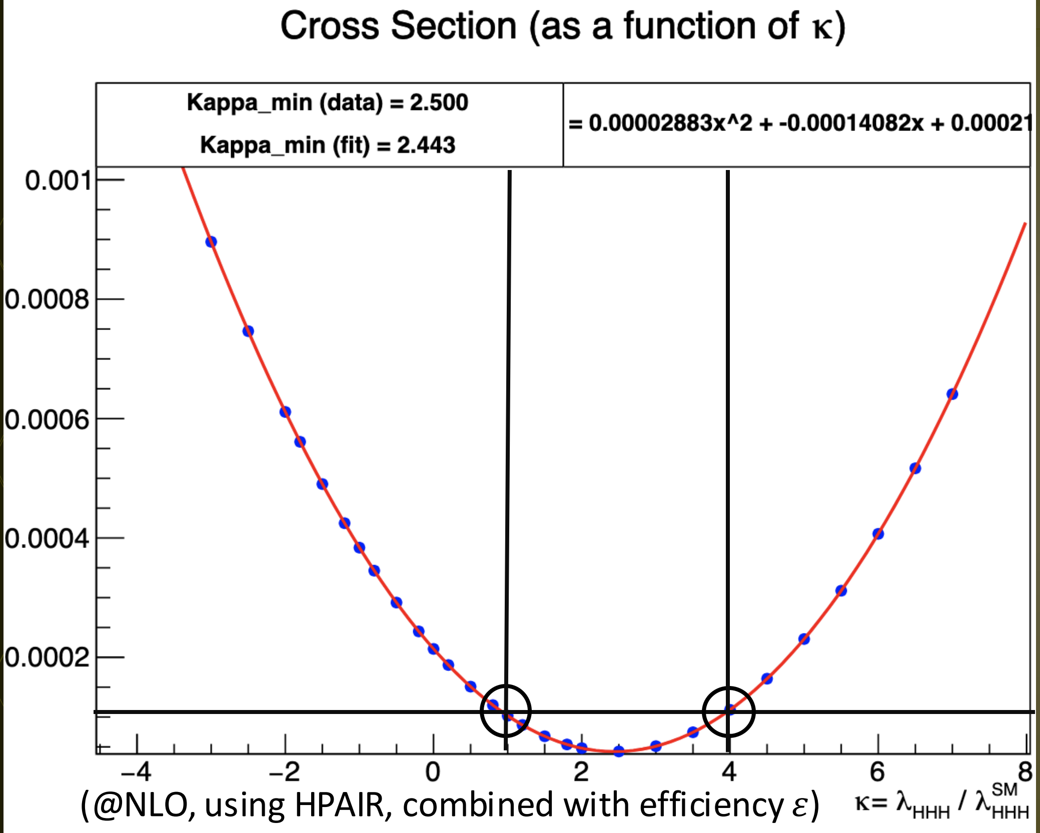

The signal cross section has very strong dependence on κ_λ. It is used in many analysis methods (like « Event counting methods »).

$-1.2 < \lambda_{obs}/\lambda_{SM} < 7.2$ [ATLAS '24]

$-1.4 < \lambda_{obs}/\lambda_{SM} < 7.0$ [CMS '24]

$-1.7 < \lambda_{\mathrm{obs}}/\lambda_{\mathrm{SM}} < 6.6$ [ATLAS $HH \to b\bar{b}\gamma\gamma$ '25]

Analysis method: Boosted Decision Trees (BDTs): machine learning (ML) algorithms.

.5 : Inside the ATLAS detector: Understanding collisions

Signal **ggF** 0.05%

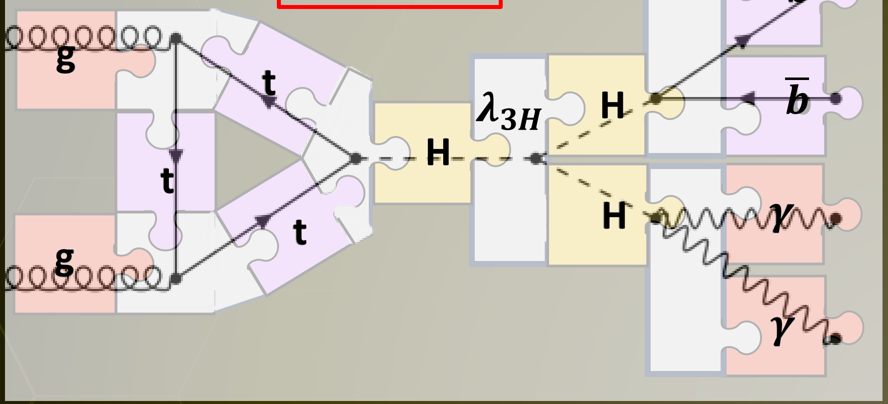

Process	LO σ [pb]
signal ggF ($\kappa_\lambda = 1.00$)	0.01983
$t\bar{t}H$	0.349
QCD $b\bar{b}\gamma\gamma$	0.05969449
Single-Higgs	0.1038

Cross-sections* σ (at LO)

Decay mode	*BR* Value
$H \to b\bar{b}$	0.5796
$H \to \gamma\gamma$	2.276×10^{-3}
$t \to Wb$	0.988

Branching ratios *BR*

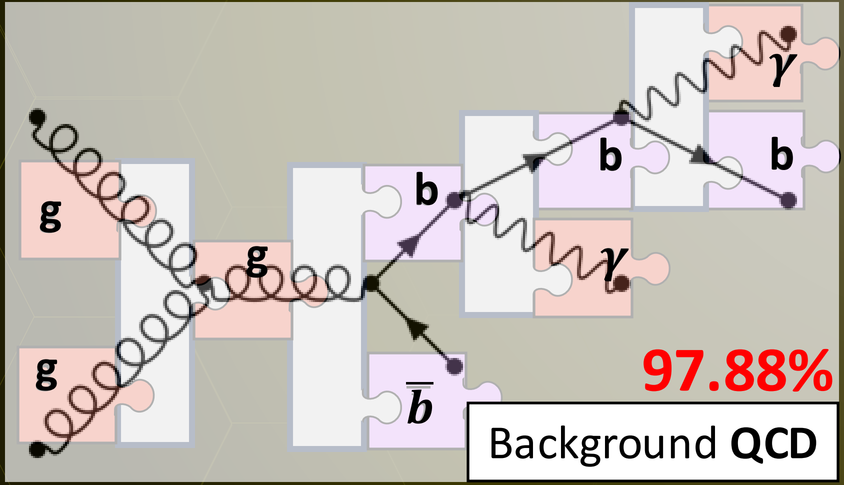

97.88%

Background **QCD**

Background **ttH**

1.6%

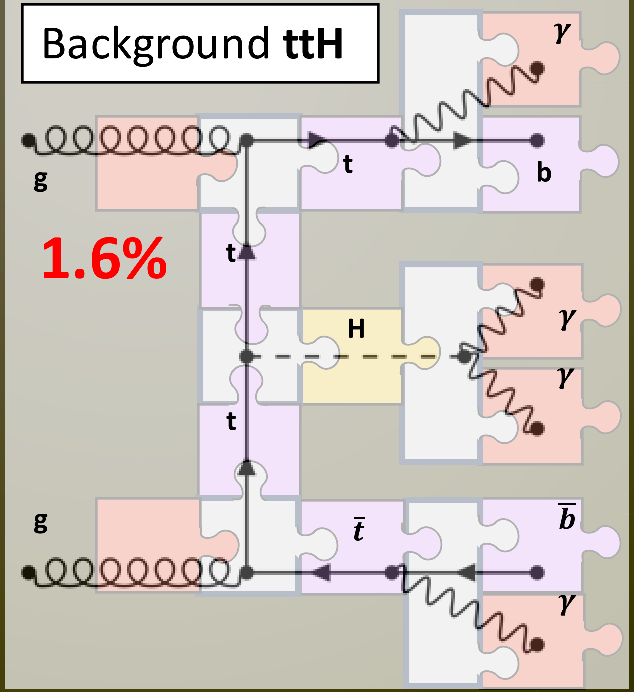

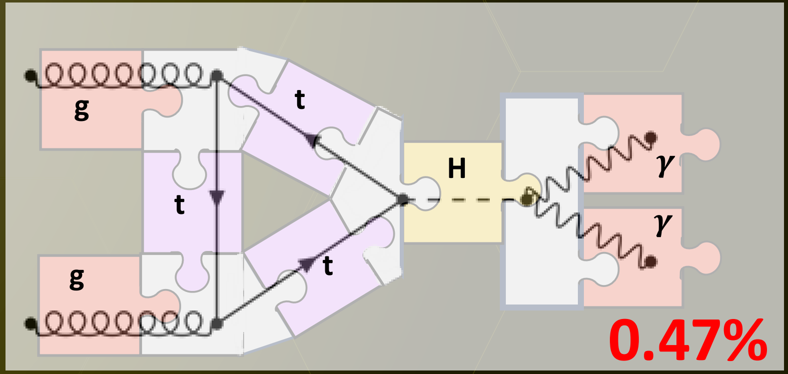

0.47%

Background **singleHiggs**

How can we overcome these challenges in order to measure λ_{3H} ?

2.1 : The Matrix Element Framework

The Matrix Element Method

<u>By definition</u>: [The MEM] statistically optimal multivariate method that maximizes both the experimental and theoretical information available to an analysis, with **minimal cuts on the data.**

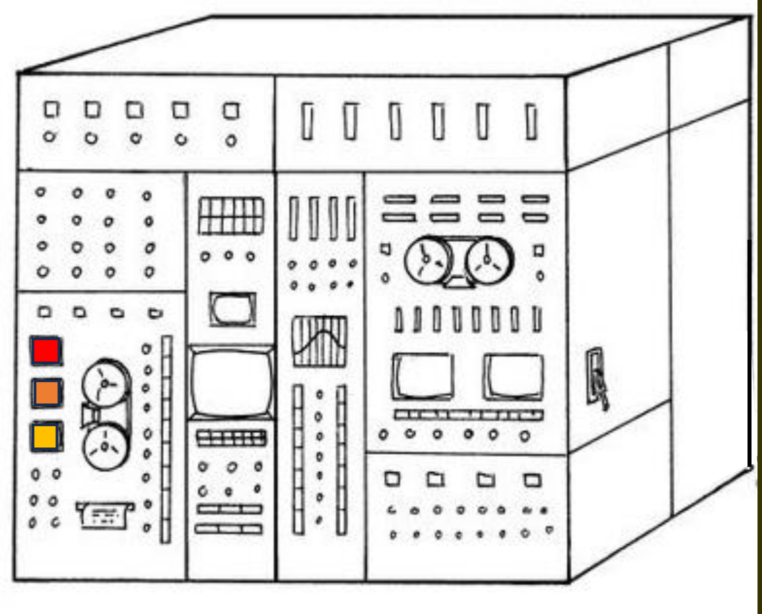

It computes a Likelihood $\mathcal{L}(\mathbf{h},\mathbf{x})$),
to observe an event **x** under the hypothesis **h**

$$\mathcal{L}^{P}_{process}(\mathbf{h}|\boldsymbol{x}^i) = \frac{d\sigma_P(pp \to \boldsymbol{x}^i; \mathbf{h}, W)}{\sigma^{obs}(pp \to F)}$$

$$\mathcal{L}^{\mathrm{p}}_{\mathrm{process}}(\mathbf{h}|\mathbf{x}^i) = \frac{1}{\sigma^{obs}_p(pp \to F)} \int_{\mathbf{y}} d\sigma_p(pp \to y; \mathbf{h}) W(\mathbf{y}, \mathbf{x}^i)$$

$$\mathcal{L}^{P}_{process}(\mathbf{h}|\boldsymbol{x}^i) = \frac{(2\pi)^4}{\sigma^{obs}_P(pp \to F)} \int_{\mathbf{y},q_1,q_2} \sum_{a_1,a_2} f_{a1}(q_1) f_{a1}(q_2) \frac{|\mathrm{M}_P(a_1a_2 \to \mathbf{y}; \mathbf{h}|^2}{q_1q_2s} W(\mathbf{y},\boldsymbol{x}^i)\delta\left(a_1 + a_2 - \sum_{j=1}^{n} y_i\right) dq_1\, dq_2 d^{4n}\mathbf{y}$$

.1 : The Matrix Element Framework

Observed events $\boldsymbol{x}^i$

Matrix element M_P

Transfer function W

$$\mathcal{L}^P_{process}\left(\mathbf{h}\middle|\boldsymbol{x}^i\right) =$$

$$\frac{(2\pi)^4}{\sigma_P^{obs}(pp \to F)} \int_{\mathbf{y},q_1,q_2} \sum_{a_1,a_2} f_{a1}(q_1) f_{a1}(q_2) \frac{|\mathrm{M}_P(a_1 a_2 \to \mathbf{y};\mathbf{h}|^2}{q_1 q_2 s} W(\mathbf{y},\boldsymbol{x}^i)\delta\left(a_1 + a_2 - \sum_{j=1}^{n} y_i\right) dq_1\, dq_2 d^{4n}\mathbf{y}$$

Total cross section for process P σ_P^{obs}

Parton density functions f

Legend:
: the experimental inputs
: the theoretical inputs

Given a fixed reconstructed event $\boldsymbol{x}^i$, we integrate over all the possible configurations of events $\boldsymbol{y}$ that could be measured as $\boldsymbol{x}^i$ by the detector.

➔ Idea: To search for $\boldsymbol{h}$ that maximizes $\mathcal{L}$

➔ hypothesis h can be: λ_{3H} value

.2 : The Matrix Element Framework: Pre-selection

Pre-selection and cuts: **minimal** (thanks to the MEM), respecting ATLAS conventions.

Used for our analysis:

Kinematic and angular selection criteria

- **Photon kinematic cuts**
  - $p_T^{\gamma\text{lead}} > 35$ GeV, $p_T^{\gamma\text{sub}} > 25$ GeV
  - $|\eta_\gamma| < 1.37$ or $1.52 < |\eta_\gamma| < 2.37$
  - $120 \text{ GeV} < m_{\gamma\gamma} < 130$ GeV
  - $p_T^{\gamma\text{lead}} > 0.35\, m_{\gamma\gamma}$, $p_T^{\gamma\text{sub}} > 0.25\, m_{\gamma\gamma}$
- ***b*-jet kinematic cuts**
  - $p_T^b > 25$ GeV
  - $|\eta_b| < 2.5$
- **Angular separations**
  - $\Delta R(\gamma,\gamma) > 0.2$
  - $\Delta R(\gamma,b) > 0.2$
  - $\Delta R(b,b) > 0.4$
  - $\Delta R(\text{rad},\gamma) > 0.2$

assuming we first managed to produced samples with $b\bar{b}\gamma\gamma$ final state.

Important distinction:

Observed events $\boldsymbol{x}^i$
(LO or NLO)

Matrix element M_P
(LO or NLO)

$$\mathcal{L}^P_{process}\left(\mathbf{h}\middle|\boldsymbol{x}^i\right) =$$

$$\frac{(2\pi)^4}{\sigma_P^{obs}(pp\to F)}\int_{\mathbf{y},q_1,q_2}\sum_{a_1,a_2} f_{a1}(q_1)f_{a1}(q_2)\frac{|\mathrm{M}_P(a_1a_2\to\mathbf{y};\mathbf{h}|^2}{q_1q_2s}W(\mathbf{y},\boldsymbol{x}^i)\delta\left(a_1+a_2-\sum_{j=1}^{n}y_i\right)dq_1\,dq_2d^{4n}\mathbf{y}$$

Important distinction:

Observed events $\boldsymbol{x^i}$
(LO or NLO)

Matrix element M_P
(LO or NLO)

Monte Carlo Events:
Can be **generated** at different orders (using softwares like MadGraph or POWHEG-BOX-V2).

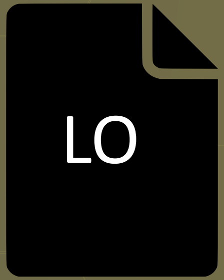

Generated events, at Leading Order (LO)

Generated events, at Next-to-Leading Order (NLO)

Matrix Element Method [MEM] **analysis** :
The order of the Matrix Element **inside the integral**, using Feynman rules.

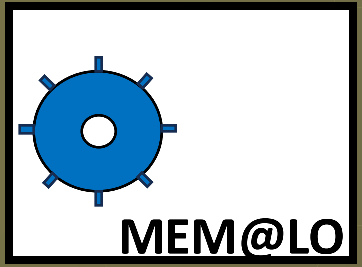

Matrix Element Method at Leading Order (MEM@LO)

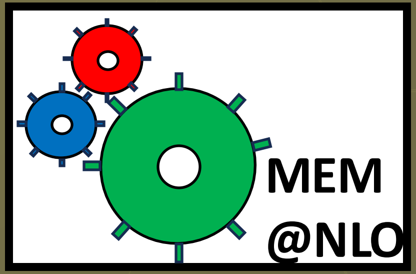

Matrix Element Method at Next-to-Leading Order (MEM@NLO)

Important distinction:

Legacy work [2019] (F.Eble, J.Stark)

Our analysis [2022 -> 2025]

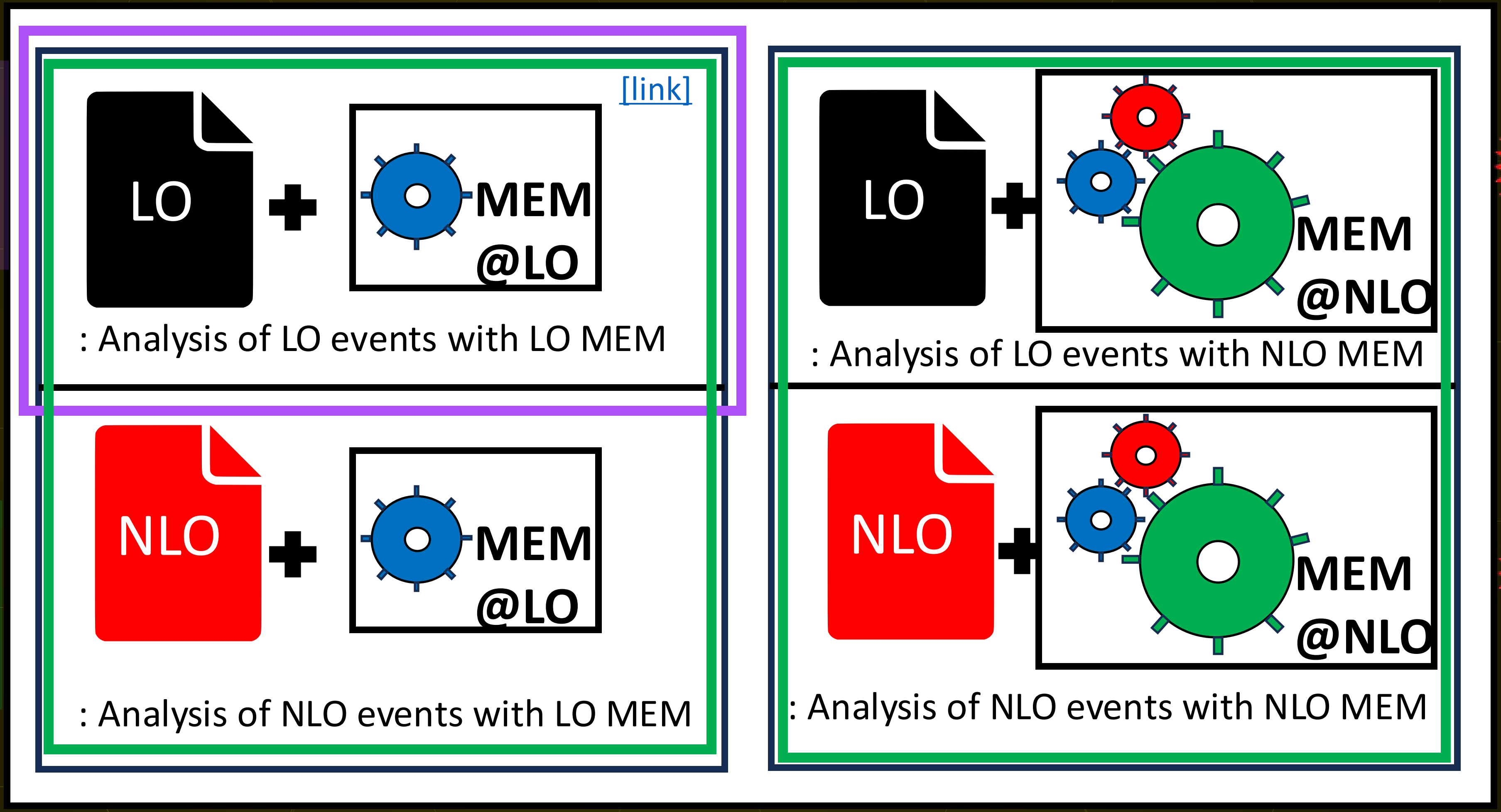

.3 : Legacy work for $b\bar{b}\gamma\gamma$ at Leading Order (LO)

General setup:

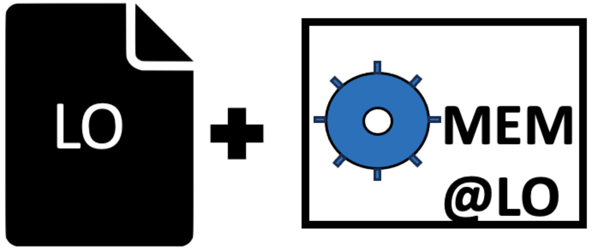

: Analysis of LO events with LO MEM

Using **MadGraph** software (MG5@NLO)

1. Computes cross-sections σ (here at LO)
2. Produce MC generated event files.

MEM integration:
using **MoMEMta** software.
MoMEMTa is a C++/Python software offering great flexibility, which separates the core components of the Matrix Element Method.

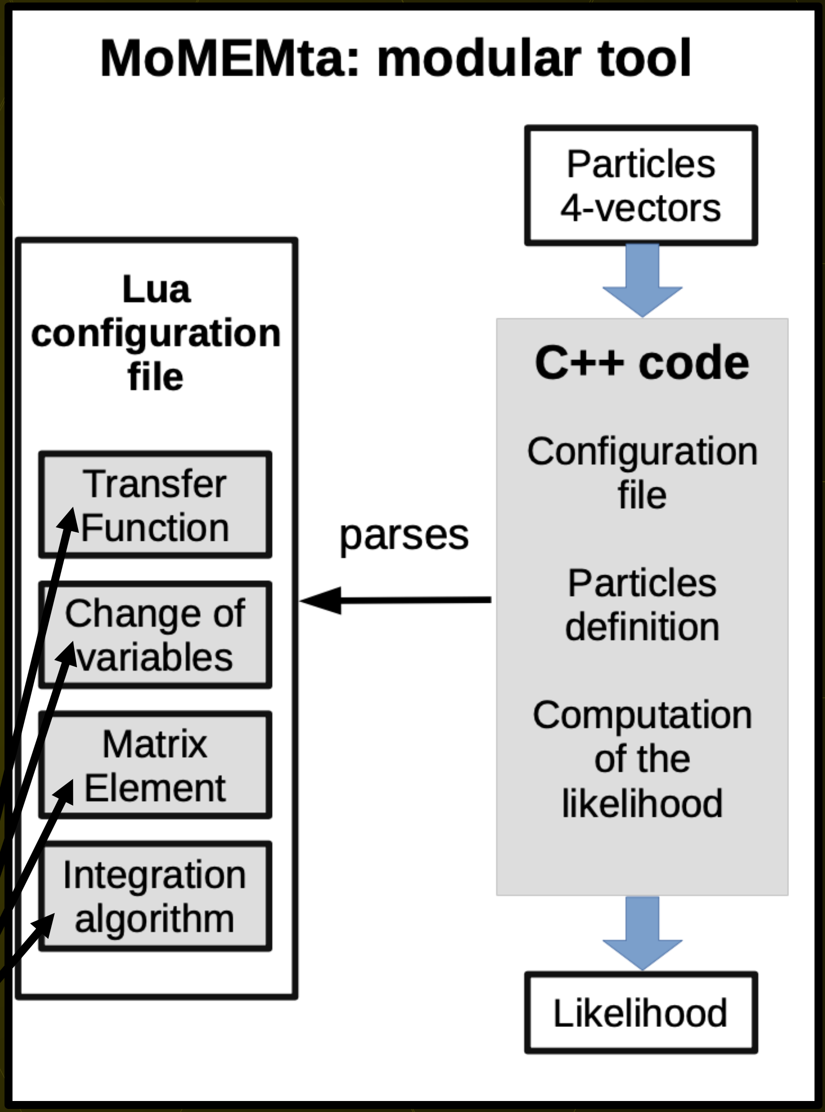

Picture taken from [legacy article]

Analysis tool: ROC

The Matrix Element Method

2

Evaluating methods discrimination power: ROC or rejection curves

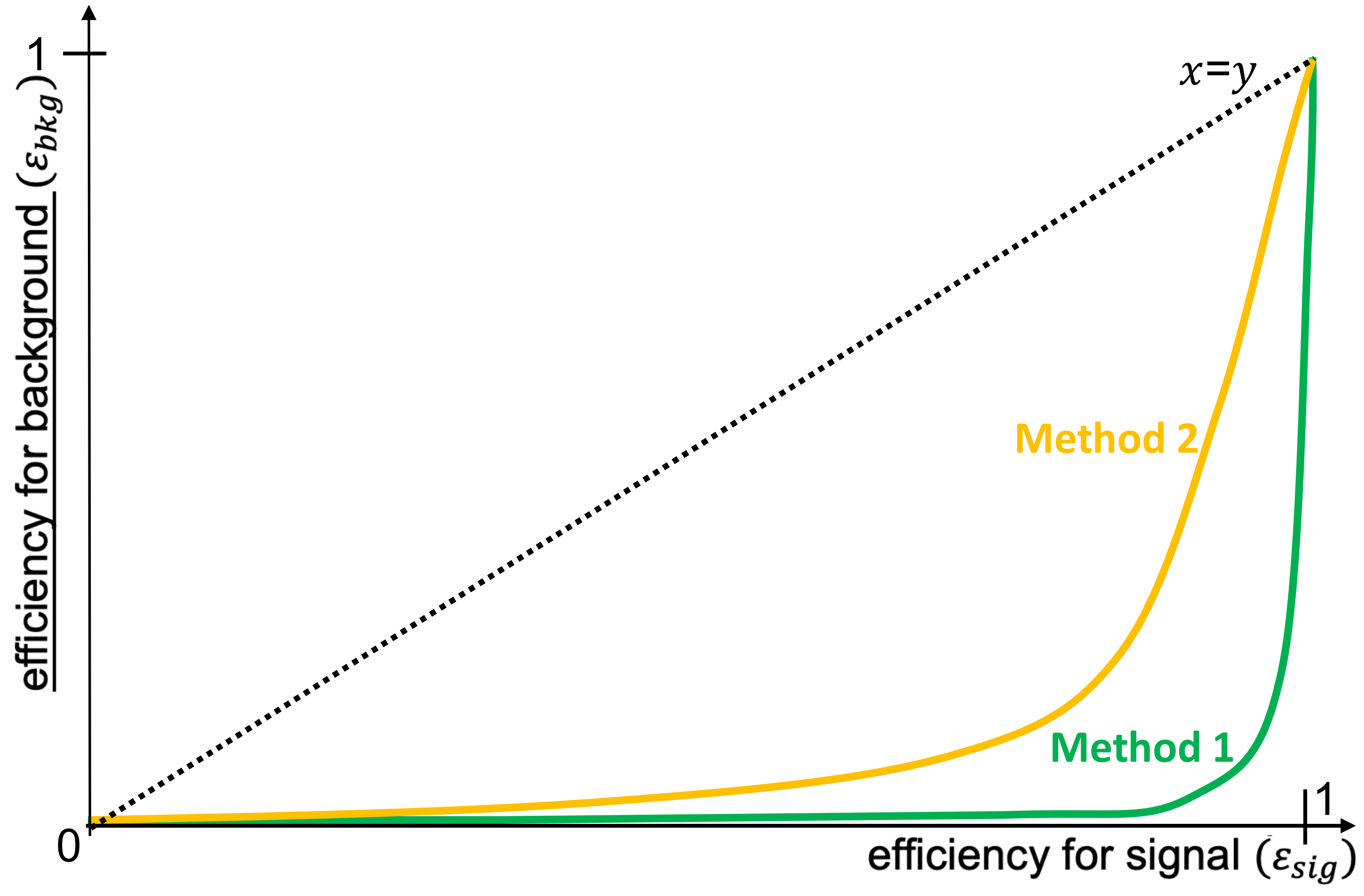

ROC "Receiver Operating Characteristics"

Graphical representation that illustrates performance of methods discrimination efficiency (signal VS background).

Given our conventions (cf. following slides) the closer the curve is to the bottom right corner, the better its discrimination power!

Analysis tool: ROC

Evaluating methods discrimination power: ROC or rejection curves

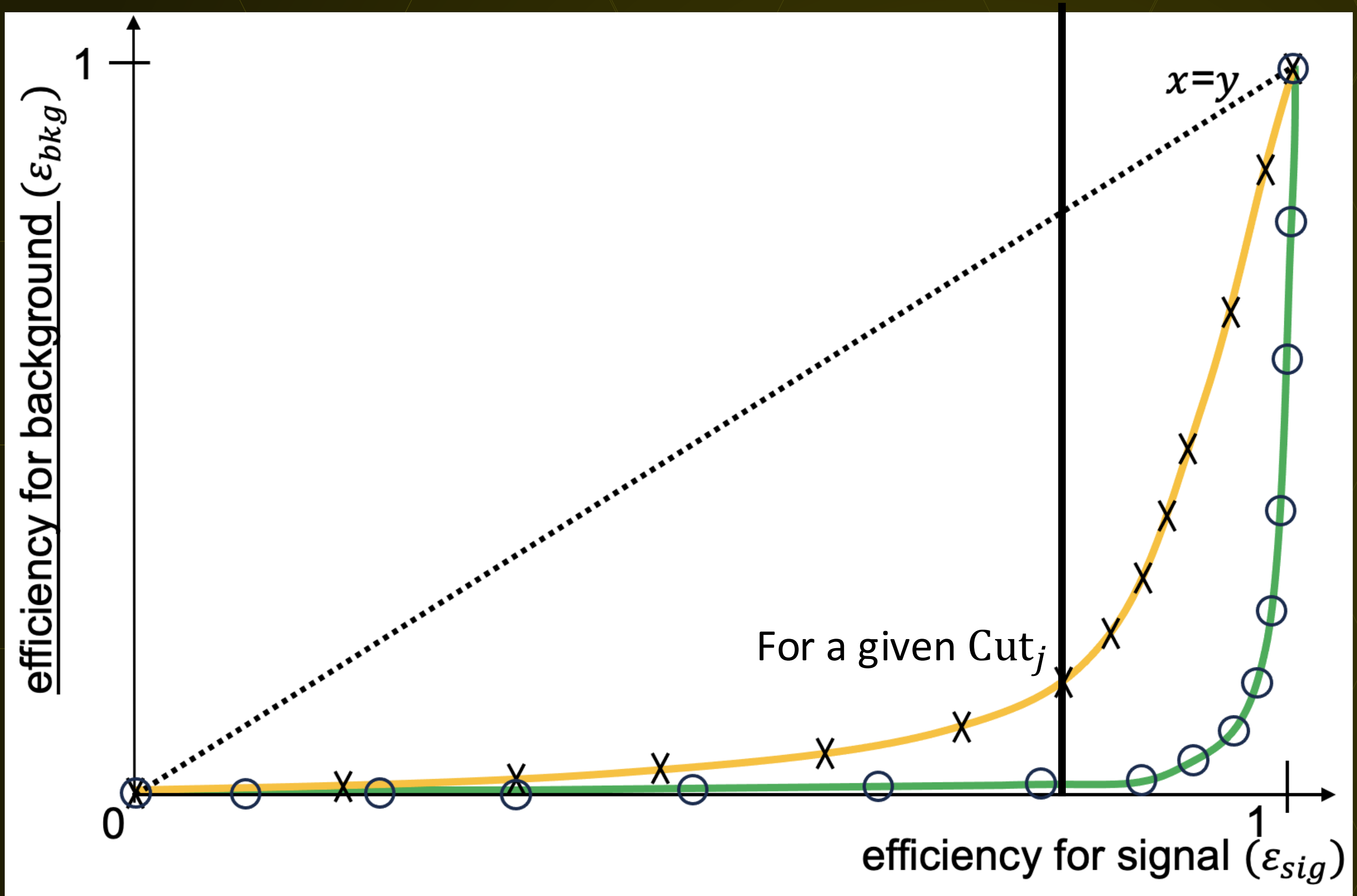

Graphical representation that illustrates performance of methods discrimination efficiency (signal VS background).

$\mathrm{Cut}_j \in [\mathbf{0}; \infty]$

If data $\boldsymbol{x}^i$ is signal: position of the point on the X-axis

Analysis tool: ROC

Evaluating methods discrimination power: ROC or rejection curves

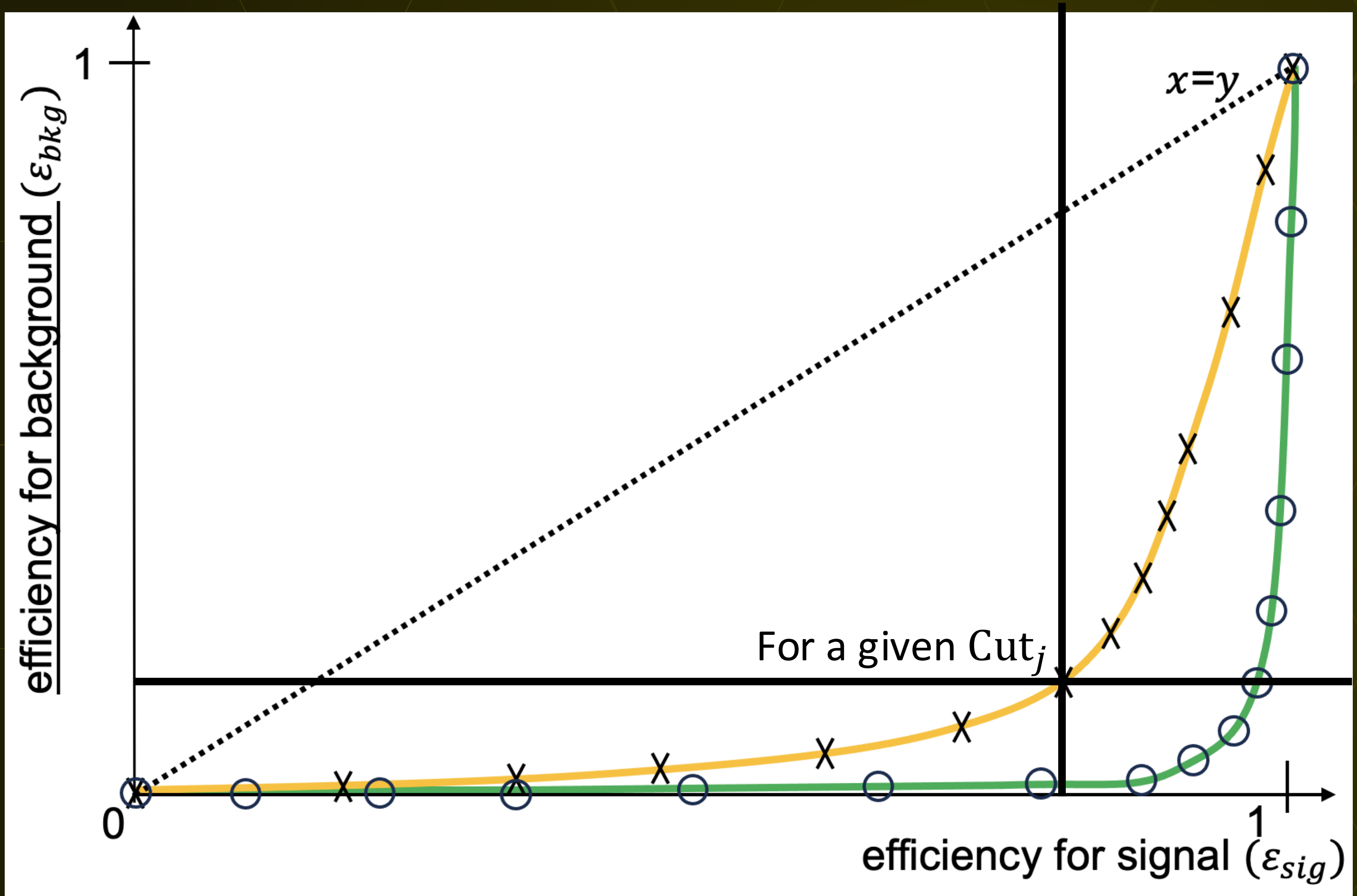

Graphical representation that illustrates performance of methods discrimination efficiency (signal VS background).

$\mathrm{Cut}_j \in [\mathbf{0}; \infty]$

If data x^i is signal: position of the point on the X-axis

Analysis tool: ROC

Evaluating methods discrimination power: ROC or rejection curves

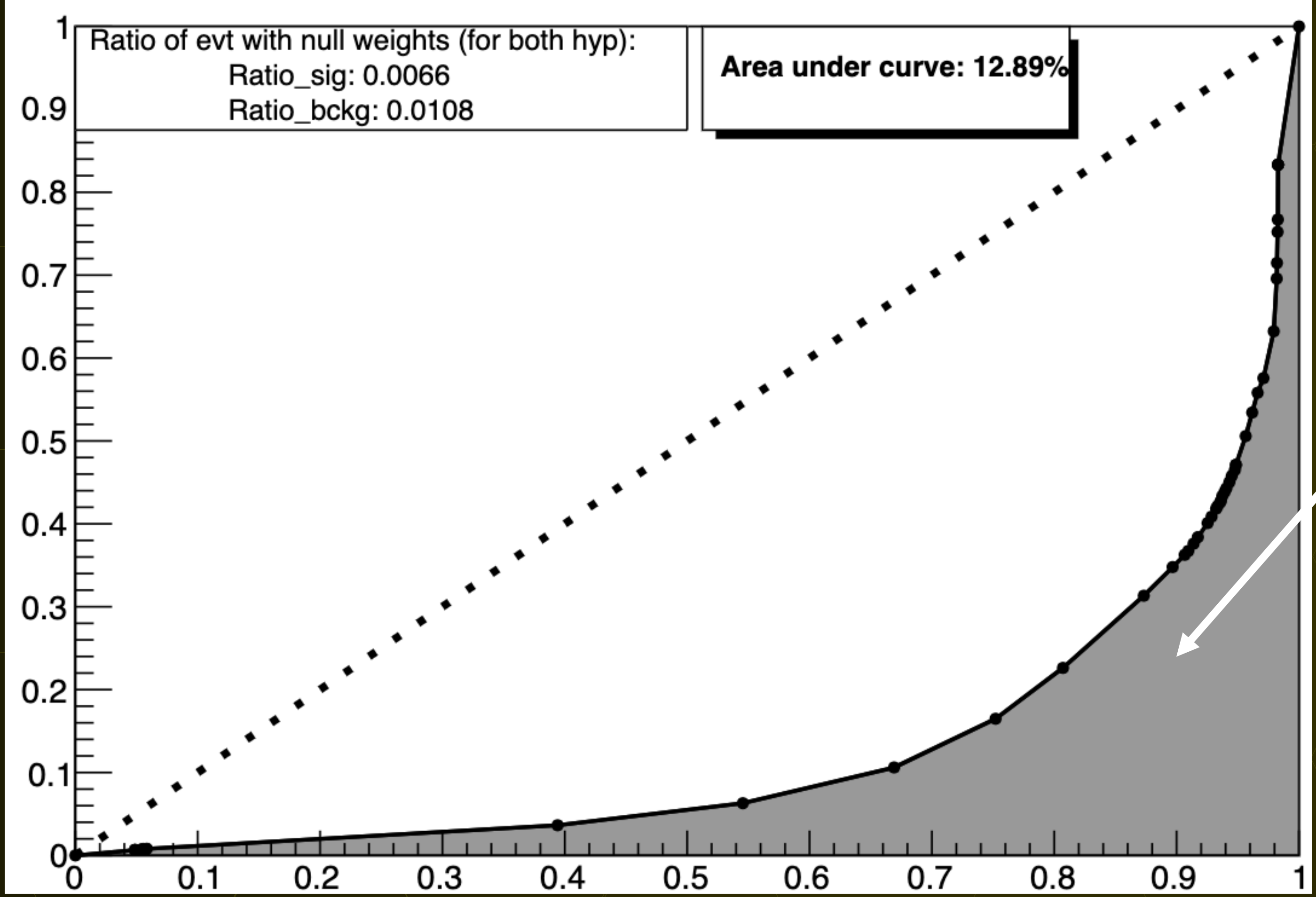

We can measure the Area Under Curve (AUC) (expressed it as a percentage)

Very helpful to quantify the method's power of discrimination.

.3 : Legacy work for $b\bar{b}\gamma\gamma$ at Leading Order (LO)

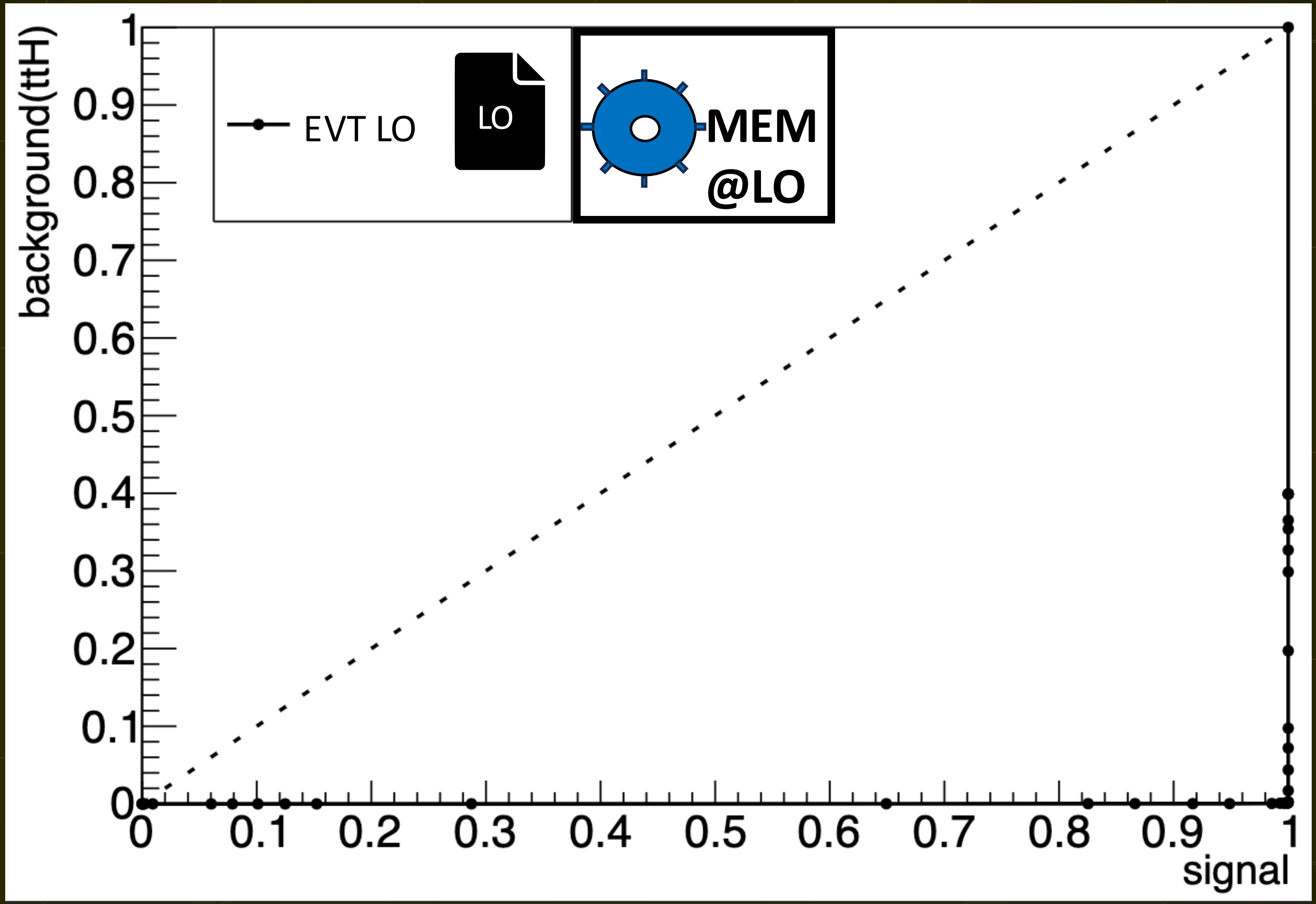

ROC curve to reproduce the Legacy work at LO.
Datasets, MEM@LO, and ROC plotting macro have been **built independently from Legacy analysis, from ground up**.

.3 : Legacy work for $b\bar{b}\gamma\gamma$ at Leading Order (LO)

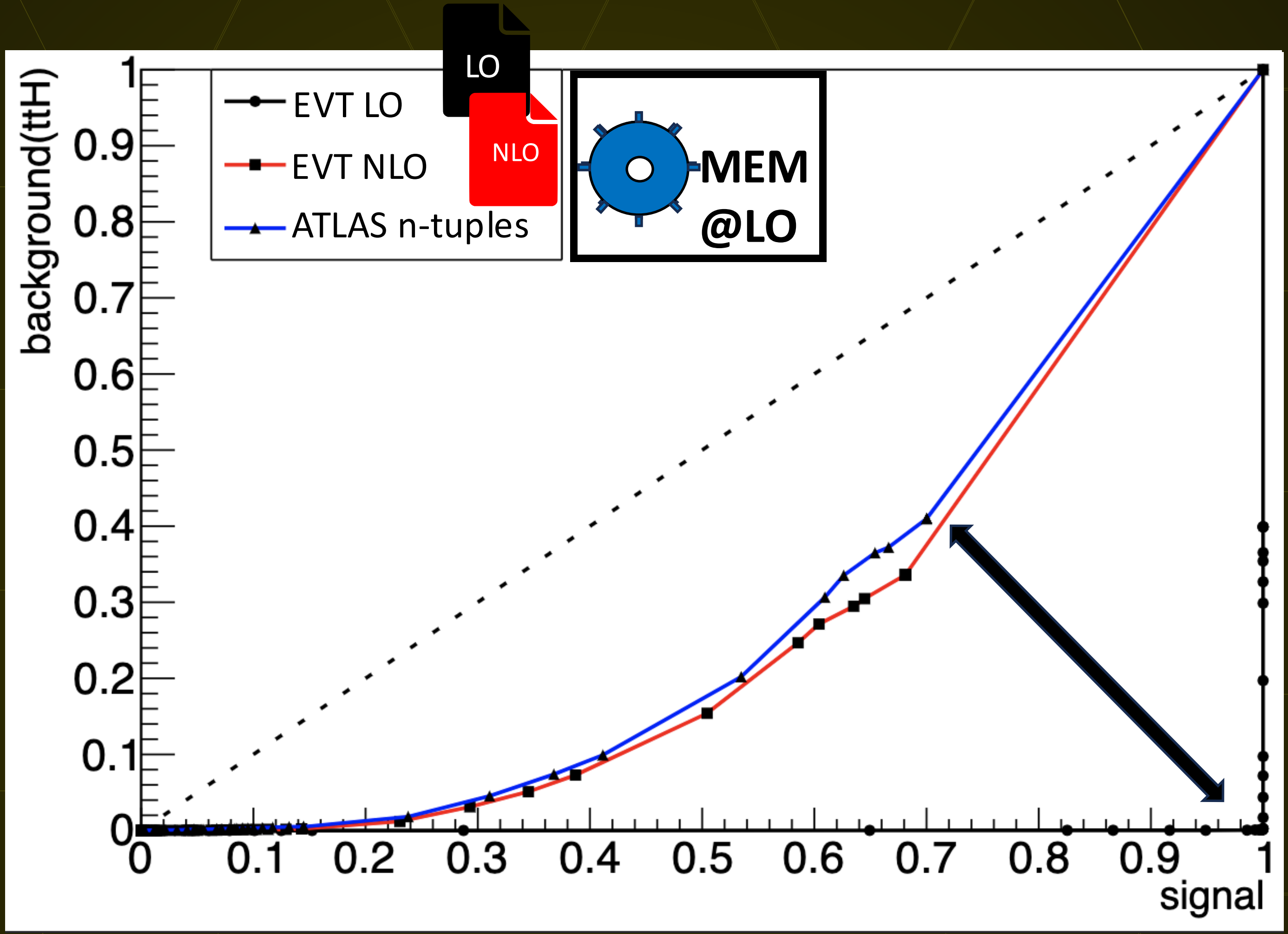

Motivates the need to construct a MEM@NLO to work on more physically accurate events.

ROC curves with the addition of new datasets: NLO MC generated events, and ATLAS n-tuples (MC generated events by the ATLAS Collaboration)

.4 : Developing a MEM@NLO

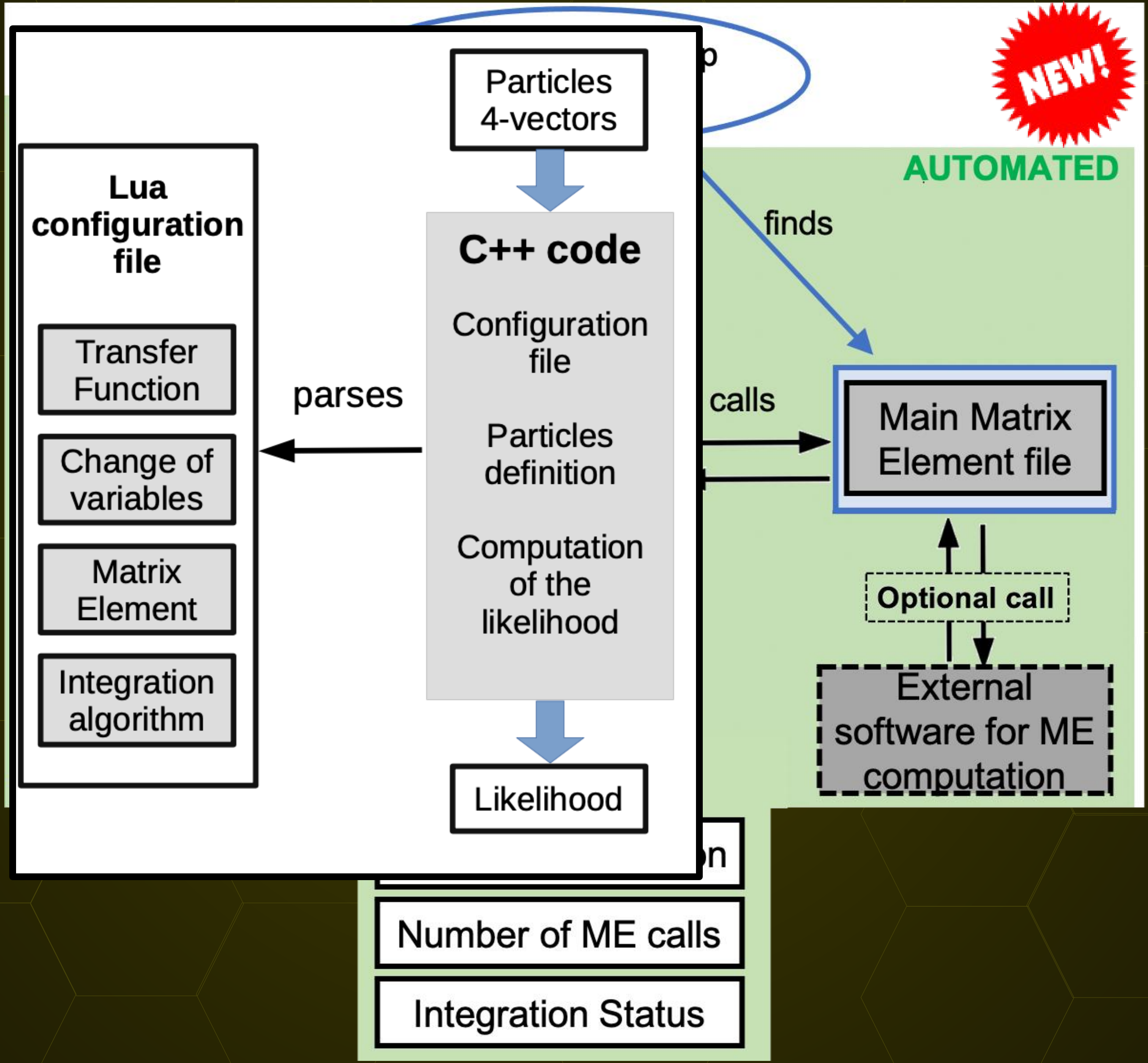

New implementation of the MEM inside MoMEMta: our MEM@NLO

2.4 : Developing a MEM@NLO

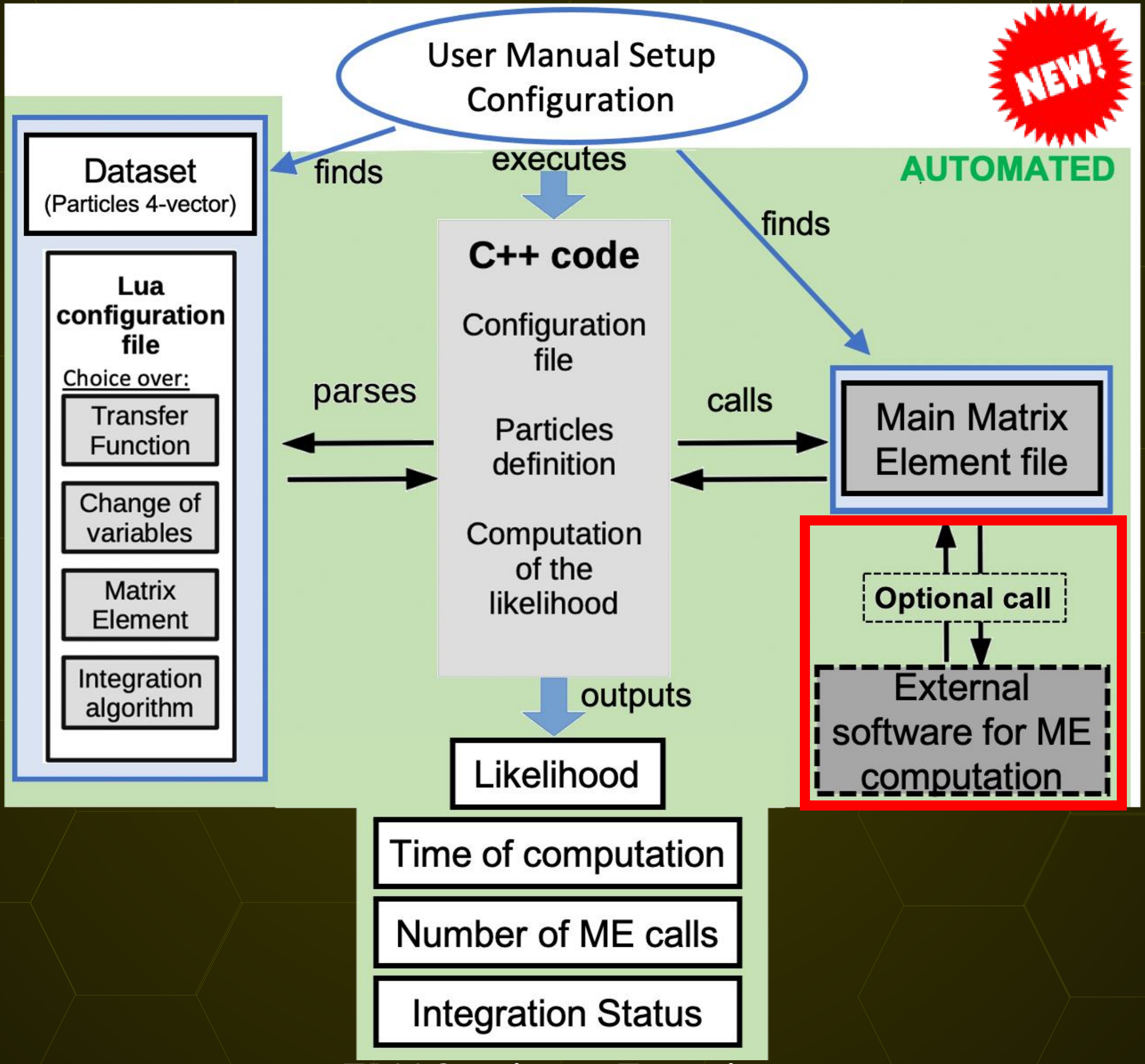

New implementation of the MEM inside MoMEMta: our MEM@NLO

Why do we need that?

Theoretical computation for NLO ME are extremely complicated.
Not possible with MadGraph for now.

.4 : Developing a MEM@NLO: Interface with POWHEG-BOX-V2

The POWHEG-BOX-V2 software

POWHEG-BOX-V2 framework plays a crucial role in particle physics analysis.

1. Cross-section calculation: fully differential NLO (or more) through numerical integration. All the different subprocess included in POWHEG-BOX-V2 share the same structure.

2. Event generation: production of NLO events (with parton showering)

Extremely usefull to the HEP community. And to us!

…Yet, it is not MEM friendly.

POWHEG-BOX-V2 is not made to allow the user to access the matrix elements and have full control over the phase-space evaluated.

.4 : Developing a MEM@NLO: Interface with POWHEG-BOX-V2

The POWHEG-BOX-V2 software

POWHEG-BOX-V2 framework plays a crucial role in particle physics analysis.

1. Cross-section calculation: fully differential NLO (or more) through numerical integration. All the different subprocess included in POWHEG-BOX-V2 share the same structure.

2. Event generation: production of NLO events (with parton showering)

Extremely usefull to the HEP community. And to us!

...Yet, it is not MEM friendly.

POWHEG-BOX-V2 is not made to allow the user to access the matrix elements and have full control over the phase-space evaluated.

.4 : Developing a MEM@NLO: Interface with POWHEG-BOX-V2

The POWHEG-BOX-V2 software

Understanding in great detail how the POWHEG-BOX-V2 work:

Main “issues”:

- Extremely well optimized.
- Extensive documentation (time consuming).
- A lot of programing languages used: python, C++, fortran (both .f and .f90), and shell scripting.
- Need to understand how every part work and how they are used by the others.

Some parts are meant to fit the POWHEG main purposes.
If taken separetly, need modifications!

.4 : Developing a MEM@NLO: Interface with POWHEG-BOX-V2

The POWHEG-BOX-V2 software

Understanding in great detail how the POWHEG-BOX-V2 work:

Main “issues”:

- Extremely well optimized.
- Extensive documentation (time consuming).
- A lot of programing languages used: python, C++, fortran (both .f and .f90), and shell scripting.
- Need to understand how every part work and how they are used by the others.

.4 : Developing a MEM@NLO: Interface with POWHEG-BOX-V2

The POWHEG-BOX-V2 software

Testing the new implementation :

First consider the LO contribution from POWHEG-BOX-V2, and compare to existing LO matrix elements from MadGraph (MG5@MC)

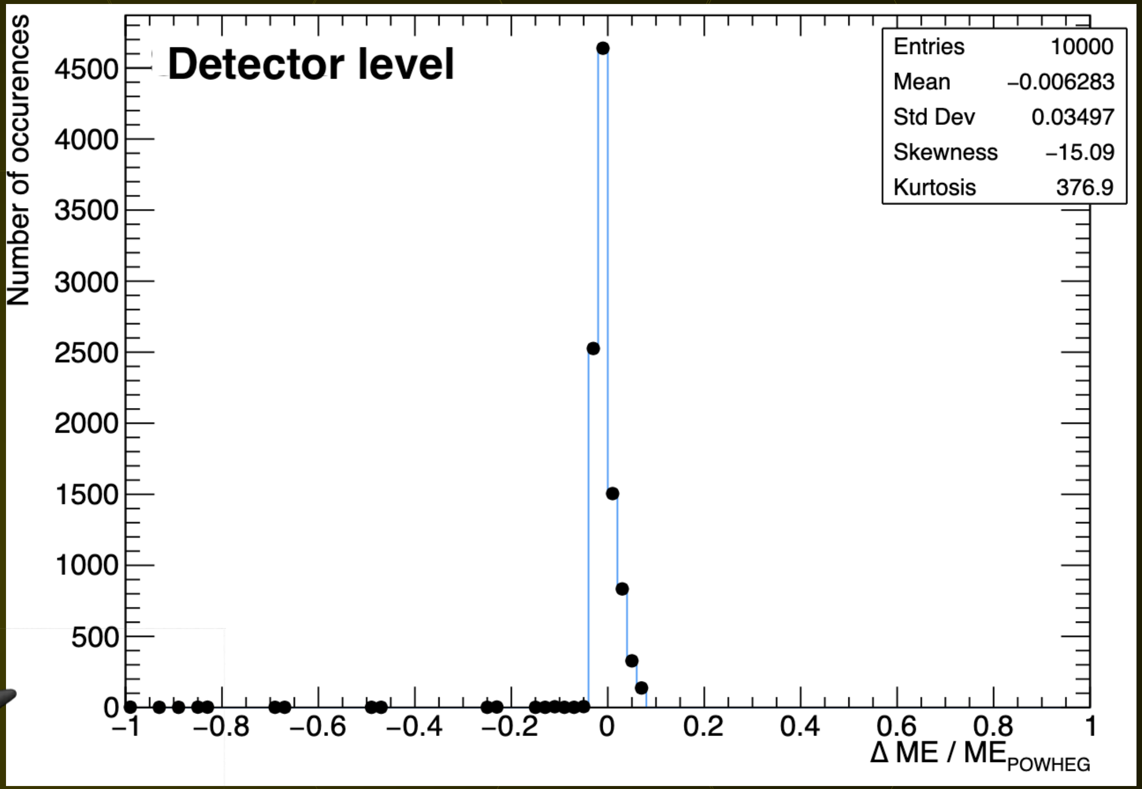

Direct comparison of the difference of ME at LO: POWHEG vs MadGraph (normalized by the POWHEG value; with the same value for α_S).

2.4 : Developing a MEM@NLO: Interface with POWHEG-BOX-V2

The POWHEG-BOX-V2 software

Main challenges presented here :

1. Used POWHEG-BOX-V2/ggHH subrepository, created by Pr.Heinrich (et al.). The Matrix Elements stop at HH production.

Solution: We added the Higgs decays by hand, from MadGraph (to POWHEG-BOX-V2).

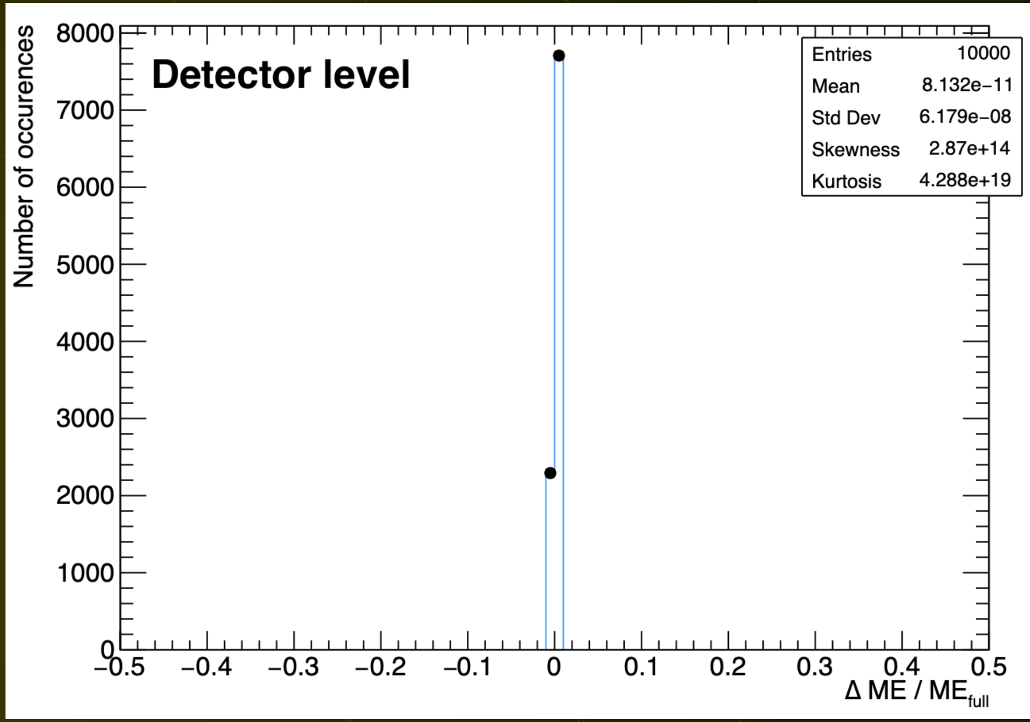

Comparison of the differences in ME value (both from MadGraph) with:
$(gg \rightarrow HH \rightarrow b\bar{b}\gamma\gamma)$ (full)
And new implementation:
2 x $(gg \rightarrow HH)$ x $(H \rightarrow b\bar{b})$ x $(H \rightarrow \gamma\gamma)$

The POWHEG-BOX-V2 software

Main challenges presented here :

1. Used POWHEG-BOX-V2/ggHH subrepository, created by Pr.Heinrich (et al.). The Matrix Elements stop at HH production.

2. Born+Virtual (BV) and Real (R) contributions do not live in the same phase-space.
   → The integrals are different.
   → the MEM should be different too.

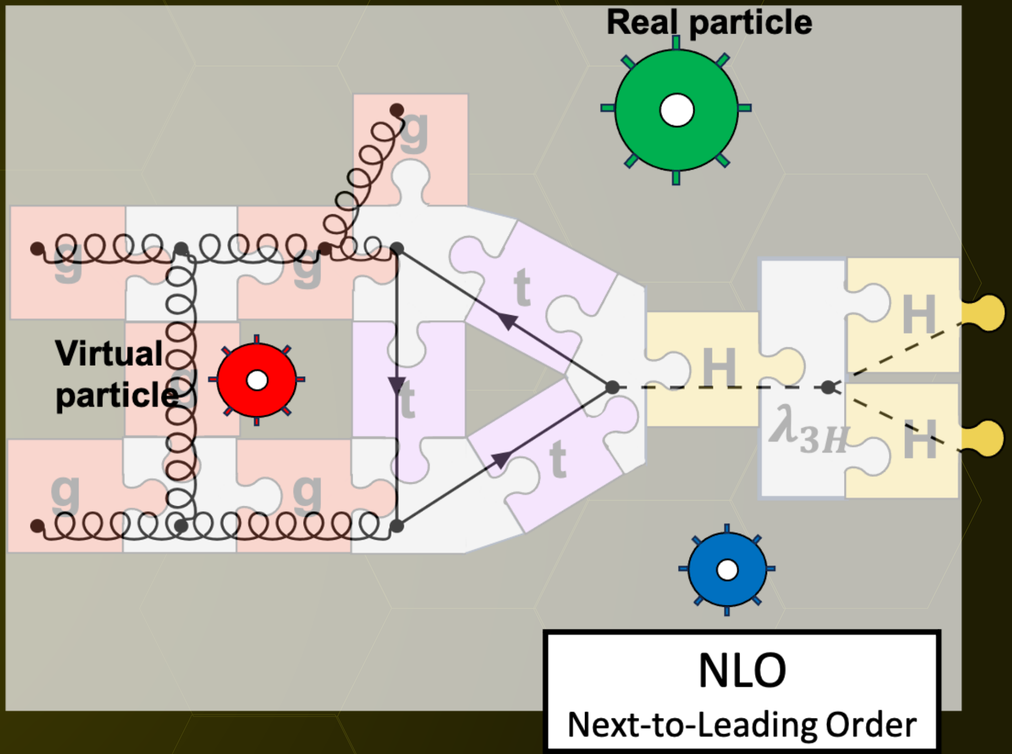

$$\sigma^{\rm NLO} = \underbrace{\int_n d\Phi_n \Big[B(\Phi_n) + V(\Phi_n)\Big]}_{\text{Born+Virtual}} + \underbrace{\int_{n+1} d\Phi_{n+1}\, R(\Phi_{n+1})}_{\text{Real}} .$$

.4 : Developing a MEM@NLO: Interface with POWHEG-BOX-V2

The POWHEG-BOX-V2 software

Main challenges presented here :

1. Used POWHEG-BOX-V2/ggHH subrepository, created by Pr.Heinrich (et al.). The Matrix Elements stop at HH production.

2. Born+Virtual (BV) and Real (R) contributions do not live in the same phase-space.
   → The integrals are different.
   → the MEM should be different too.

3. Degeneracy in the definition of Next-to-Leading Order (NLO) due to parton-shower.

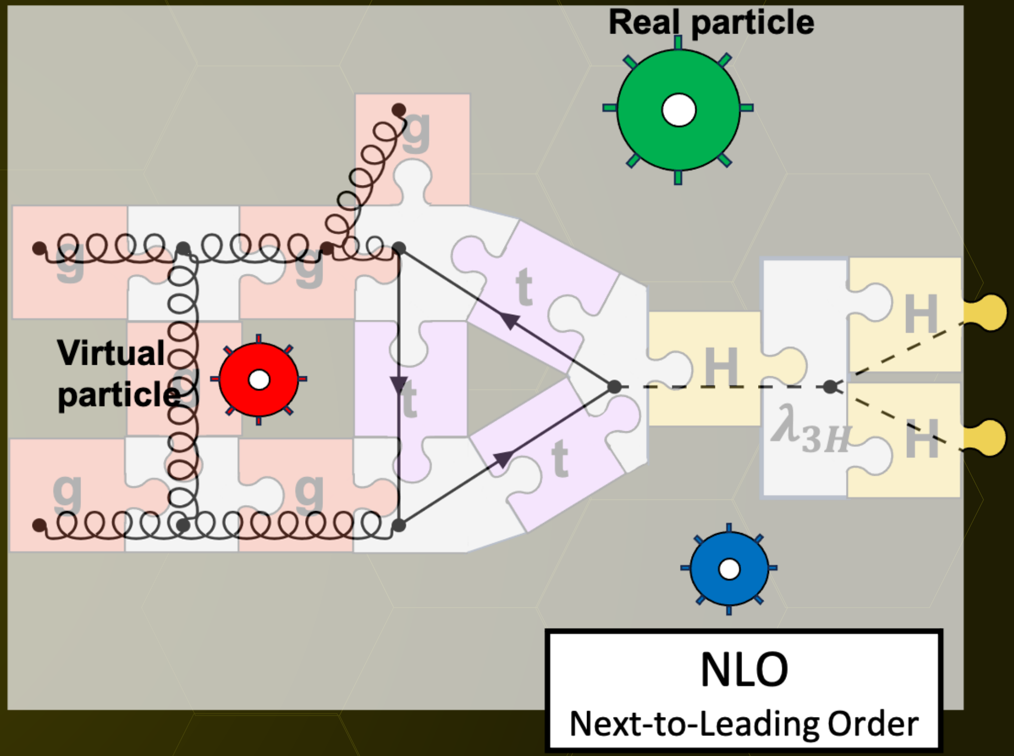

2

The Matrix Element Method

.4 : Developing a MEM@NLO: Interface with POWHEG-BOX-V2

Degeneracy in the definition of Next-to-Leading Order (NLO)

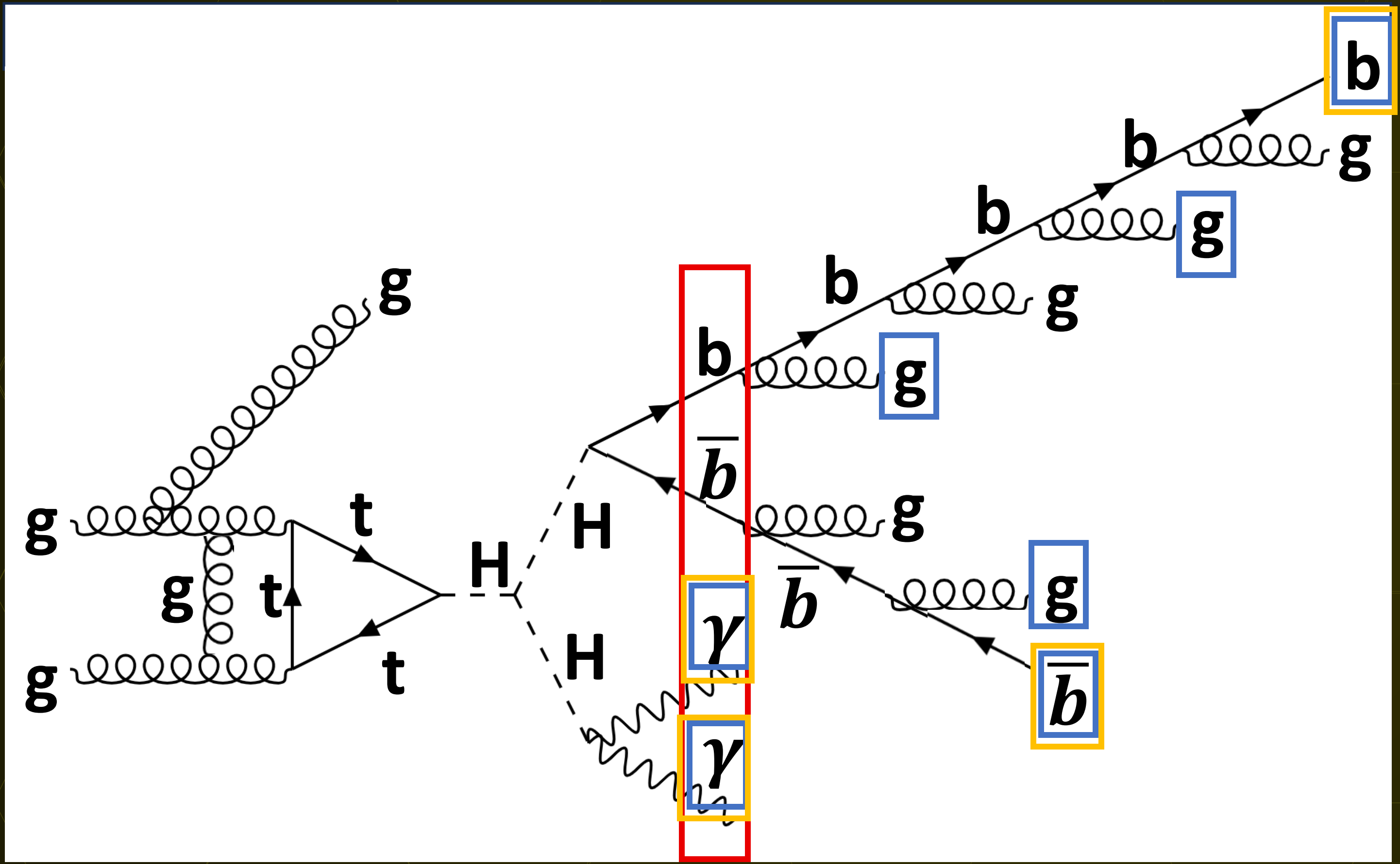

Parton shower with PYTHIA (inside POWHEG-BOX-V2)

We modified the PYTHIA script to create 3 different files:

NLO — **ISR** "Initial State Radiation"

NLO — **FSRdr** "Final State Radiation ΔR": Include every shower radiation within $\Delta R < 0.4$.
where $\Delta R = \sqrt{\eta^2 + \phi^2}$

NLO — **FSRend** "Final State Radiation"

.4 : Developing a MEM@NLO: Interface with POWHEG-BOX-V2

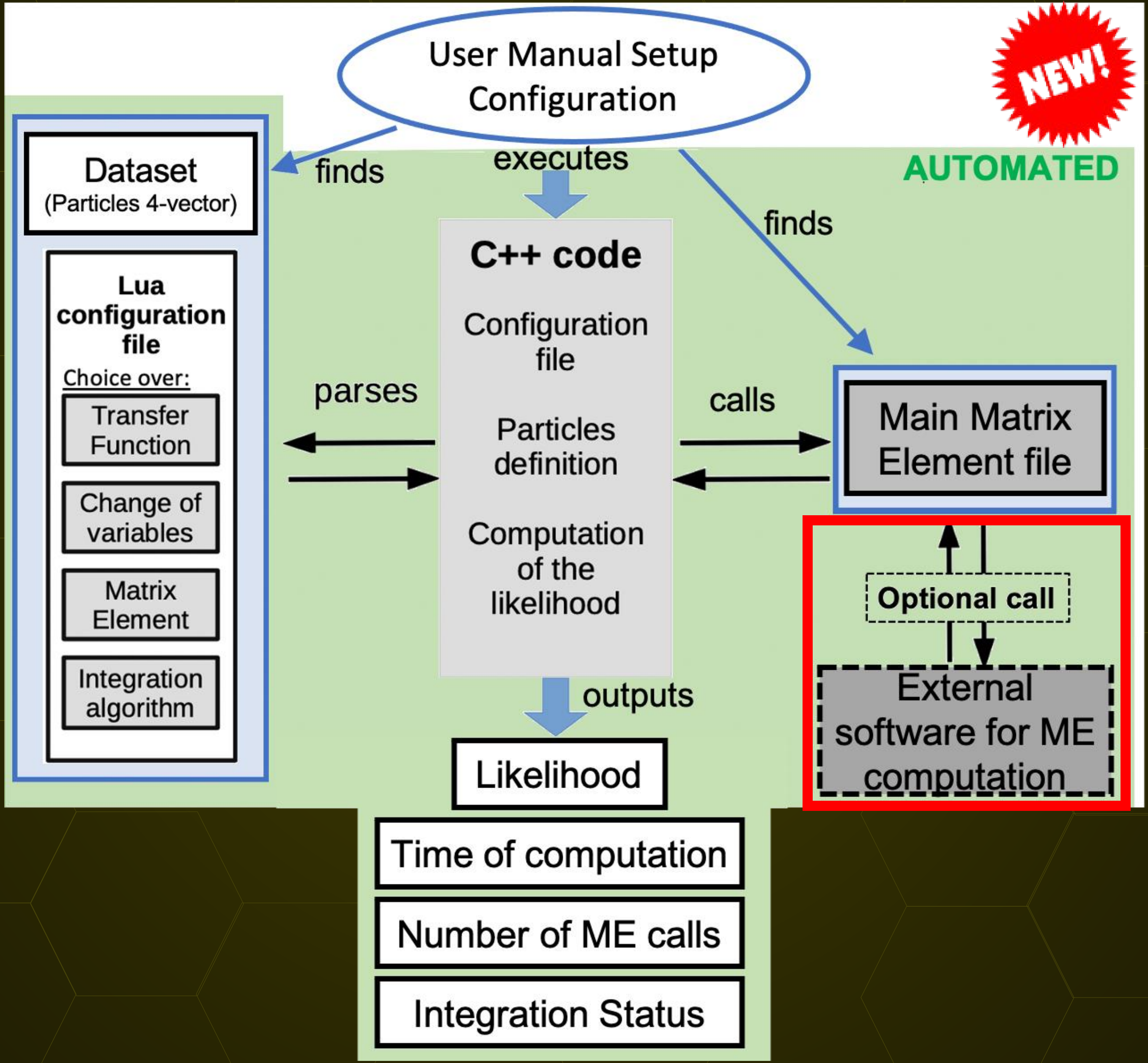

New implementation of the MEM inside MoMEMta: our MEM@NLO

Why do we need that?

Theoretical computation for NLO ME are extremely complicated.
Not possible with MadGraph for now.

.4 : Developing a MEM@NLO: Change of variables

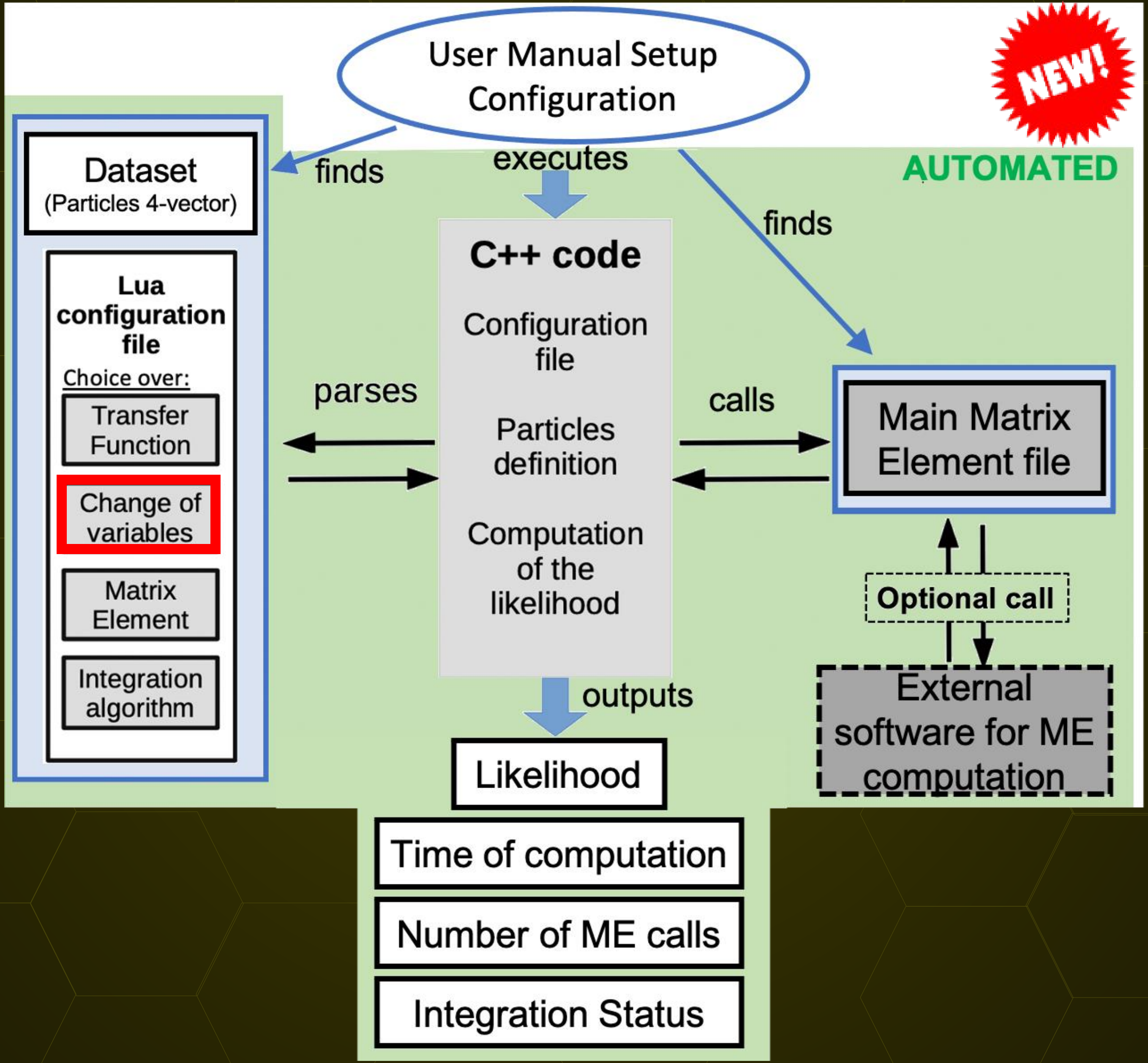

.4 : Developing a MEM@NLO: Change of variables

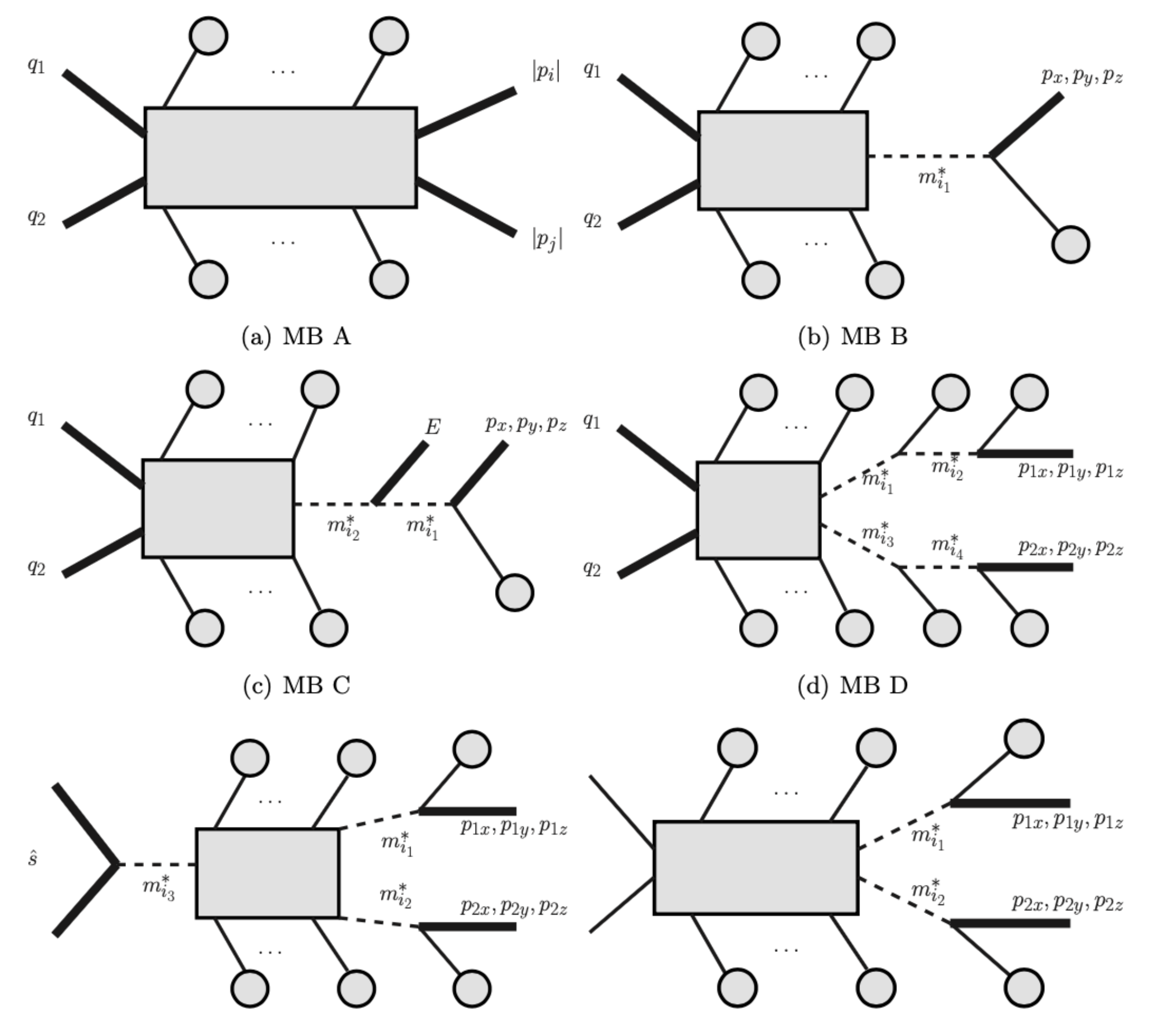
(a) MB A (b) MB B (c) MB C (d) MB D (e) MB E (f) MB F

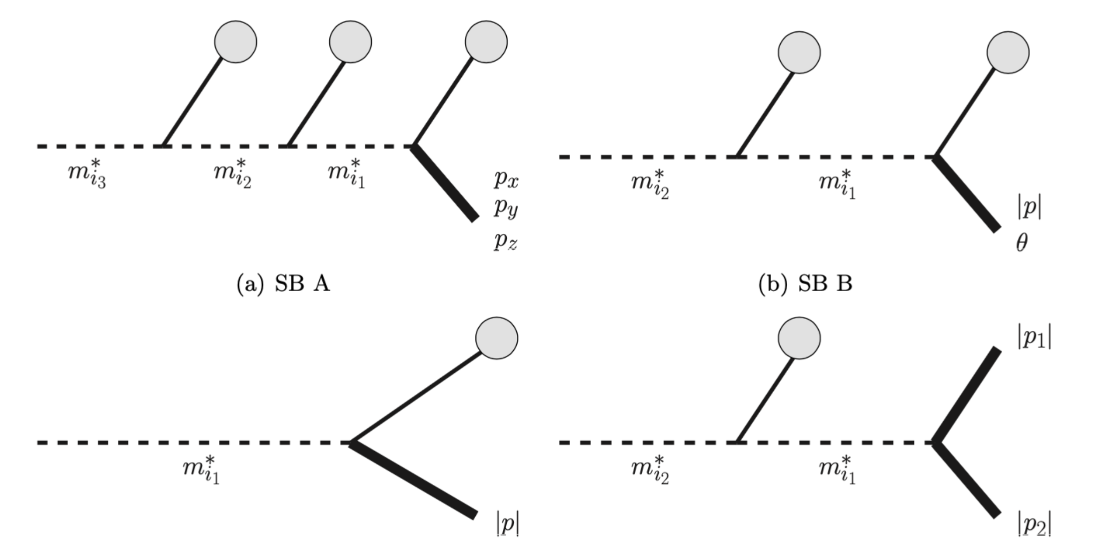
(a) SB A (b) SB B (c) SB C/D (d) SB E

Main and Secondary Blocks

Definition « Blocks » : Choices of integration variable (and substitutions) made to break down a complex process into manageable configuration.

.4 : Developing a MEM@NLO: Change of variables

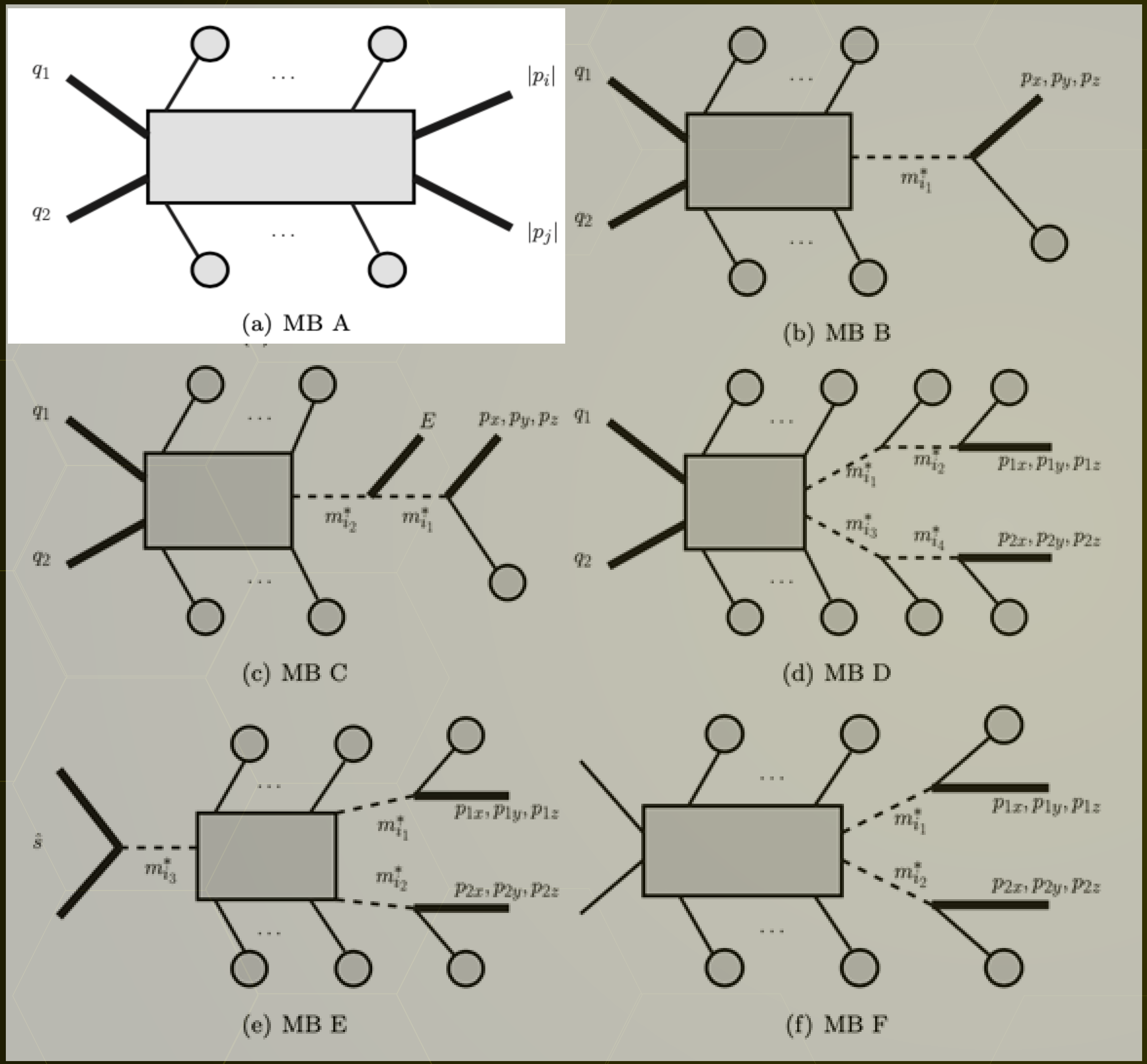

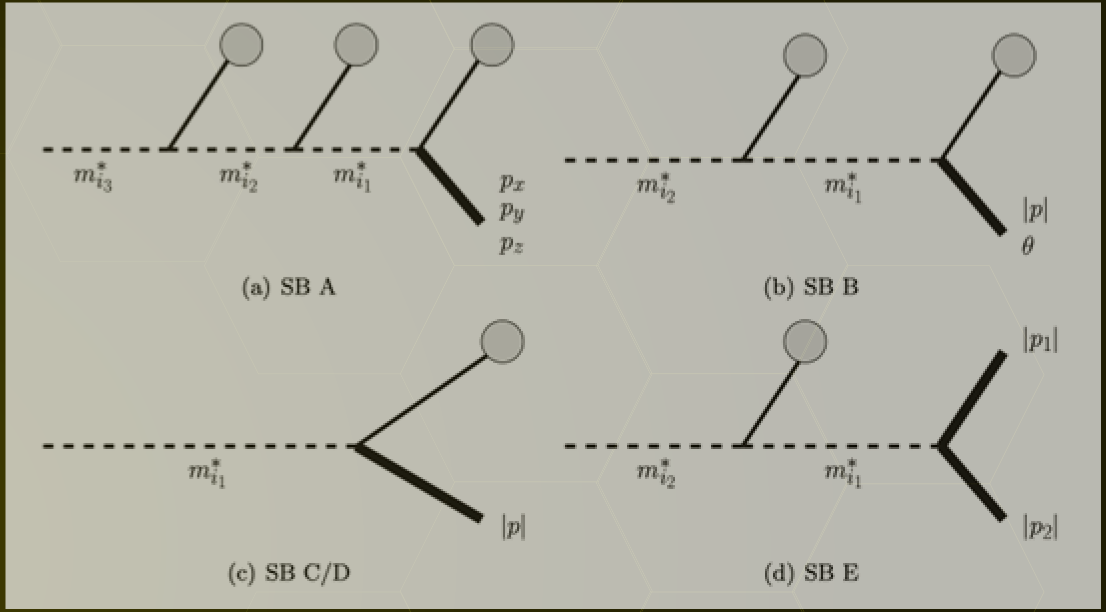

Main and Secondary Blocks

Definition « Blocks » : Choices of integration variable (and substitutions) made to break down a complex process into manageable configuration.

.4 : Developing a MEM@NLO:

Main Block A:

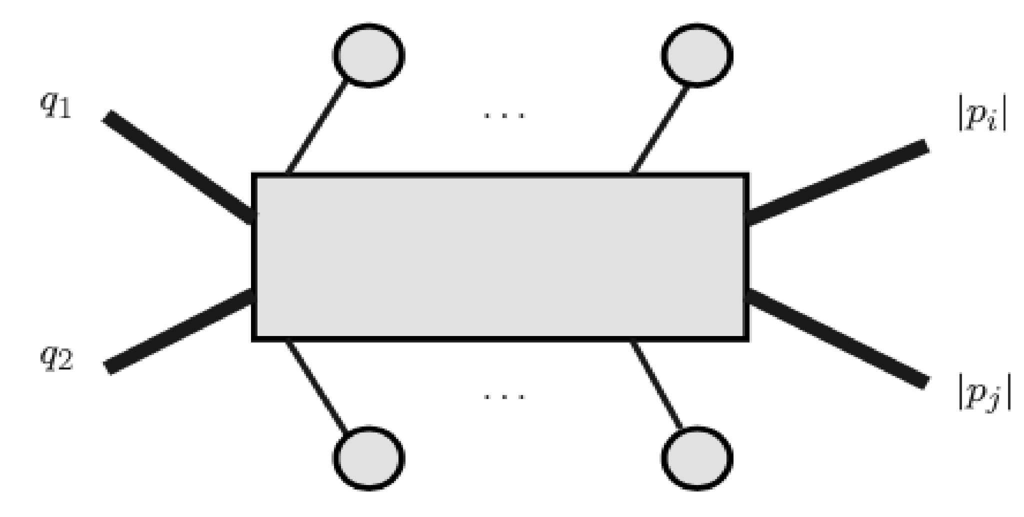

(a) MB A

$$dq_1\,dq_2\,\frac{d^3p_1}{(2\pi)^3 2E_1}\,\frac{d^3p_2}{(2\pi)^3 2E_2}\,(2\pi)^4\,\delta^4(P_{in}-P_f)$$

$$\downarrow$$

$$\frac{1}{16\pi^2 E_1 E_2}\,d\theta_1\,d\theta_2\,d\varphi_1\,d\varphi_2 \cdot J$$

$$\frac{1}{(2\pi)^3}\frac{1}{(2\pi)^3}(2\pi)^4\frac{1}{4E_1E_2}\,dq_1dq_2\,d^3p_1\,d^3p_2\,\delta^4(P_{in}-P_{out})$$

$$=\frac{1}{(2\pi)^2}\frac{1}{4E_1E_2}\,dq_1dq_2\,dp_{x1}dp_{y1}dp_{z1}dp_{x2}dp_{y2}dp_{z2}\,\delta^4(P_{in}-P_{out})$$

$$=\frac{1}{(2\pi)^2}\frac{1}{4E_1E_2}\,J_2J_4\,dE_+dE_-\,J_3\,dp_1d\theta_1d\varphi_1\,dp_2d\theta_2d\varphi_2\,\delta^4(P_{in}-P_{out})$$

$$=\frac{1}{(2\pi)^2}\frac{1}{4E_1E_2}\,J_2J_3J_4\left[dE_+dE_-\,\delta(E_+-E_{out})\,\delta(E_--P_{z,out})\right]$$

$$\cdot J_1\left[dP_x\,dP_y\,\delta(-P_x)\,\delta(-P_y)\right]d\theta_1d\varphi_1\,d\theta_2d\varphi_2$$

we integrate out the deltas:

$$=\frac{1}{(2\pi)^2}\frac{1}{4E_1E_2}\,J_1J_2J_3J_4\,d\theta_1d\varphi_1\,d\theta_2d\varphi_2$$

to compare with

$$=\frac{1}{16\pi^2}\frac{1}{E_1E_2}\,J\,d\theta_1d\varphi_1\,d\theta_2d\varphi_2$$

which gives:

$$J=\frac{1}{(2\pi)^2}\frac{1}{4E_1E_2}\times 16\pi^2E_1E_2\,J_1J_2J_3J_4$$

$$=J_1J_2J_3J_4$$

$$=\frac{1}{\sin\theta_1\sin\theta_2(\cos\varphi_1\sin\varphi_2-\sin\varphi_1\cos\varphi_2)}\,\frac{4}{s}\cdot p_1^2\sin\theta_1\,p_2^2\sin\theta_2\cdot\frac{1}{2}$$

$$=p_1^2p_2^2\,\frac{2}{s}\,\frac{1}{(\cos\varphi_1\sin\varphi_2-\sin\varphi_1\cos\varphi_2)}$$

$(= J_{manual}$ $\neq \mathcal{J}_{code}$

.4 : Developing a MEM@NLO: Change of variables

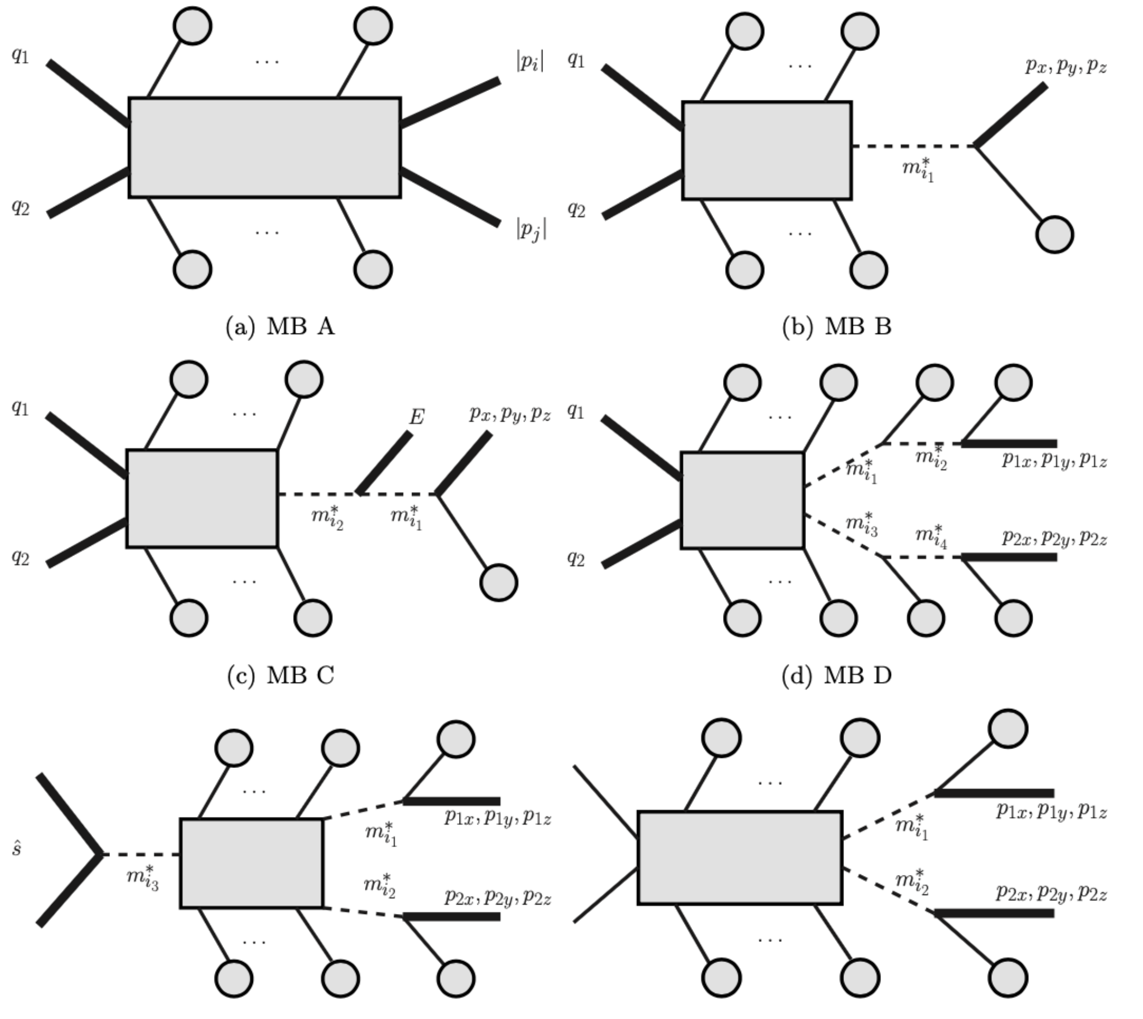

(a) MB A (b) MB B (c) MB C (d) MB D (e) MB E (f) MB F

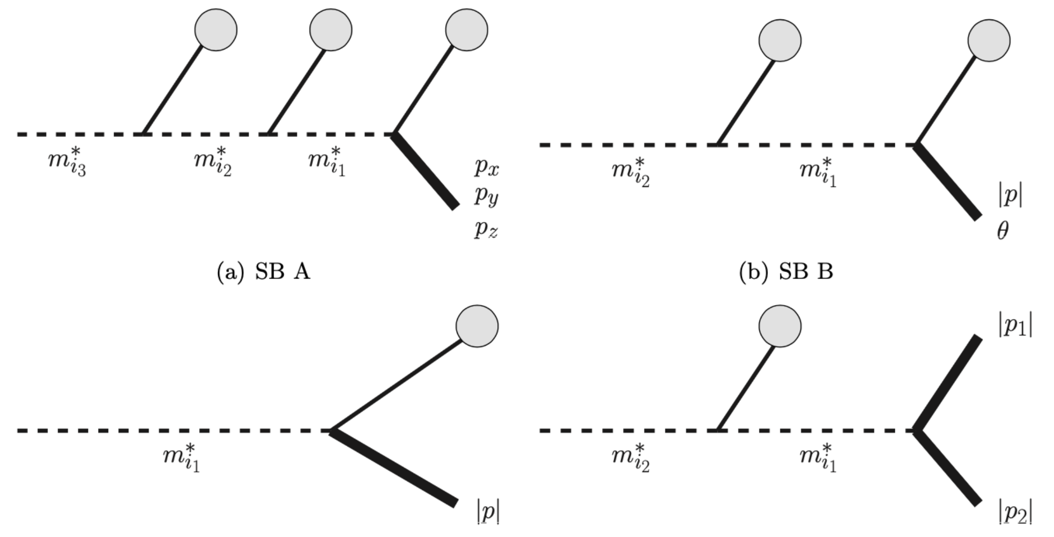

(a) SB A (b) SB B (c) SB C/D (d) SB E

None of these existing Blocks can properly deal with additional NLO invisible radiation (i.e. not "NLO friendly").

So we create our own !

2

The Matrix Element Method

.4 : Developing a MEM@NLO: Change of variables

Main Block N:

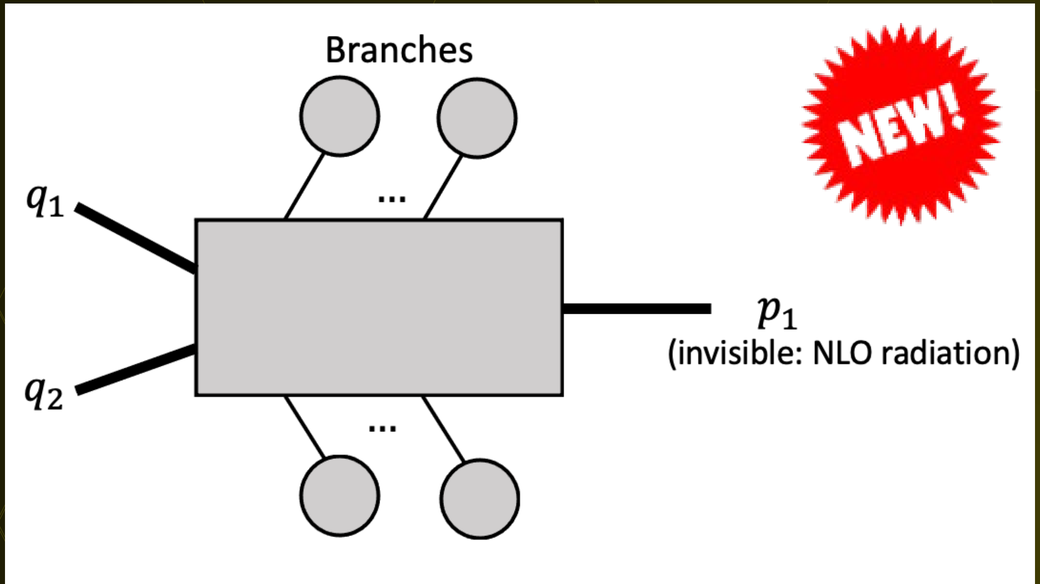

$$dq_1\, dq_2\, \frac{d^3p_1}{(2\pi)^3\, 2E_{p_1}}\, (2\pi)^4\, \delta^{(4)}(In - Out)$$

$$\downarrow$$

$$\prod \frac{1}{E_{p_1}} \cdot dp_{1z} \cdot |\det(J)|$$

$$\frac{1}{(2\pi)^3}\,(2\pi)^4\, \frac{1}{2E_1}\, dq_1\, dq_2\, dp_1^3\, \delta^4(P_{in} - P_{out})$$

$$= \frac{\prod}{E_{p_1}}\, dq_1\, dq_2\, dp_{1x}\, dp_{1y}\, dp_{1z}\, \delta^4(P_{in} - P_{out})$$

$$= \frac{1}{2}\, \frac{\prod}{E_{p_1}}\, dp_{1z}\, dP_x\, dP_y\, dP_z\, dE\, \delta(P_x)\, \delta(P_y)\, \delta(P_z)\, \delta(E)$$

we integrate out the deltas:

$$= \frac{1}{2}\, \frac{\prod}{E_{p_1}}\, dp_{1z}$$

Where $\frac{1}{2}$ is the determinant of the Jacobian for the changes of integration variables.

.4 : Developing a MEM@NLO: Change of variables

Main Block N:

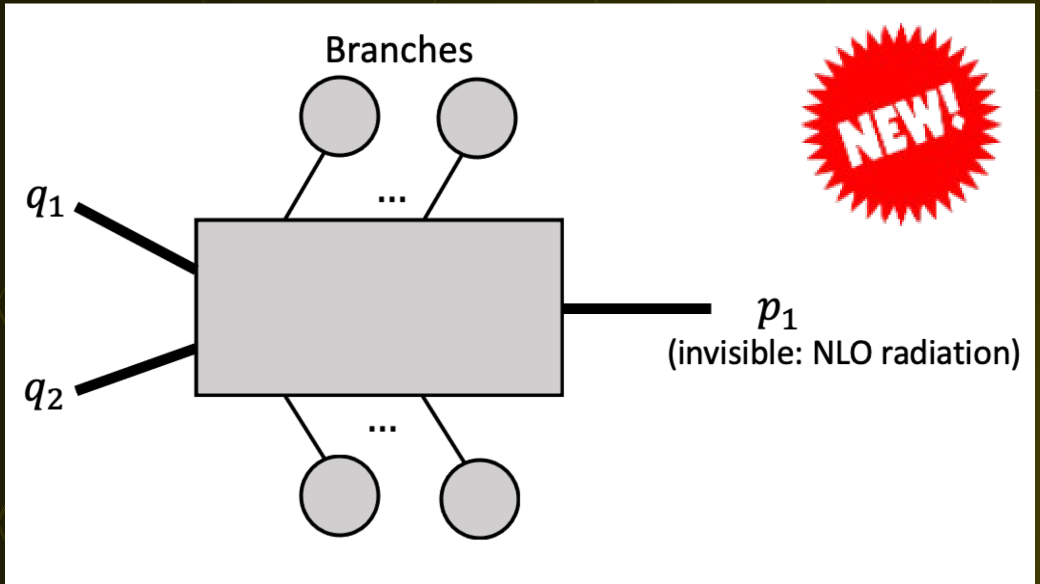

Where $\frac{1}{2}$ is the determinant of the Jacobian for the changes of integration variables.

$$\det(J) = \frac{1}{\det(J^{-1})} = \frac{1}{2}$$

The corresponding Jacobian is derived from the system:

$$\begin{cases} p_{1x} = -P_x, \\ p_{1y} = -P_y, \\ q_1 + q_2 = P_z, \\ q_1 - q_2 - \sqrt{p_{1x}^2 + p_{1y}^2 + p_{1z}^2} = E_T, \end{cases}$$

where P_x, P_y, P_z and E_T are the total sum of the respective contributions from all the final particles $b\bar{b}\gamma\gamma$

$$J^{-1} = \begin{pmatrix} \frac{\partial P_x}{\partial p_{1x}} & \frac{\partial P_x}{\partial p_{1y}} & \frac{\partial P_x}{\partial q_1} & \frac{\partial P_x}{\partial q_2} \\ \frac{\partial P_y}{\partial p_{1x}} & \frac{\partial P_y}{\partial p_{1y}} & \frac{\partial P_y}{\partial q_1} & \frac{\partial P_y}{\partial q_2} \\ \frac{\partial P_z}{\partial p_{1x}} & \frac{\partial P_z}{\partial p_{1y}} & \frac{\partial P_z}{\partial q_1} & \frac{\partial P_z}{\partial q_2} \\ \frac{\partial E_T}{\partial p_{1x}} & \frac{\partial E_T}{\partial p_{1y}} & \frac{\partial E_T}{\partial q_1} & \frac{\partial E_T}{\partial q_2} \end{pmatrix} = \begin{pmatrix} -1 & 0 & 0 & 0 \\ 0 & -1 & 0 & 0 \\ 0 & 0 & 1 & 1 \\ -\frac{p_{1x}}{E_{p_1}} & -\frac{p_{1y}}{E_{p_1}} & 1 & -1 \end{pmatrix}$$

$$\det\left(J^{-1}\right) = \left|(-1)(-1)\cdot\det\begin{pmatrix} 1 & 1 \\ 1 & -1 \end{pmatrix}\right| = \left|\det\begin{pmatrix} 1 & 1 \\ 1 & -1 \end{pmatrix}\right| = |-2| = 2$$

.4 : Developing a MEM@NLO: Change of variables

Validation for our new Main Block N:

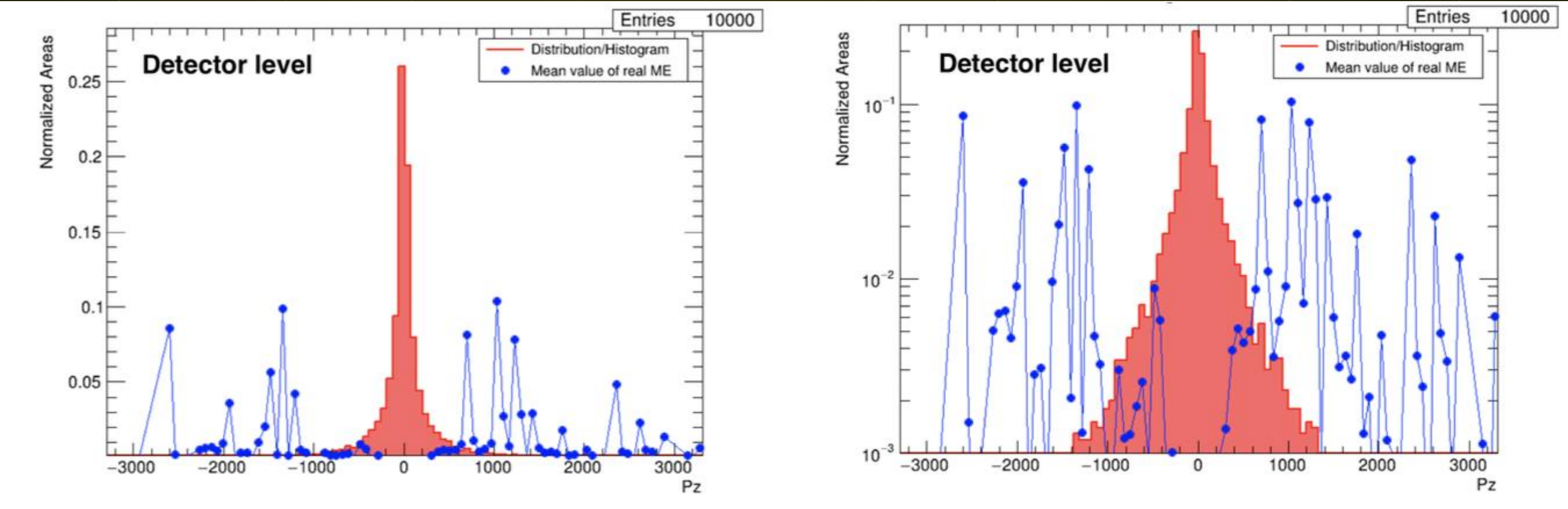

(a) Real ME Only

(b) with Y-axis in log

1st step:

- in blue: The mean value of the real matrix element evaluated for each events (for each bin of p_z value).
- in red: The distribution of the p_z component of NLO radiation, for signal ggF events.

.4 : Developing a MEM@NLO: Change of variables

Validation for our new Main Block N:

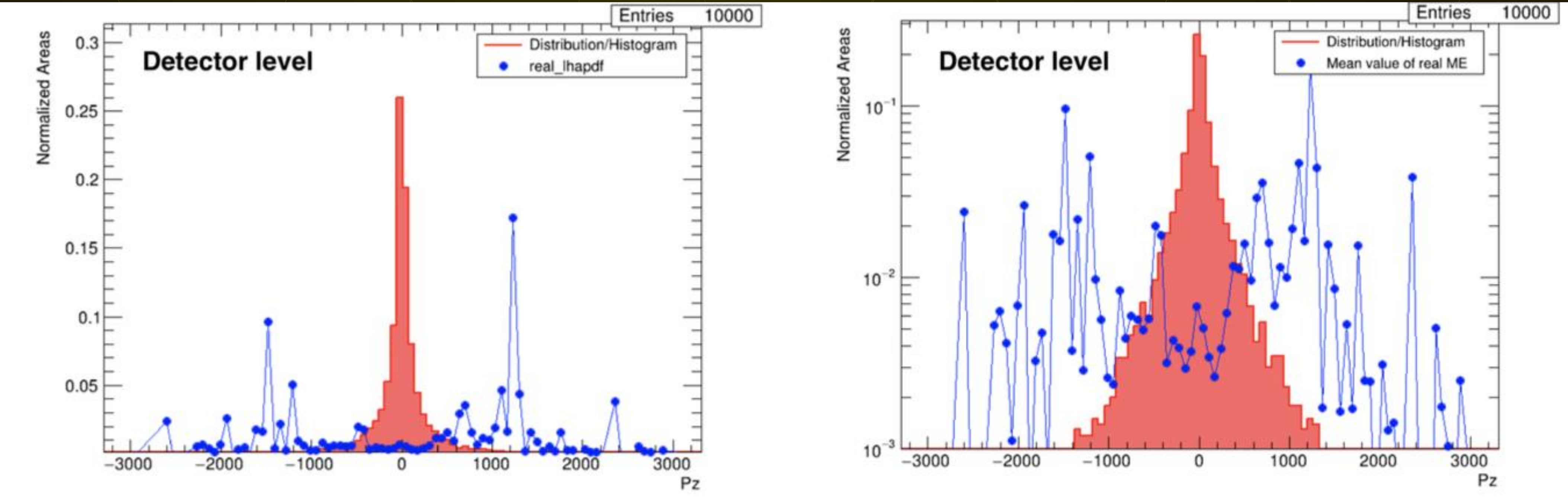

(c) Real ME + PDF

(d) with Y-axis in log

2nd step:

- in blue: The mean value of the real matrix element evaluated for each events (for each bin of p_z value) + the Parton Density Functions (PDF) f_q.

- in red: The distribution of the p_z component of NLO radiation, for signal ggF events.

.4 : Developing a MEM@NLO: Change of variables

Validation for our new Main Block N:

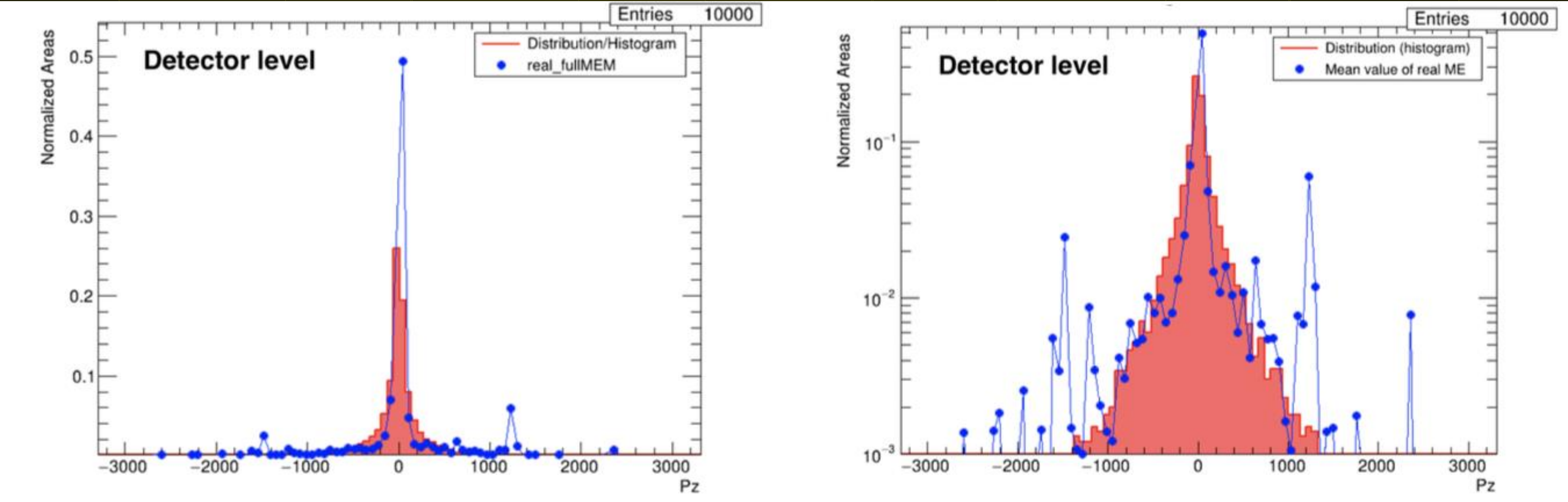

(e) Full Real Integrand

(f) with Y-axis in log

3rd step:

- in blue: The mean value of the real matrix element evaluated for each events (for each bin of p_z value) + the Parton Density Functions (PDF) f_q + the **full** phase-space Jacobian.

- in red: The distribution of the p_z component of NLO radiation, for signal ggF events.

.4 : Developing a MEM@NLO: Change of variables

Collinear treatement:

Naïve idea: we allow generation of the NLO radiation in any angular direction.

Yet some configurations lack physical interpretation.

The idea is simple, when the NLO radiation is generated in such speficic cases, its energy is removed from the corresponding b-jet ("inverse smearing").

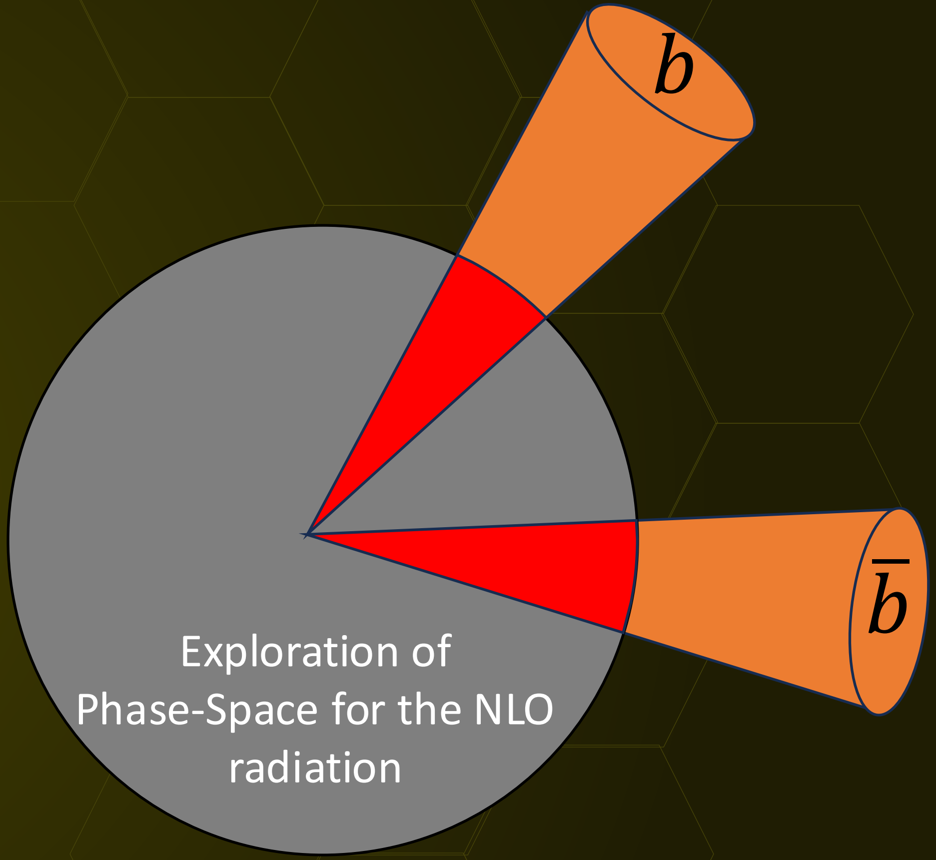

.4 : Developing a MEM@NLO: Change of variables

Determination of the Infrared (IR) and Ultraviolet (UV) limits

Process	$p_T^{\min}$	$p_T^{\max}$	$E^{\min}$	$E^{\max}$	$\lvert p_z\rvert^{\min}$	$\lvert p_z\rvert^{\max}$
$gg \to HH$ (ggF)	15	300	15	1550	2	$\sqrt{E^2_{\max} - p^2_{T,\min}}$
$t\bar{t}H$	12	500	20	1875	1	$\sqrt{E^2_{\max} - p^2_{T,\min}}$
QCD background	10	330	15	1800	0.05	$\sqrt{E^2_{\max} - p^2_{T,\min}}$
singleHiggs	20	182	20	1620	2	$\sqrt{E^2_{\max} - p^2_{T,\min}}$

Choice of integration limits for the kinematic variables for the additional NLO radiation.

Additional kinematic cuts to ensure that integrals remain well defined (i.e. no divergence).

For NLO radiations, typically impose limits on transverse momentum p_t, energy E, or longitudinal momentum p_z.

.4 : Developing a MEM@NLO: Change of variables

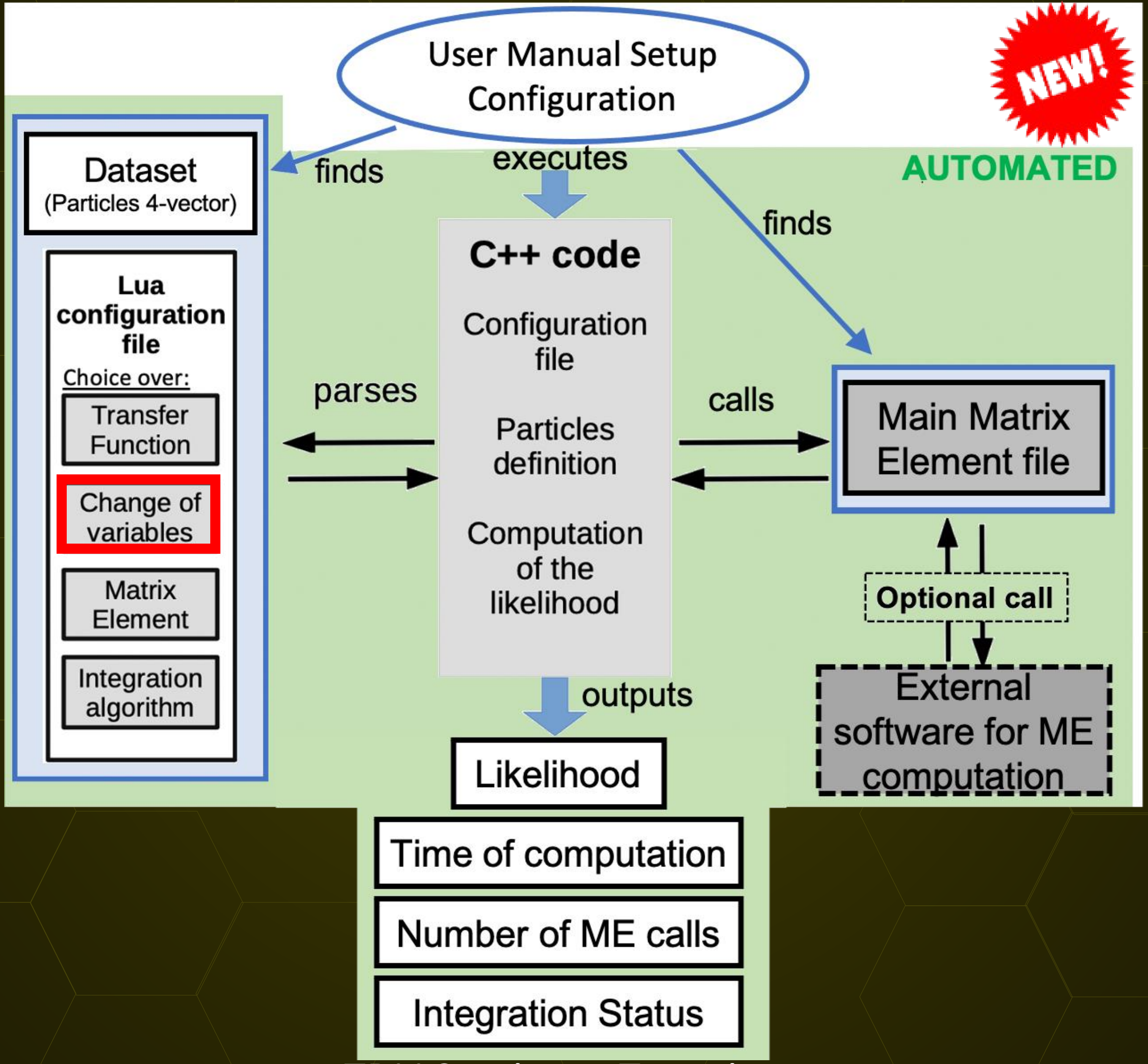

.4 : Developing a MEM@NLO: Transfer Function

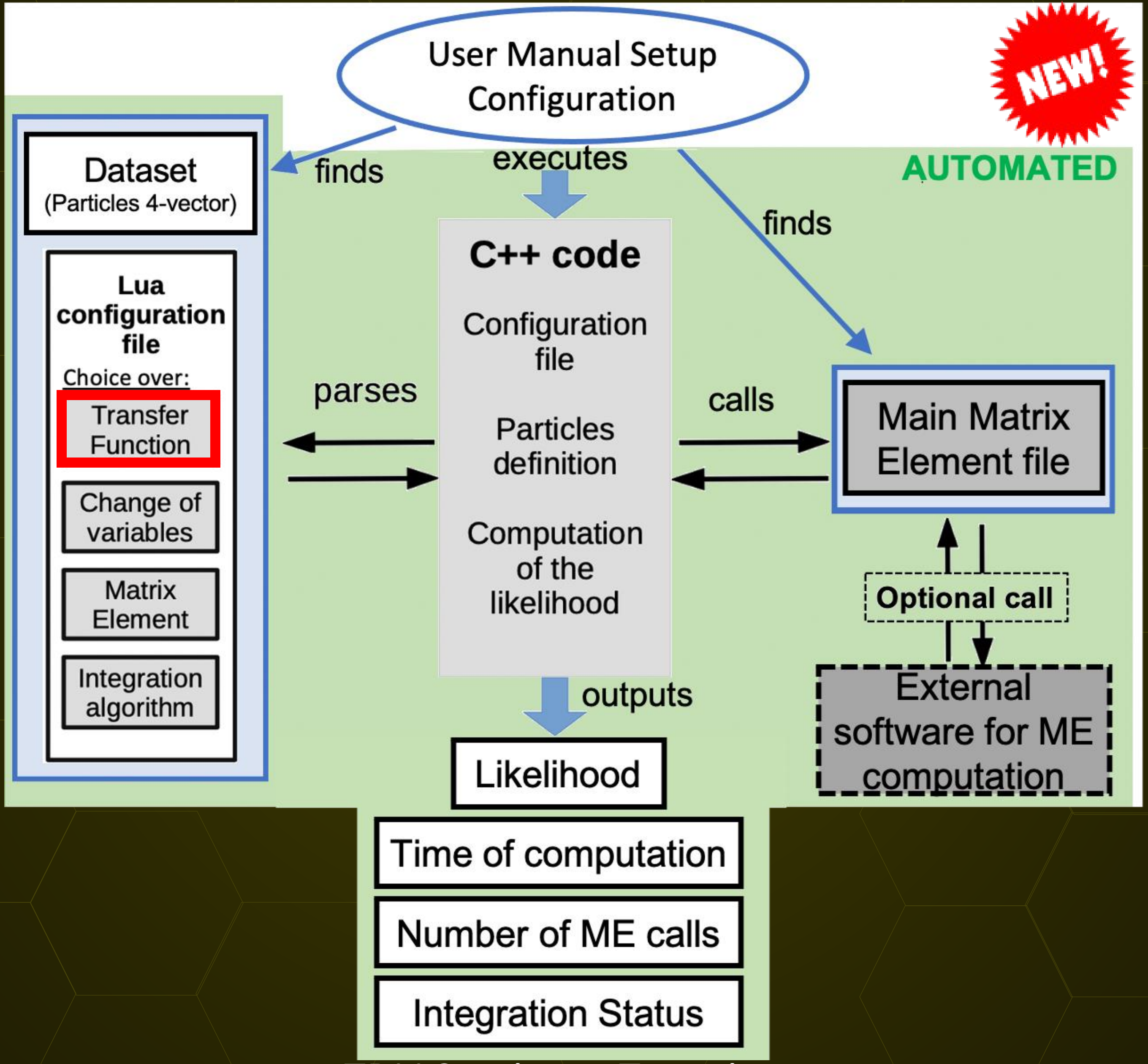

.4 : Developing a MEM@NLO: Transfer Function

Transfer functions $W(y; x^i)$

Aims to construct a set of new values **y** from the data $\mathbf{x^i}$, and computes how likely it would be to obtain to $\mathbf{x^i}$ from **y.**

Describe the resolution of the detector and impact on the reconstructed kinematics in the data. :

- Simple assumption on the gaussian width σ_E (ratio over the reco energy E):

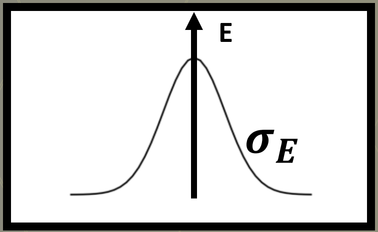

$$\frac{\sigma_E}{E_{\text{reco}}} \approx 1\% \quad \text{for photons,} \qquad \frac{\sigma_E}{E_{\text{reco}}} \approx 10\% \quad \text{for } b\text{-jets.}$$

- More advanced (what is considered physical in the ATLAS Collaboration). Not implemented inside MoMEMta.

$$\frac{\sigma_E}{E_{\text{reco}}} = \frac{S}{\sqrt{E_{\text{reco}}}} + C + \frac{N}{E_{\text{reco}}}$$

.4 : Developing a MEM@NLO: Transfer Function

Transfer functions $W(y; x^i)$

Aims to construct a set of new values **y** from the data $\mathbf{x^i}$, and computes how likely it would be to obtain to $\mathbf{x^i}$ from **y.**

Describe the resolution of the detector and impact on the reconstructed kinematics in the data. :

- Simple assumption on the gaussian width σ_E (ratio over the true energy E):

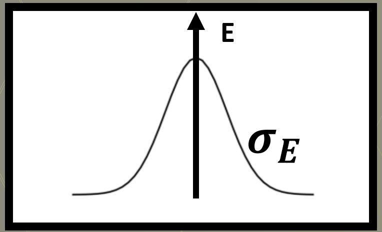

$$\frac{\sigma_E}{E_{\text{reco}}} \approx 1\% \quad \text{for photons,} \qquad \frac{\sigma_E}{E_{\text{reco}}} \approx 10\% \quad \text{for } b\text{-jets.}$$

Simple assumption was enough for our present work. No significant improvement came from the more advanced assumption.

.4 : Developing a MEM@NLO: Transfer Function

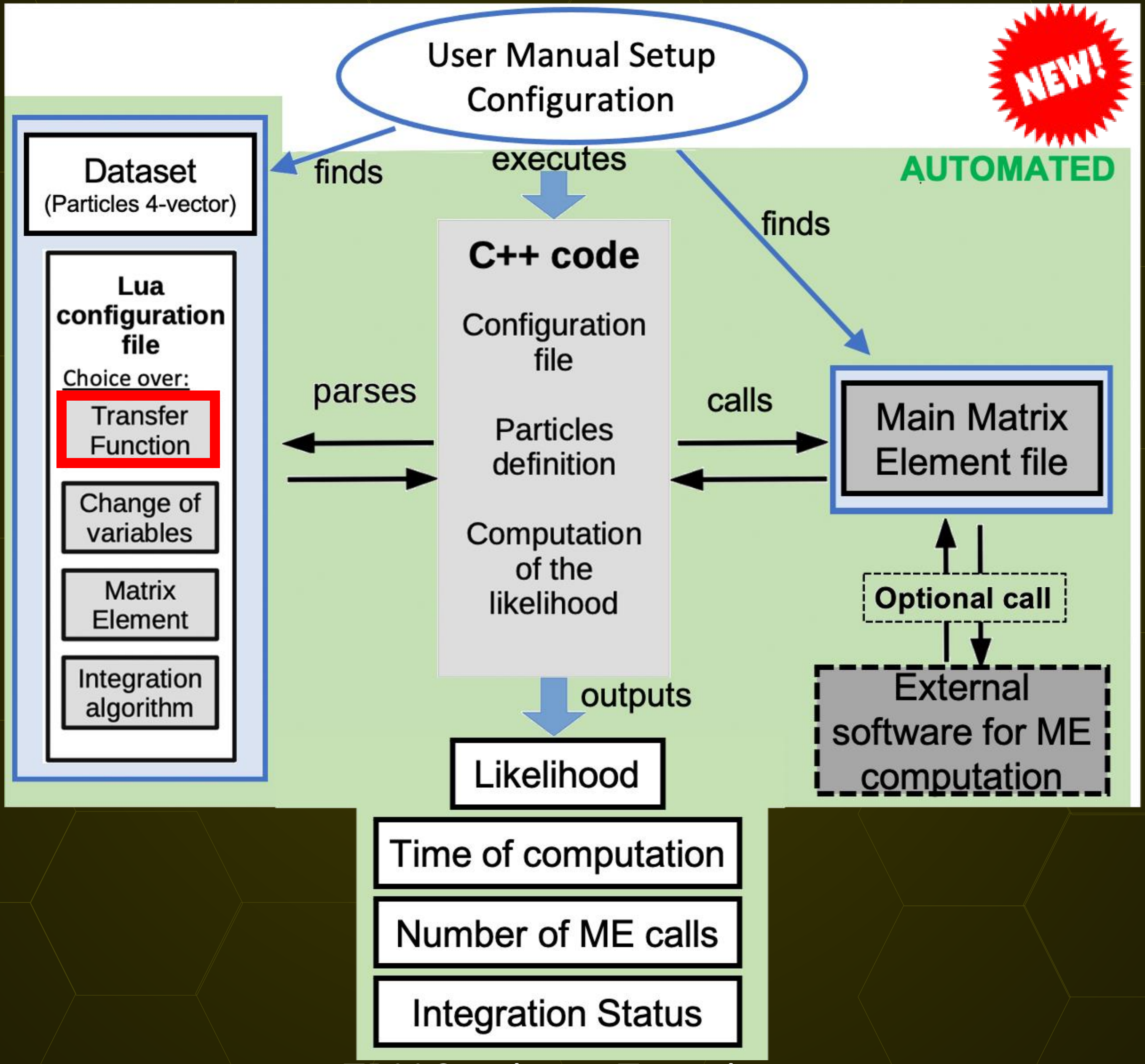

.4 : Developing a MEM@NLO: Integration algorithms

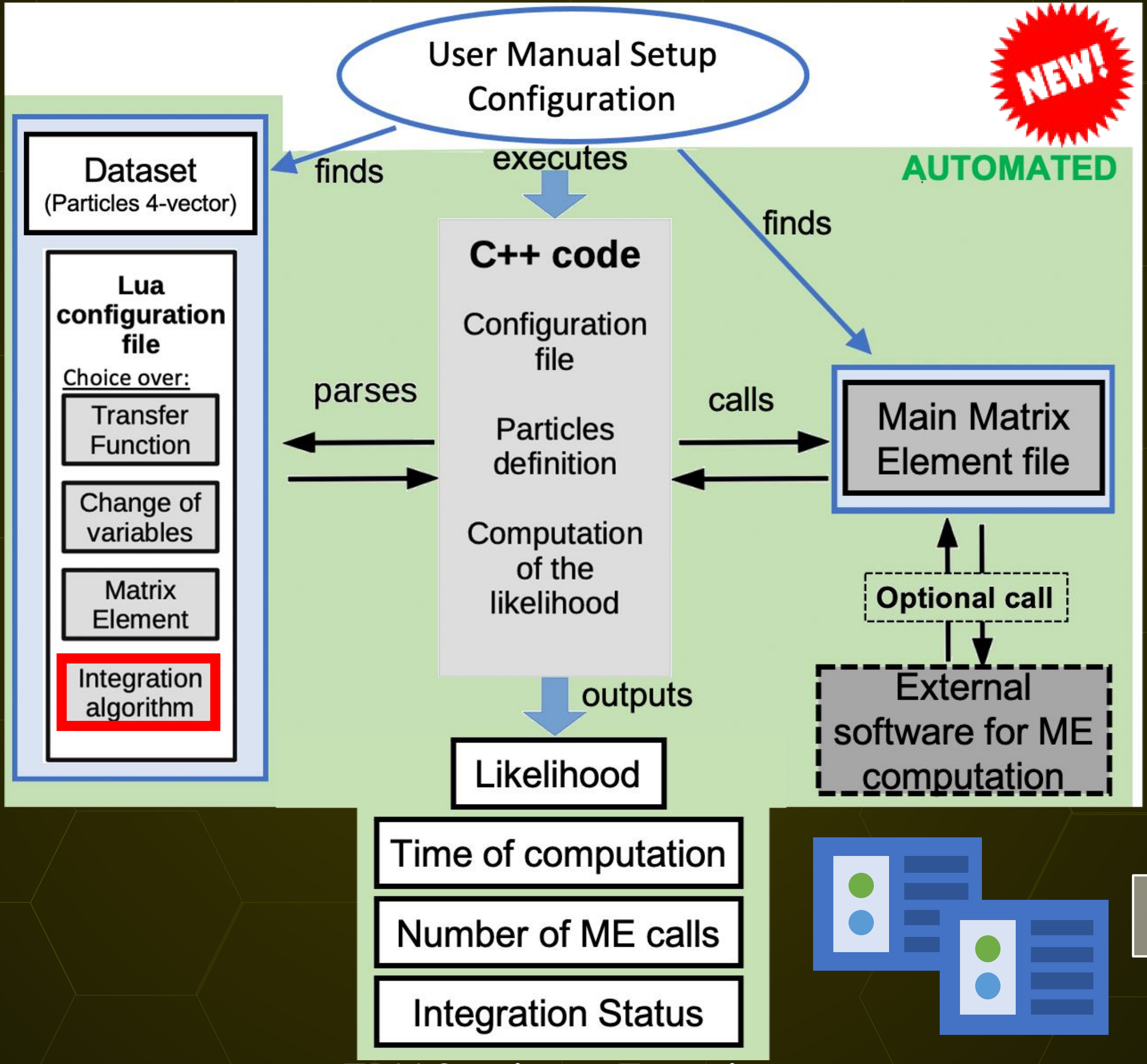

DIVONNE,
VEGAS,
CUBA,
…

MEM Outputs

.5 : Developing a MEM@NLO: Automated framework

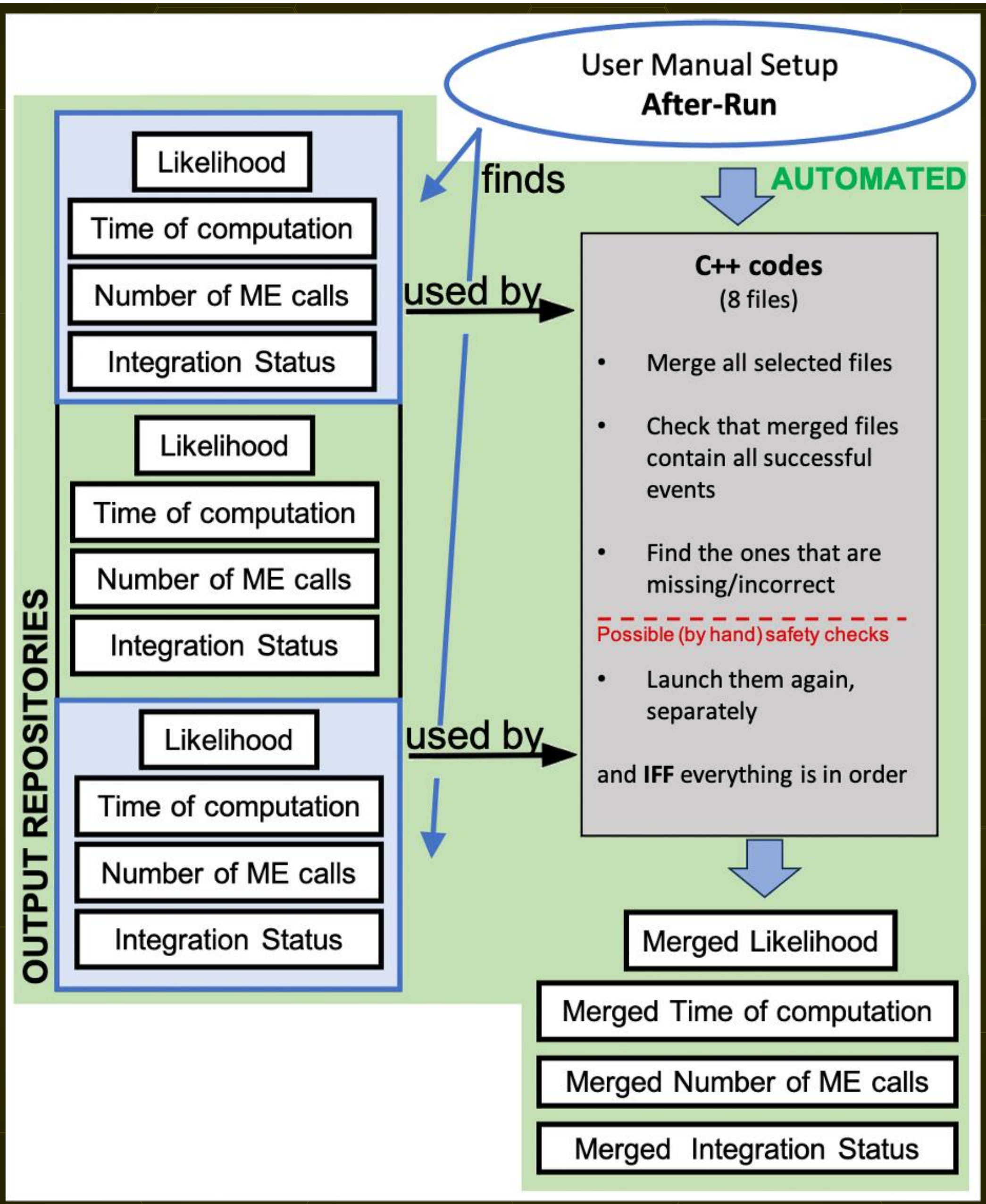

An other automated framework:
After the MEM outputs

Analysis tool: Extraction of κ_λ using Likelihood scans

Constructing the Kinematic Likelihood $\mathcal{L}_{kinematic}(\kappa_\lambda)$:

$$\mathcal{L}^{\mathrm{p}}_{\mathrm{process}}(\mathbf{h}|\mathbf{x}^i) = \frac{1}{\sigma_p^{obs}(pp \to F)} \int_{\mathbf{y}} d\sigma_p(pp \to y; \mathbf{h}) W(\mathbf{y}, \mathbf{x}^i)$$

The MEM produces a likelihood for each process: $\mathcal{L}^P_{process}(\mathbf{h}|x^i)$, for a given event x^i.

$$\mathcal{L}_{\mathrm{event}}(\mathbf{h}|\mathbf{x}^i) = \sum_{p=1}^{n_p} f_p(\mathbf{h}) \mathcal{L}^p_{\mathrm{process}}(\mathbf{h}|\mathbf{x}^i),$$

Construct event likelihood $\mathcal{L}_{event}(\mathbf{h}|x^i)$ by summing over all processes, for a given event x^i.

$$\boxed{\mathcal{L}_{\mathrm{kinematic}}(\mathbf{h}|\mathcal{D})} = \prod_{i=1}^{N} \mathcal{L}_{\mathrm{event}}(\mathbf{h}|\mathbf{x}^i)$$

Finally,
construct kinematic likelihood $\mathcal{L}_{kinematic}(\mathbf{h}|D)$ by multiplying each $\mathcal{L}^P_{event}(\mathbf{h}|x^i)$, for a given dataset D.

Analysis tool: Extraction of κ_λ using Likelihood scans

Constructing the Yield Likelihood $\mathcal{L}_{yield}(\kappa_\lambda)$:

The signal cross section has very strong dependence on κ_λ.

For our MEM, this information is used inside: $\mathcal{L}_{yield}(\kappa_\lambda)$.

$$\boxed{\mathcal{L}_{\text{yield}}(\kappa)} = \frac{\lambda(\kappa)^{N_{\text{obs}}} e^{-\lambda(\kappa)}}{N_{\text{obs}}!}, \quad \lambda(\kappa) = N_{\text{sig}}(\kappa) + N_{\text{bkg}}$$

Assuming number of observed events N_{obs} follows a Poisson distribution.

The yield likelihood $\mathcal{L}_{yield}(\kappa_\lambda)$ is the Poisson probability with parameter $\lambda(\boldsymbol{\kappa})$ to observe N_{obs} events (for a given integrated luminosity).
$N_{sig}(\boldsymbol{\kappa})$ and N_{bkg} correspond to the theoretically expected number of signal and background events.

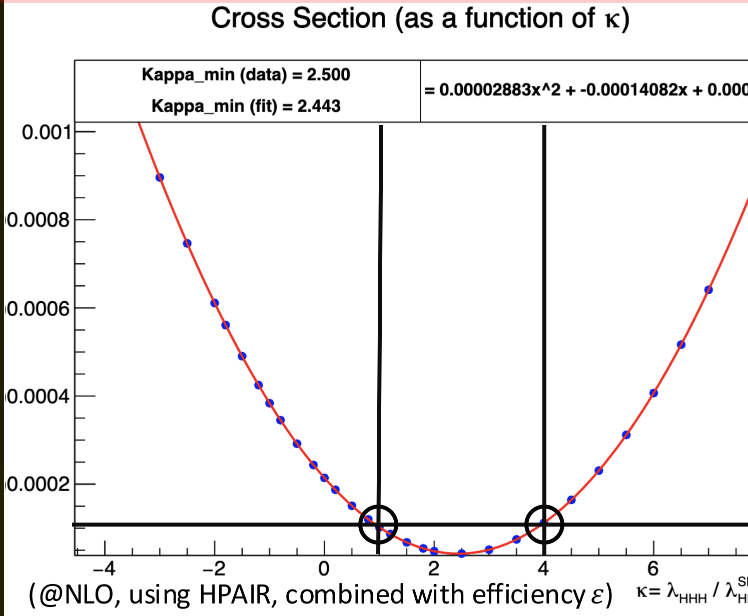

(@NLO, using HPAIR, combined with efficiency ε)

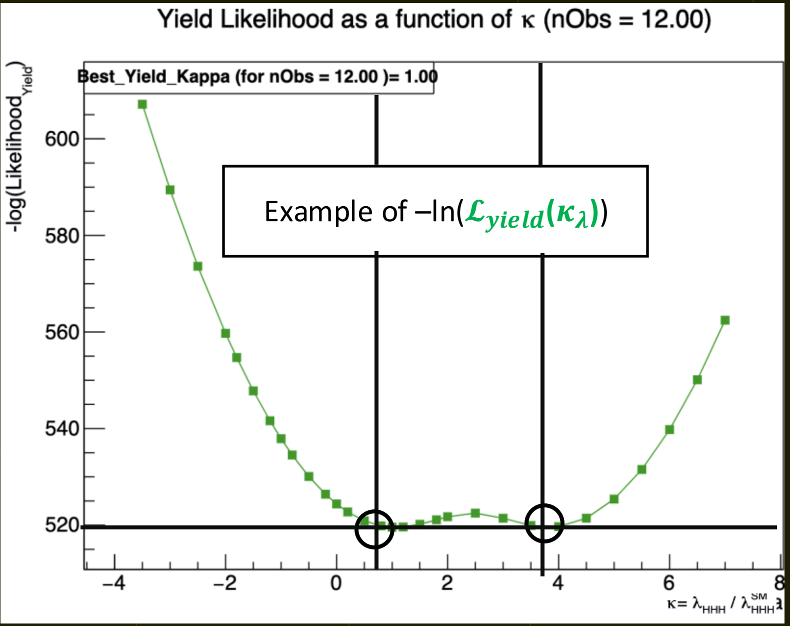

Analysis tool: Extraction of κ_λ using Likelihood scans

Constructing the Extended Likelihood $\mathcal{L}_{\text{extended}}(\kappa_\lambda)$:

$$\boxed{\mathcal{L}_{\text{ext}}(\kappa)} = \underbrace{\prod_{i=1}^{N_{\text{obs}}} \mathcal{L}_{\text{event}}(\kappa|\mathbf{x}^i)}_{\text{Kinematic term}} \times \underbrace{\mathcal{L}_{\text{yield}}(\kappa)}_{\text{Yield term}}$$

Combines the MEM expertise, and the theoretical prediction.

Analysis tool: Extraction of κ_λ using Likelihood scans

Method of minimum negative log-likelihood (NLL)

$$\mathcal{L}_{\text{ext}}(\kappa) = \underbrace{\prod_{i=1}^{N_{\text{obs}}} \mathcal{L}_{\text{event}}(\kappa|\mathbf{x}^i)}_{\text{Kinematic term}} \times \underbrace{\mathcal{L}_{\text{yield}}(\kappa)}_{\text{Yield term}}$$

Combines the MEM expertise, and the theoretical prediction.

$$-\ln \mathcal{L}_{\text{ext}}(\kappa) = -\sum_{i=1}^{N_{\text{obs}}} \ln \mathcal{L}_{\text{event}}(\kappa|\mathbf{x}^i) + \lambda(\kappa) - N_{\text{obs}} \ln \lambda(\kappa) + \mathrm{C}$$

Main advantages of using NLL:

- numerical stability.
- Easy measurement of the uncertainty σ_h on the best value $\hat{\kappa}$

Analysis tool: Extraction of κ_λ using Likelihood scans

Example of Likelihood scan:

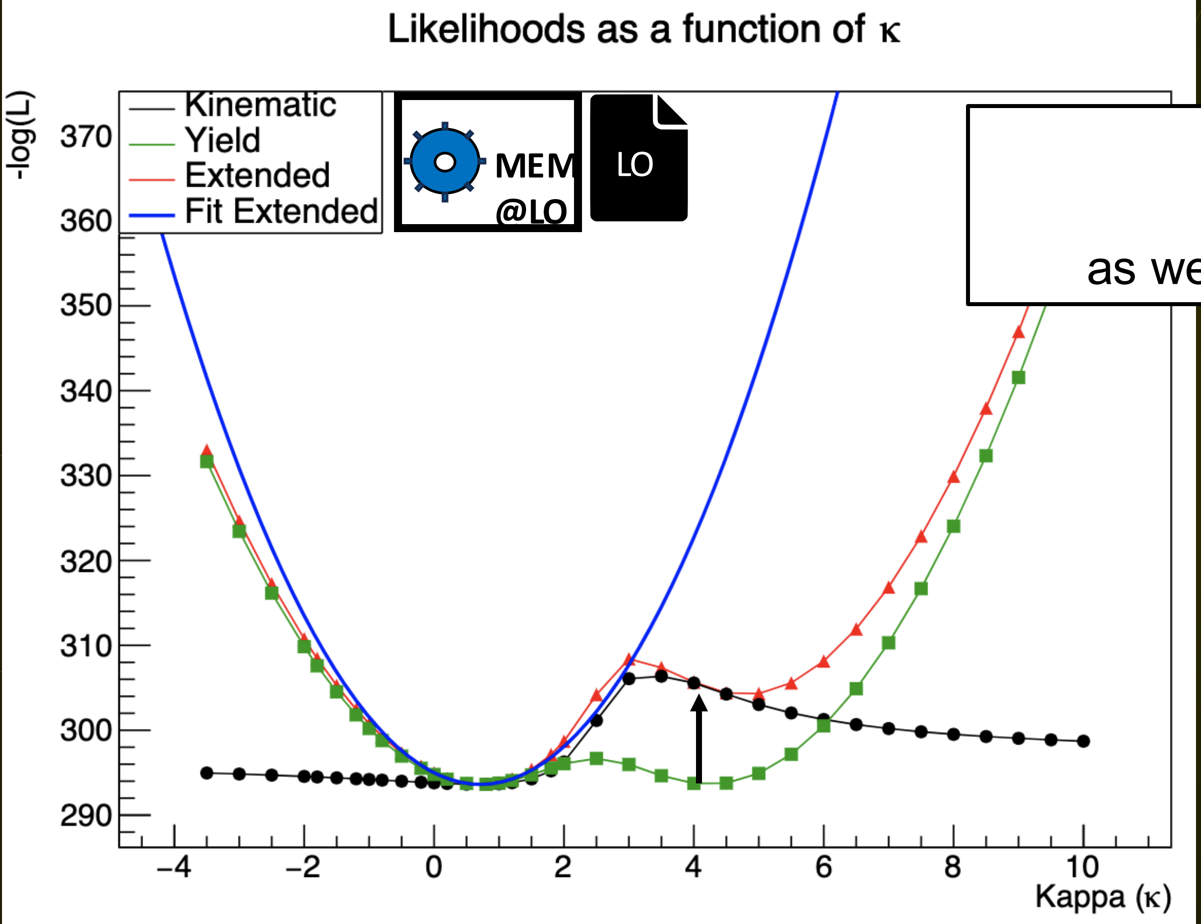

Likelihood scan for LO signal only with MEM@LO

Here you can see the 3 Likelihoods: $\mathcal{L}_{kinematic}$, $\mathcal{L}_{yield}$, and $\mathcal{L}_{extended}$ as well as a **Parabolic Fit** around $\mathcal{L}_{extended}$'s minimum.

For a given pseudo-dataset (i.e. subset of the dataset *D*)

(plotting macros have been **built independently from Legacy analysis, from ground up**)

Analysis tool: Extraction of κ_λ using Likelihood scans

Example of Likelihood scan performance:

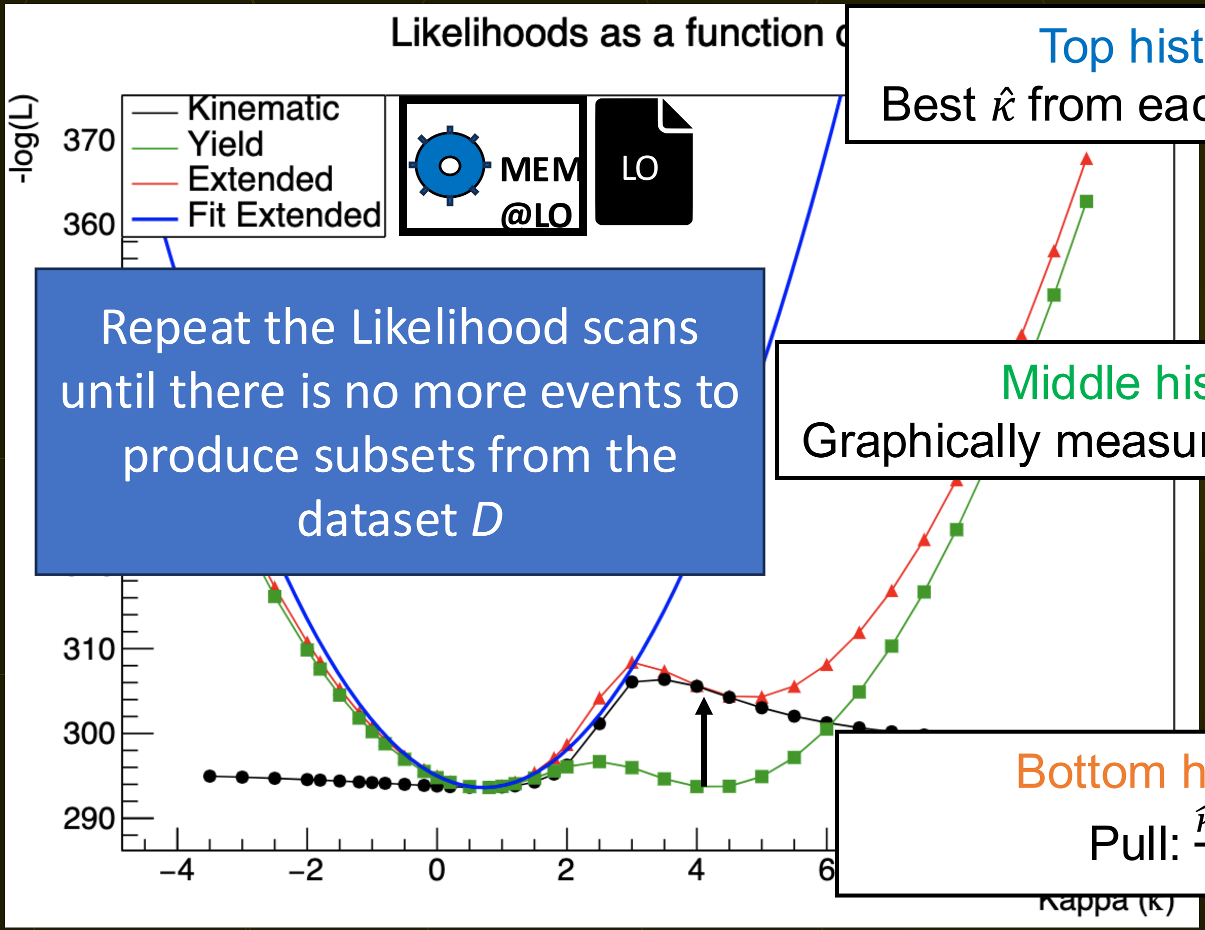

Repeat the Likelihood scans until there is no more events to produce subsets from the dataset *D*

Likelihood scan for LO signal only with MEM@LO

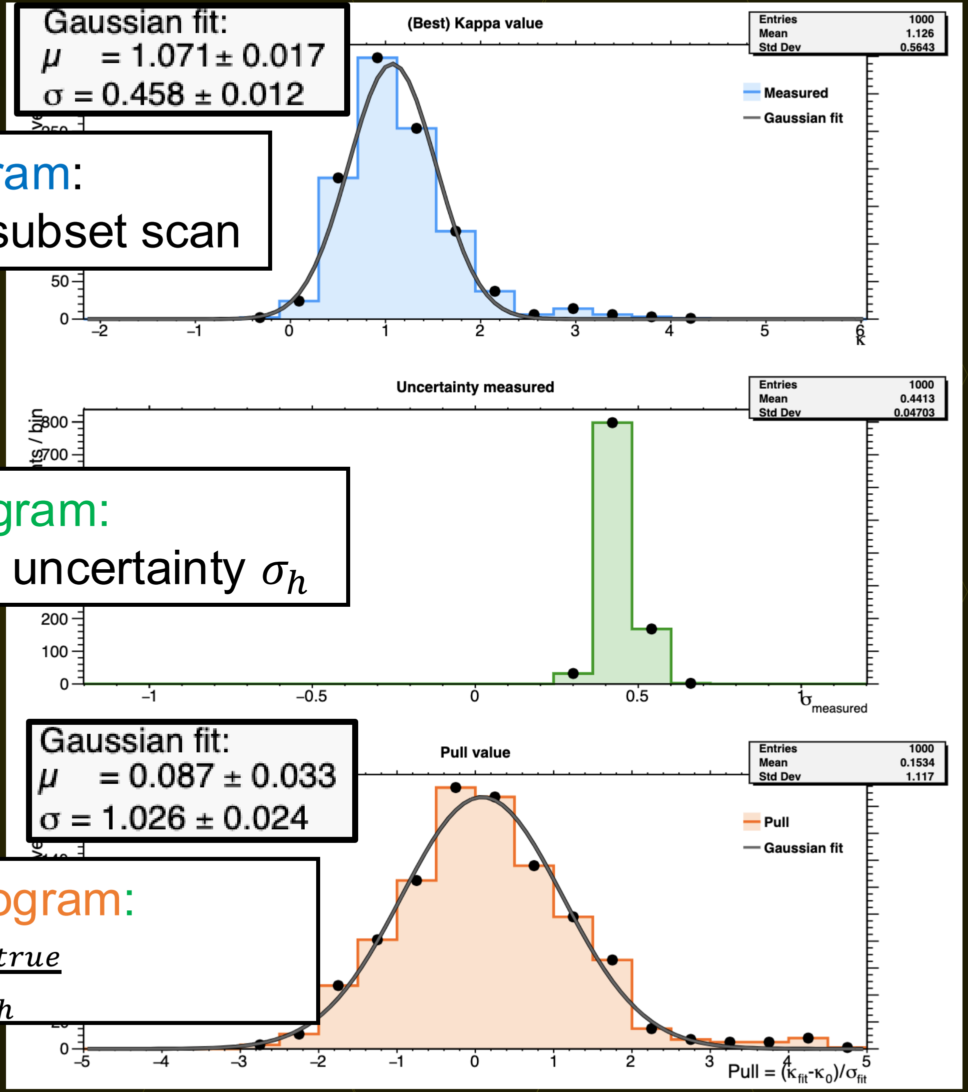

Gaussian fit:
$\mu = 1.071 \pm 0.017$
$\sigma = 0.458 \pm 0.012$

Top histogram: Best $\hat{\kappa}$ from each subset scan

Middle histogram: Graphically measured uncertainty σ_h

Gaussian fit:
$\mu = 0.087 \pm 0.033$
$\sigma = 1.026 \pm 0.024$

Bottom histogram: Pull: $\frac{\hat{\kappa}-\kappa_{true}}{\sigma_h}$

Likelihood scan performance

3.1 : Progress during this PhD: Our contributions

Results

✓ Legacy analysis paper

✓ Our PhD productions

What we did for our MEM analysis:

Processes		Signal (ggF)	Background (ttH)	Background (QCD di-photon)	Background (singleHiggs)
ROC	MEM@ **LO**	✗	✓✓	✓	✓
	MEM@ **NLO**	✗	✓	✓	✓
Likelihood Scans	MEM@ **LO**	✓✓	✓	✓✓	✓
	MEM@ **NLO**	✓	✓	✓	✓

For given (set of) files: LO events, NLO [ISR, …], ATLAS n-tuples.

The coverage of this **entire** table largely made possible with dedicated automated frameworks.

.2 : Impact of MEM@NLO on the ROC

for ttH bakcground

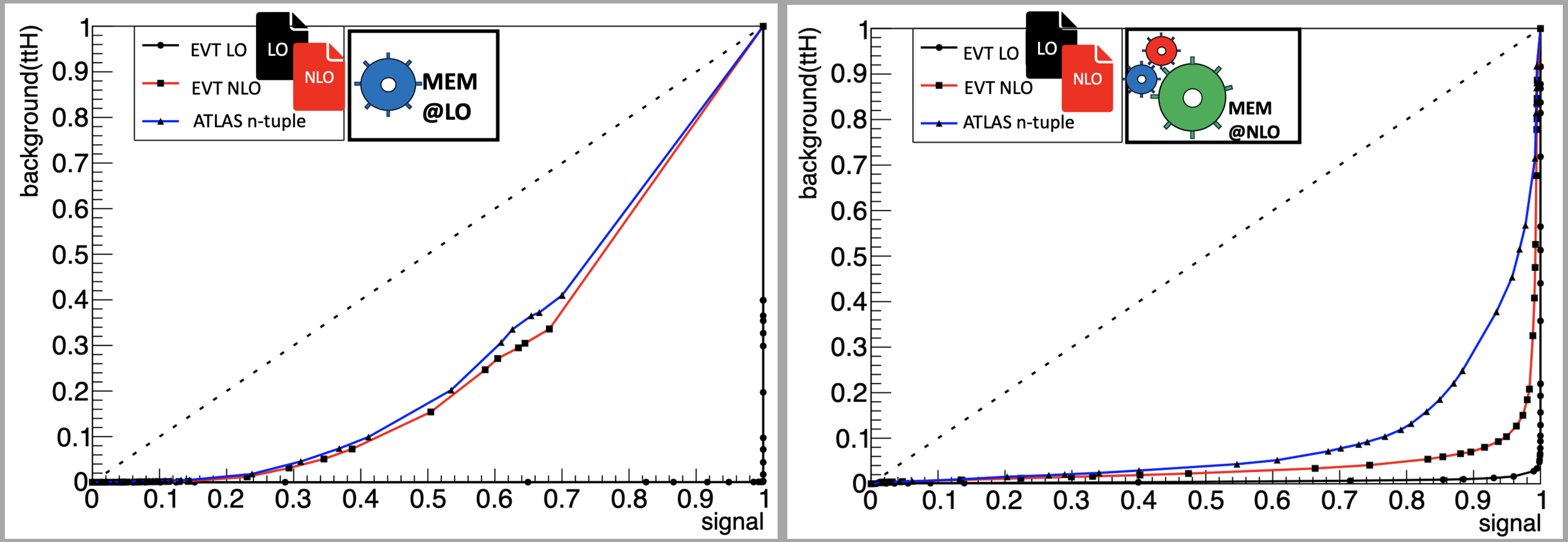

	MEM@LO	MEM@NLO
AUC for NLO ISR (%)	22.98	4.09
AUC for ATLAS n-tuples (%)	29.28	9.69

Results

.2 : Impact of MEM@NLO on the ROC

For QCD di-photon bakcground

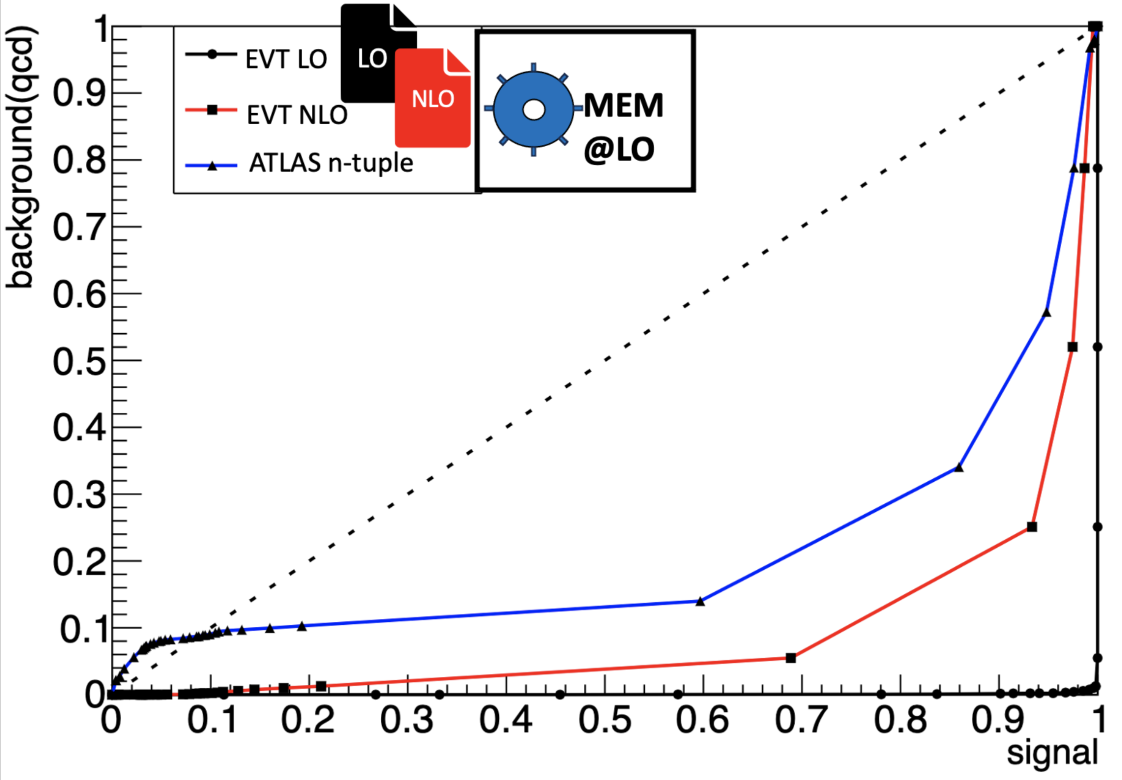

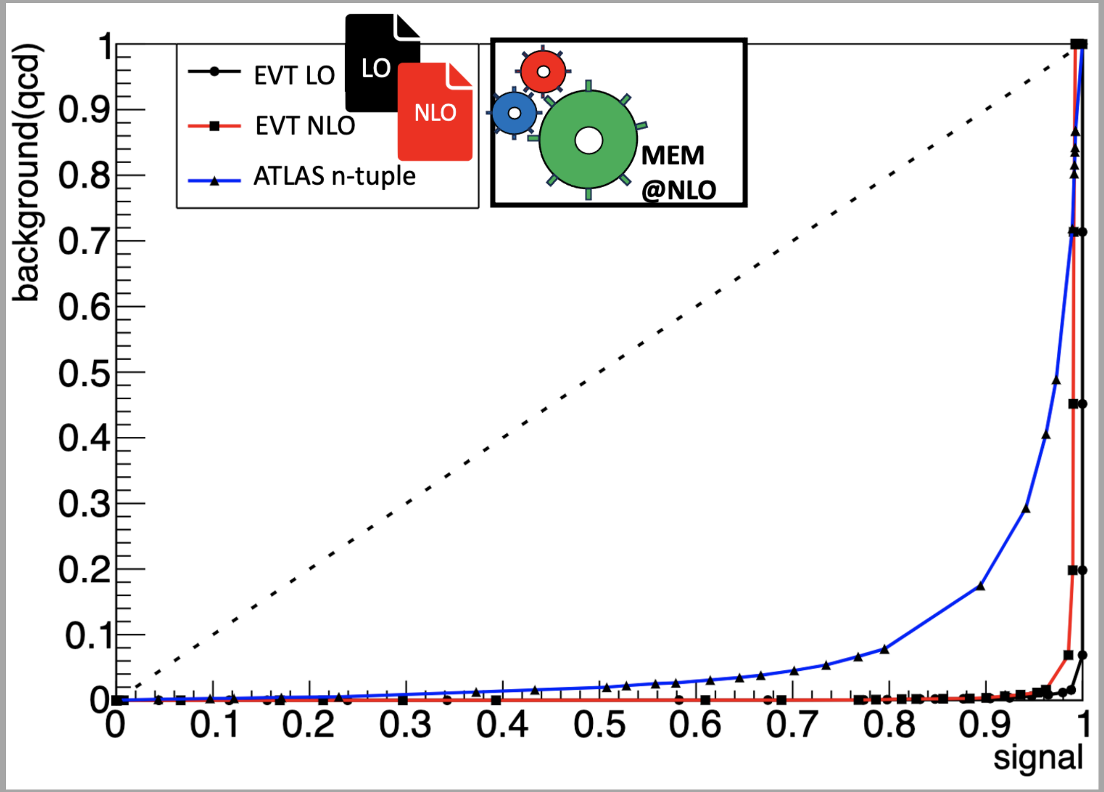

	MEM@LO	MEM@NLO
AUC for NLO ISR (%)	9.05	1.18
AUC for ATLAS n-tuples (%)	20.96	7.08

.2 : Impact of MEM@NLO on the ROC

For singleHiggs bakcground

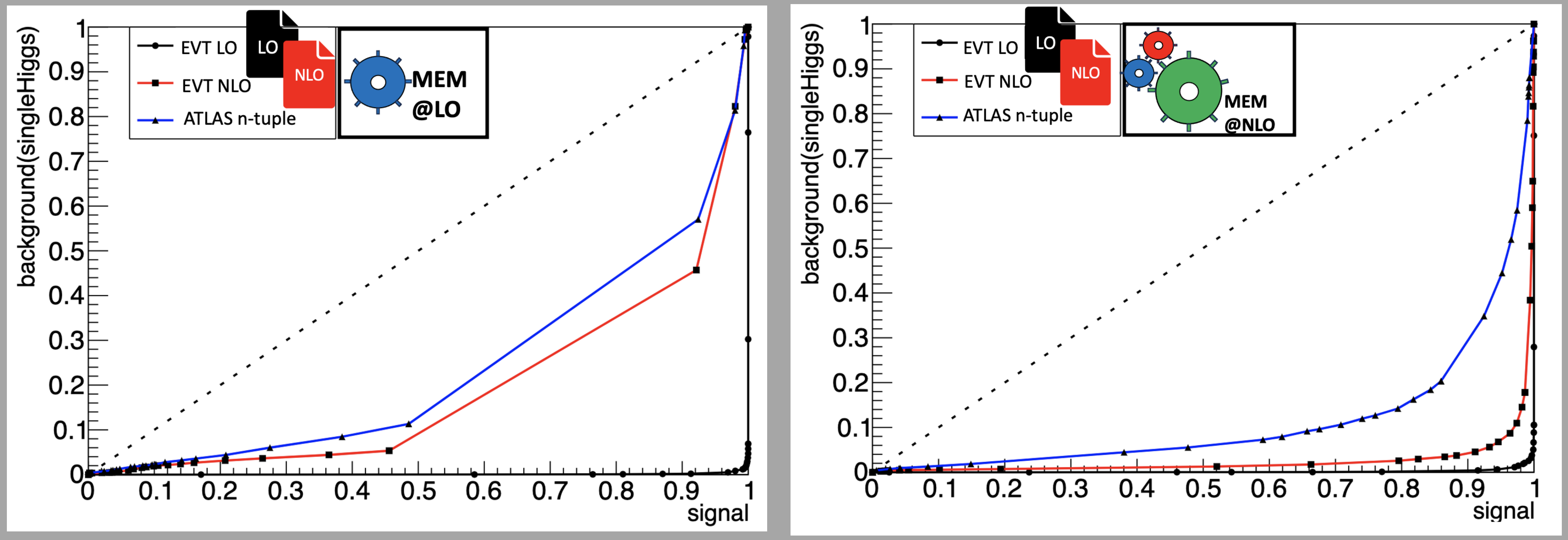

	MEM@LO	MEM@NLO
AUC for NLO ISR (%)	18.87	3.12
AUC for ATLAS n-tuples (%)	23.33	11.33

3

Results

.3 : Impact of MEM@NLO on the Likelihood scans

For signal only sample

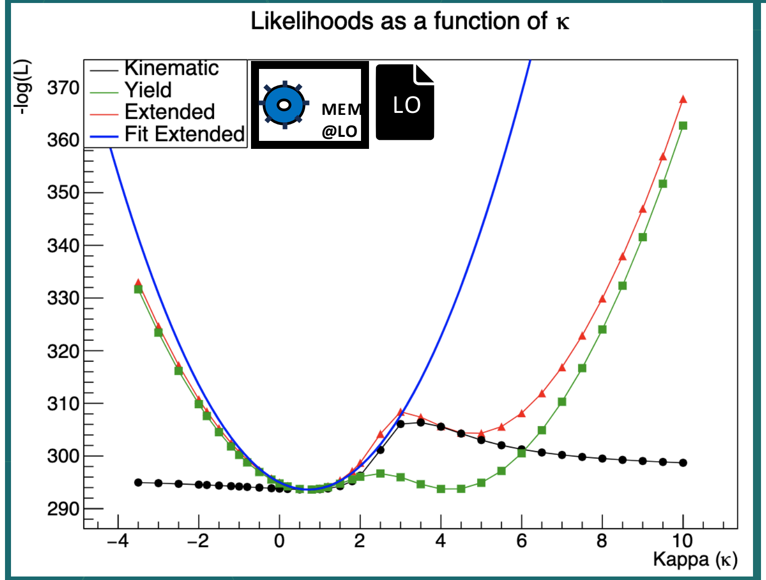

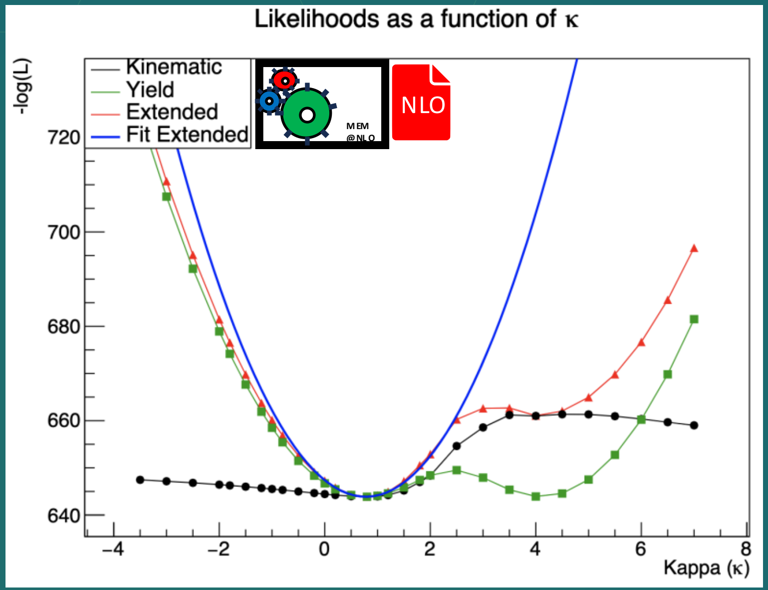

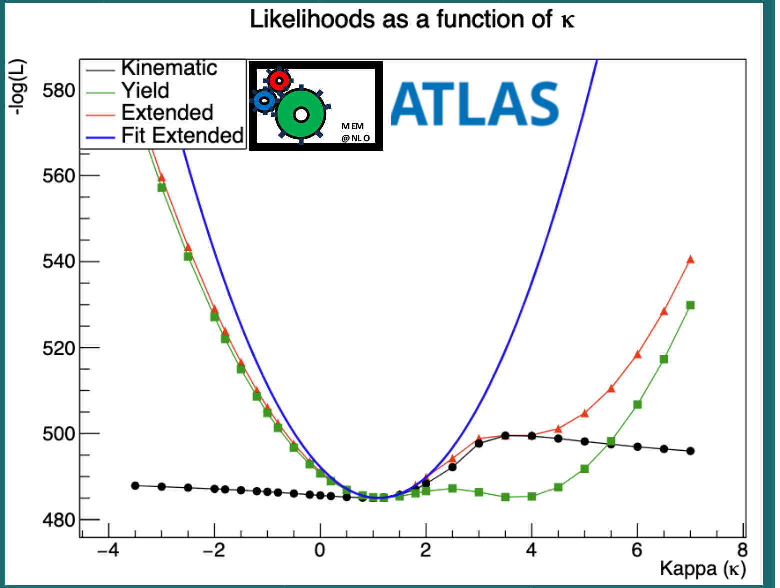

LO with MEM@LO

NLO [ISR] with MEM@NLO

ATLAS n-tuples with MEM@NLO

.3 : Impact of MEM@NLO on the Likelihood scan performances

For signal only sample

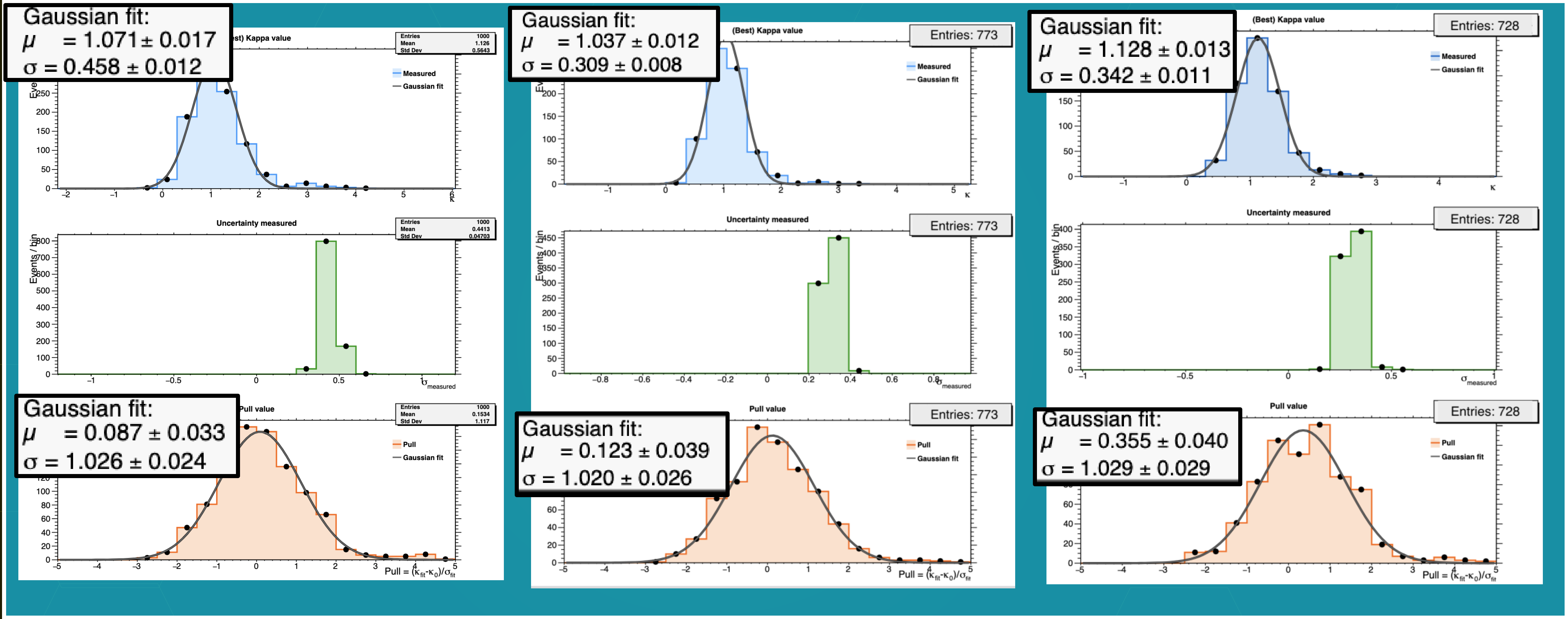

AUC for NLO ISR	LO	NLO	ATLAS
Value of $\hat{\kappa} \pm \sigma$	1.071 ± 0.458	1.037 ± 0.309	1.128 ± 0.342

.3 : Impact of MEM@NLO on the Likelihood scan performances

3

Results

For {signal + ttH} sample

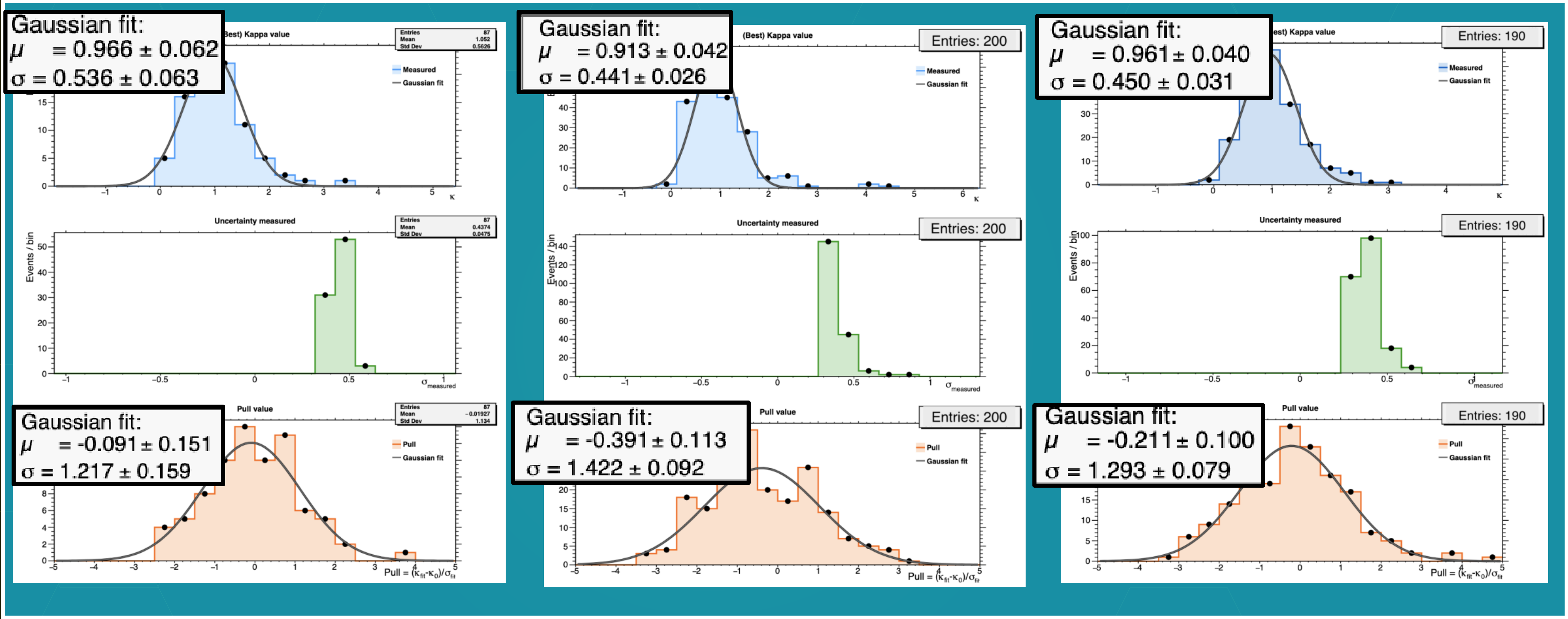

AUC for NLO ISR	LO	NLO	ATLAS
Value of $\hat{\kappa} \pm \sigma$	0.966 ± 0.536	0.913 ± 0.441	0.961 ± 0.450

3

Results

.3 : Impact of MEM@NLO on the ROC

For {signal + ttH + QCD+ singleHiggs} sample

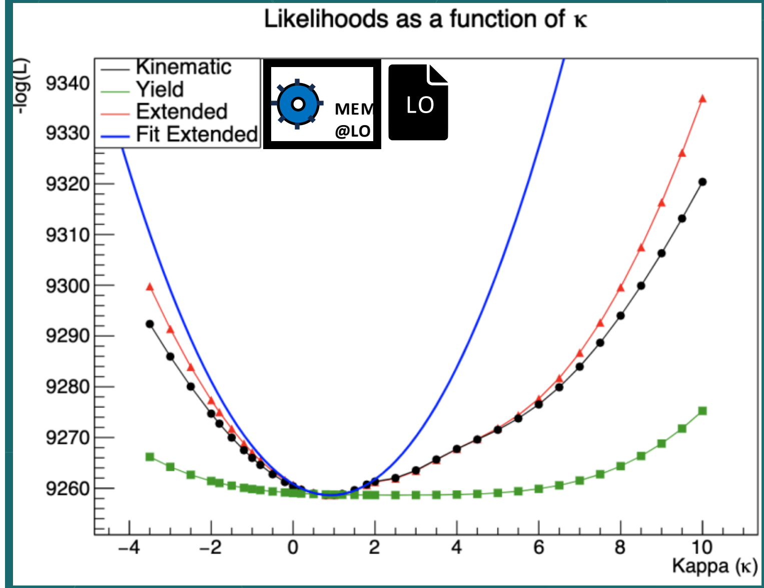

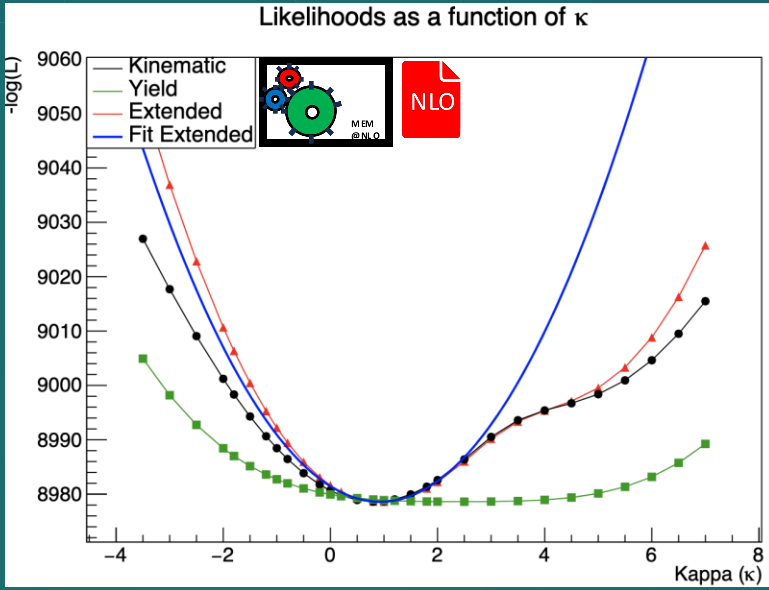

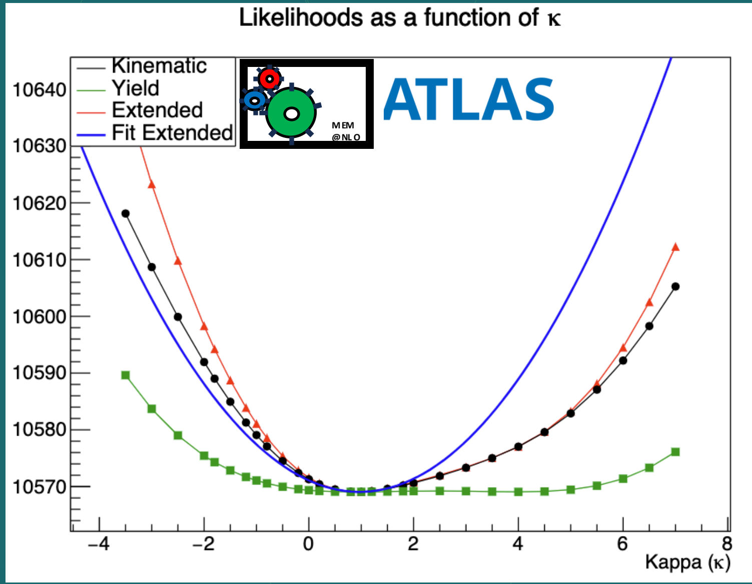

LO
with MEM@LO

NLO [ISR]
with MEM@NLO

ATLAS n-tuples
with MEM@NLO

3

.3 : Impact of MEM@NLO on the Likelihood scan performances

Results

For {signal + ttH + QCD+ singleHiggs} sample

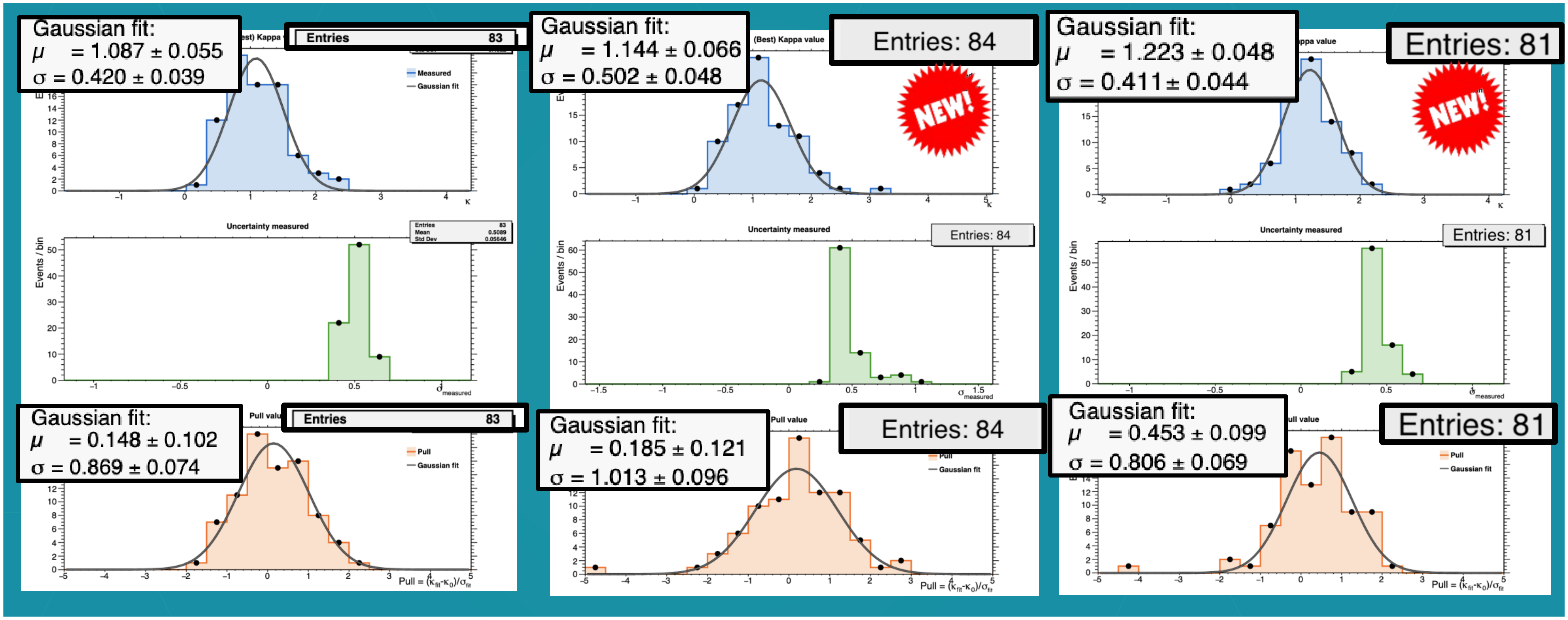

AUC for NLO ISR	LO	NLO	ATLAS
Value of $\hat{\kappa} \pm \sigma$	$1.087 \ \pm 0.420$	$1.144 \ \pm 0.502$	$1.223 \ \pm 0.411$

.4 : Results summary: NLO [ISR]

NLO

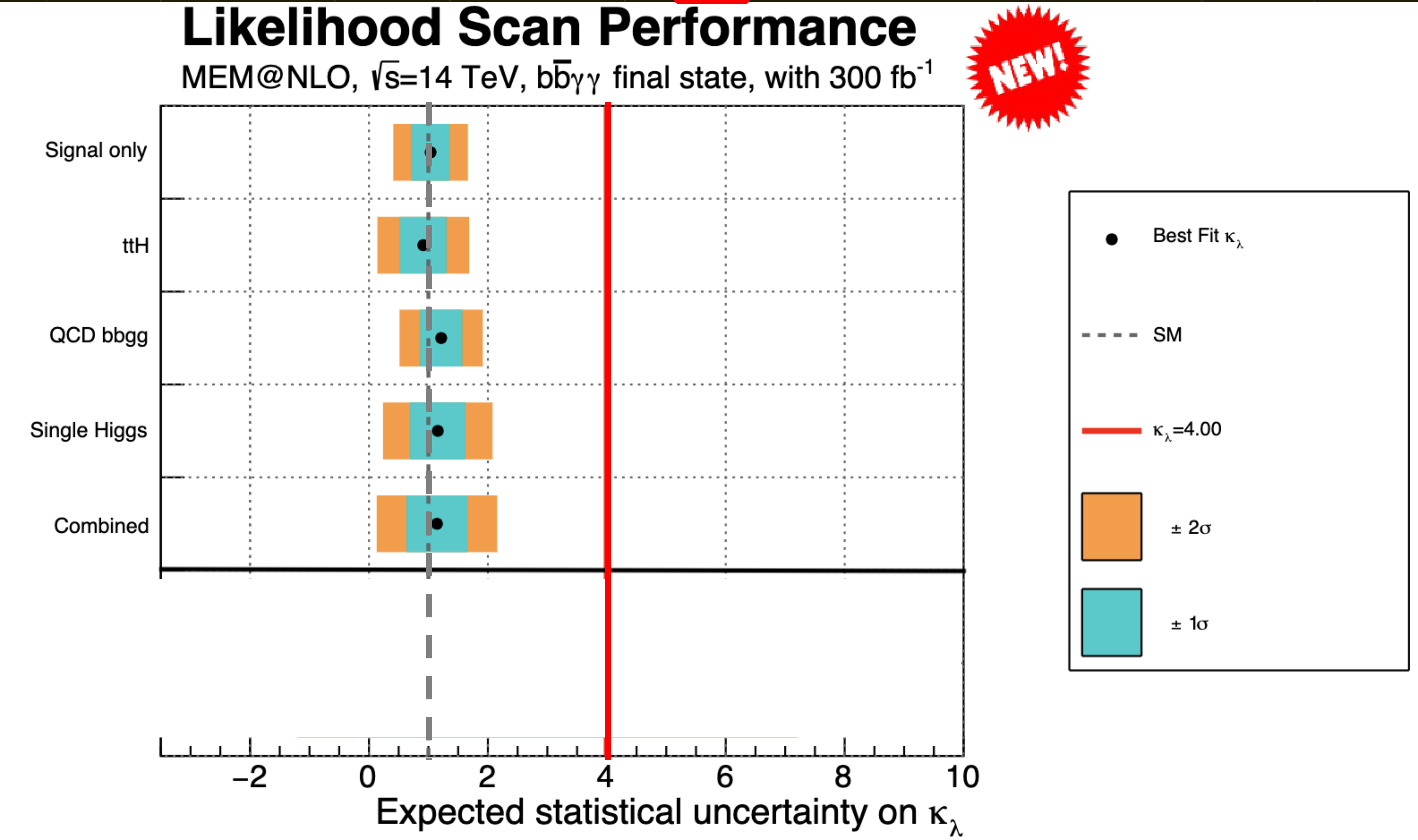

3

Results

3

Results

.4 : Results summary: ATLAS n-tuples

ATLAS

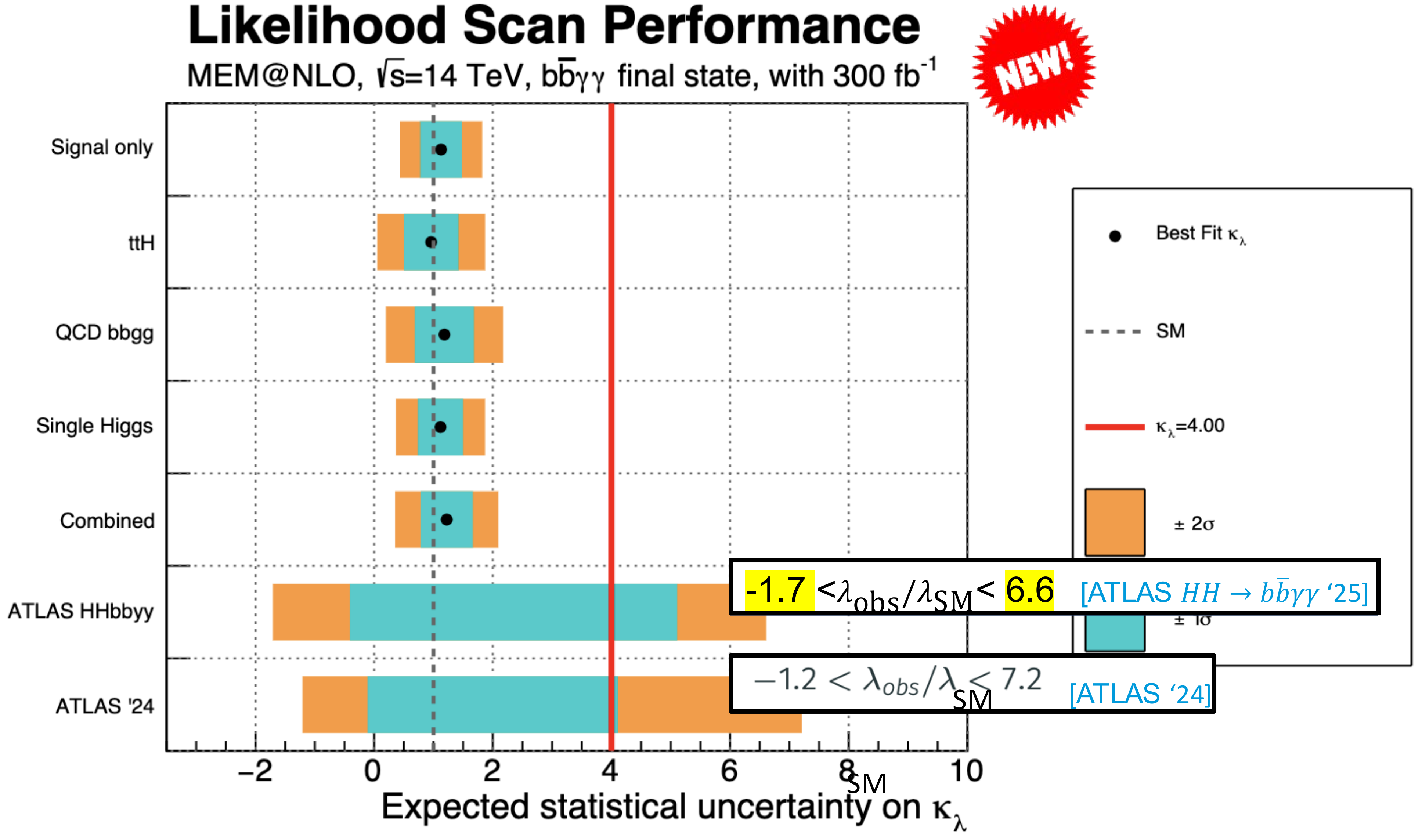

4 Conclusion

Summary

Measurement of the Higgs boson trilinear self-coupling λ_{3H} remains of great importance.

We developed the first Next-to-Leading Order Matrix Element Method (MEM@NLO) in the context of the $gg \to HH \to b\bar{b}\gamma\gamma$ channel, to measure it.

Validation against NLO Monte-Carlo samples and ATLAS n-tuples show:

- κ_λ = 1.144 with an associated uncertainty σ_κ = 0.50 on NLO ISR events.
- κ_λ = 1.223 with an associated uncertainty σ_κ = 0.41 on ATLAS events.

Outlook:

Our work focused on MC simulated data, but framework ready for deployment on Run-3 datasets.
Looking ahead, the MEM@NLO could also be extended to other final states ($b\bar{b}\tau\tau$, $b\bar{b}b\bar{b}$,…), to SMEFT interpretations at full NLO accuracy, or other @NLO applications.

Thank you very much for your attention!